GROUNDWATER AVAILABILITY OF THE BARTON SPRINGS SEGMENT OF
THE EDWARDS AQUIFER, TEXAS: NUMERICAL SIMULATIONS THROUGH
2050

by

Bridget R. Scanlon, Robert E. Mace*, Brian Smith**, Susan Hovorka, Alan R. Dutton,
and Robert Reedy

prepared for

Lower Colorado River Authority
under contract number UTA99-0

October 2001

GROUNDWATER AVAILABILITY OF THE BARTON SPRINGS SEGMENT OF
THE EDWARDS AQUIFER, TEXAS: NUMERICAL SIMULATIONS THROUGH
2050

by

Bridget R. Scanlon, Robert E. Mace*[1], Brian Smith**, Susan Hovorka, Alan R. Dutton,
and Robert Reedy

prepared for

Lower Colorado River Authority
under contract number UTA99-0

October 2001

[1] This study was initiated while Dr. Mace was an employee at the Bureau of Economic
Geology and his involvement primarily included initial model development and
calibration.

CONTENTS

Figures

Tables

ABSTRACT

A two-dimensional, numerical groundwater-flow model was developed for the Barton Springs segment of the Edwards aquifer to evaluate groundwater availability and predict water levels and spring flow in response to increased pumpage and droughts during the period 2001 through 2050. A steady-state model was developed on the basis of average recharge for a 20-yr period (1979 through 1998) and pumpage values for 1989. Transient simulations were conducted using monthly recharge and pumping data for a 10-yr period (1989 through 1998) that includes periods of low and high water levels. Values of hydraulic conductivity were estimated by calibrating the steady-state model using trial and error and automated inverse methods. Good agreement was found between measured and simulated flow at Barton Springs (root mean square error [RMS error, average of squared differences in measured and simulated discharges] 12 cfs), between measured and simulated water levels at different times and between measured and simulated water levels in many of the monitoring wells. To assess the impact of future pumpage and potential future droughts on groundwater availability, transient simulations were conducted using extrapolated pumpage for 10-yr periods (2001 through 2050) and average recharge for a 3-yr period and recharge from the 1950's drought for the remaining 7 yr. Results of these simulations were compared with those using average recharge and future pumpage. Predicted water-level declines in response to future pumpage under average recharge conditions are small (≤ 35 ft), whereas water-level declines under future drought conditions were much greater (≤270 ft). Simulated spring discharge in response to future pumpage under average recharge decreased proportionally to future pumpage (2 cfs per decade), whereas spring discharge decreased to 0 cfs in response to future pumpage under drought-of-record conditions. Management of water resources under potential future drought conditions should consider enhanced recharge and conservation measures.

INTRODUCTION

This modeling study focuses on a segment of the Edwards aquifer within and adjacent to Austin, Texas, that discharges into Barton Springs and Cold Springs and is hydrologically distinct from the rest of the Edwards aquifer. This region, referred to as the Barton Springs segment of the Edwards aquifer, constitutes the sole source of water to about 45,000 residents. Barton Springs pool was created when a dam was installed immediately downstream of the

spring and it also serves as a municipal swimming pool in Zilker Park, downtown Austin. The Barton Springs salamander, listed as an endangered species, is restricted to the region immediately surrounding the spring. Increased population growth and recent droughts (1996) have focused attention on groundwater resources and sustainability of spring flow. A combination of increased pumpage and severe drought could severely impact future water resources.

A numerical groundwater flow model is a tool that can help in assessing the impacts of current and future pumpage on groundwater resources and spring discharge. A groundwater flow model numerically represents the aquifer using a computer. Information about the aquifer, such as water levels, recharge, and spring discharge, provides input to the model and helps us evaluate the reliability of the model. A calibrated groundwater model can provide a valuable tool for evaluating the impact of pumping and drought on an aquifer.

The objective of this study was to evaluate long-term groundwater availability in response to future pumpage and potential future droughts. To meet this objective, it was necessary to develop a two-dimensional numerical, finite-difference groundwater model of the Barton Springs segment of the Edwards aquifer. This model will provide (1) a management tool to the Barton Springs Edwards Aquifer Conservation District (BSEACD) and to the Regional Water Planning Group and (2) a tool for evaluating groundwater availability under drought-of-record conditions. This report describes the construction and calibration of the numerical model and the results of predictive simulations of water levels and spring discharge for the next 50 yr based on projected demands from the Regional Water Planning Group and the BSEACD.

The various components of the modeling study included (1) developing a conceptual model that included our current understanding of the geology, (2) quantifying groundwater recharge from stream-gage records, (3) calibrating a steady-state model using average recharge for a 20-yr period (1979–1998) and trial and error and automated inverse methods, (4) running a transient model for a 10-yr period (1989–1998), (5) conducting sensitivity analyses to determine the primary controls on the simulations, and (6) running predictive simulations through 2050. This report describes (1) the study area, previous work, and hydrogeologic setting used to develop the conceptual model; (2) the code, grid, and recharge assigned during model construction; (3) calibration of the steady-state model to estimate the hydraulic conductivity distribution; (4) the transient model for the 10-yr period; (5) sensitivity analysis for the steady-state and transient model; and (6) predictions of water-level changes and spring discharge under

future pumpage and drought-of-record conditions; (7) the limitations of the current model; and (8) suggestions for improvements.

The model developed in this study differs from the previous two-dimensional, finite-difference model developed by Slade and others (1985) in the grid resolution (minimum 500 ft versus a minimum of 1,500 ft) in explicitly representing the aquifer thickness in the simulation, in simulating transient flow for a long time (10 yr versus 5 mo), and in predicting groundwater availability under increased pumpage and potential future droughts for the period through 2050. The spatially distributed model developed in this study allows the effect of pumpage in different regions of the model area to be assessed, which is not possible with the lumped parameter model developed by Barrett and Charbeneau (1996). More details on these other models are provided in the Previous Work section.


STUDY AREA


The Barton Springs segment of the Edwards aquifer constitutes the study area and includes parts of Travis and Hays Counties (fig. 1). The study region is within the Lower Colorado Region (Region K) water-planning group and includes the Barton Springs/Edwards Aquifer Conservation District (fig. 2). The model boundaries are all hydrologic boundaries and include the Mount Bonnell fault to the west, which acts as a no-flow boundary (Senger and Kreitler, 1984); a groundwater divide to the south along Onion Creek (Guyton and Associates, 1958); the "bad-water" line to the east; and the Colorado River (Town Lake) to the north. Groundwater circulation in the Edwards aquifer decreases to the east and total dissolved solids (TDS) increase. The bad-water line marks the zone where TDS exceeds 1,000 mg/L, which generally coincides with Interstate 35. The groundwater divide in the south separates the Barton Springs segment from the San Antonio segment of the Edwards aquifer, which discharges into Comal and San Marcos Springs.


Physiography and Climate

Physiographically the aquifer lies on the transition between the Edwards Plateau to the west and the Blackland Prairie to the east. The topography of the area is that of the Rolling


3

Prairie province. Surface elevations range from about 1,050 ft in the southwest to about 250 ft along the east margin (fig. 3).

The study area is in the subtropical humid climate zone (Larkin and Bomar, 1983). Annual precipitation ranges from 11 to 65 inches (1860 through 2000), a figure which is based on records from a NOAA station located north of the study area at Camp Mabry and Mueller Airport in Austin (fig. 4a). Long-term mean annual precipitation is 33.5 inches (fig. 4a). Precipitation occurs primarily in the spring and fall, mainly as a result of mixing of cool fronts and warm, moist air from the Gulf of Mexico. Convectional thunderstorms result in small amounts of rain in the summer. Mean annual gross lake evaporation is 66 inches (Larkin and Bomar, 1983).

The Edwards aquifer is unconfined in the outcrop area where recharge occurs and in part of the section to the east, where it is overlain by the Del Rio Clay (fig. 1). Farther to the east, the aquifer is confined by the Del Rio Clay. Approximately 80 percent of the aquifer is unconfined, and the remainder is confined (Slade and others, 1985).

Geology

The Barton Springs segment of the Edwards aquifer is a hydrologically significant element within an aquifer system developed in thick and regionally extensive Lower Cretaceous carbonates that underlie large areas of Texas. The components make up the northern segment of the Edwards aquifer, the Barton Springs segment, the San Antonio segment, and the Edwards-Trinity Plateau and Trinity aquifers (fig. 5).

The sediments hosting these aquifers were deposited when a Lower Cretaceous sea-level rise flooded the North American craton. Two transgressive–regressive cyclic genetic sequences are represented by conglomerate, sandstone, shale, and limestone in the lower and middle Trinity Group (Moore, 1996). Continued transgression recorded by cyclic sedimentation resulted in deposition of two thick carbonate-dominated sequences of the Glen Rose Formation in the upper Trinity Group overlain by four sequences that comprise the Edwards aquifer and facies-equivalent limestones (fig. 6). Edwards Group and temporally equivalent limestones and marls are recognized as far north as the Texas Panhandle, where they subcrop beneath the Ogallala Formation. Water depth continued to increase cyclically through part of the Late Cretaceous, but sedimentary patterns were modified by deposition of a number of shales separated by limestone

4

and chalk. The first of these shale units is the Del Rio Formation, which forms the aquitard at the top of the Edwards Group over a wide area, and which is overlain by the Buda Formation (dominantly limestone) and the Eagle Ford Formation (dominantly shale). Maximum water depth is represented by deposition of the Austin Chalk over a wide area. Maximum water depth was followed by progradation, aggradation, and sea-level fall, during which clastics, including the Taylor and Navarro Formations, were the dominant deposits.

The major episode of structural deformation affecting aquifer development was uplift of the Edwards Plateau along the Balcones Fault Zone. This deformation occurred along a sinuous trend extending from Dallas through Austin and San Antonio and west toward Del Rio. Uplift of the Edwards Plateau began in the Miocene and during the creation of the regional hydraulic gradient. Normal faulting along en echelon faults and graben systems that yielded a total of 1,400 ft down-to the coast displacement across the Barton Springs segment accommodated uplift. Major faults trend north-northeast.

Uplift along the Balcones Fault Zone, followed by erosion, has resulted in stripping of younger units to expose the Glen Rose Formation to the west. This area is commonly described as the contributing zone to the Edwards aquifer. It is characterized by creeks that are maintained by spring flow. The recharge zone is the area where diverse stratigraphic units that form the Edwards aquifer crop out. The recharge zone is approximately coincident with the west edge of the Balcones Fault Zone, and structural and rock properties combine to create effective pathways for rapid recharge from streams. At the east edge of the study area, where less uplift has occurred, the aquifer is confined by younger, low-permeability units, including the Del Rio Clay, Eagle Ford Formation, Austin Chalk, Taylor, and Navarro Formations. Although faults are less easily mapped in weak and poorly exposed shales at the east edge of the study area, examination of subsurface structure shows that this area is within the Balcones Fault Zone.

PREVIOUS WORK

Numerical models of groundwater flow in the Barton Springs segment of the Edwards aquifer were previously developed by Slade and others (1985) and Barrett and Charbeneau (1996). Slade and others (1985) developed a two-dimensional numerical groundwater flow model for the part of the Edwards aquifer that discharges at Barton Springs by using a finite difference code written by Trescott and others (1976). The purpose of the modeling study was to

determine the spatial distribution of hydraulic parameters and to assess different water-management scenarios that included increased pumpage and enhanced recharge. The model grid consisted of 318 active cells, with cell spacing ranging from about 1,500 to 8,000 ft. A steady-state model was developed for mean recharge conditions that corresponded to long-term average discharge at Barton Springs (53 cfs). Recharge was estimated from stream-loss records. The model did not explicitly represent aquifer thickness, although thickness was incorporated in the transmissivity data. Calibration of the steady-state model was used to determine the spatial distribution of transmissivity, which varied from 100 ft$^2$ d$^{-1}$ in the west part of the aquifer to more than 1 million ft$^2$ d$^{-1}$ near Barton Springs. A transient model was developed for a 5-mo period. Calibration of the transient model yielded values of specific yield and storage coefficient for the aquifer. Predictive simulations, conducted by using projected pumpage for the year 2000, indicated that the aquifer would be dewatered in the southwest part of the study area and major declines would occur in the southeast area. However, another simulation that included use of recharge enhancement predicted a rise in potentiometric surface of about 50 ft in the southwest part of the aquifer and moderate water-level declines in the southeast zone. The model developed by Slade and others (1985) is not appropriate for regional water planning because the model was developed with a code that is no longer in use (Trescott and others, 1976), the grid cell size is large (minimum 1,500 ft), the aquifer thickness is not explicitly represented in the model, and the transient simulation period was short (5 mo).

Barrett and Charbeneau (1996) developed a new type of lumped parameter model to predict the impacts of urban development on the quantity and quality of water in the Barton Springs segment of the Edwards aquifer. The aquifer was divided into five cells corresponding to the five watersheds in the region. A single well was used to represent conditions in each cell. The model successfully reproduced measured water levels and average nitrogen concentrations in the Edwards aquifer and at Barton Springs. Increased urbanization was simulated by estimating changes in creeks that recharge the system. The results indicate that increased development will reduce spring flow and increase nitrogen concentrations in the aquifer. The resolution of the model (cells equivalent to river basins) is too coarse to evaluate the impact of more local pumpage on spring discharge; therefore, the lumped parameter model is inadequate for regional water planning.

# HYDROGEOLOGIC SETTING

The hydrogeologic setting describes the aquifer and hydrologic features and hydraulic properties that influence groundwater flow in the aquifer. For this study, we built on previous surface mapping to develop two new subsurface structure maps and an isopach map.

The hydrogeologic framework developed for this model was based on previous work. An unpublished geologic map in ARC/INFO Geographic Information System (GIS) provided the interpretation of bedrock geology at the surface (figs. 7, 8) (Hauwert and others, 1997). Maps of parts of the area were published by Small and others (1996) and Hanson and Small (1995). The other major data input was an unpublished notebook of subsurface well log data and a table of depth to top of formations compiled by Nico Hauwert for BSEACD (N. Hauwert, 1998, unpublished data). Following the convention developed in the San Antonio segment of the Edwards aquifer, we consider the interval between the regionally extensive markers at the top of the Glen Rose Formation and the base of the Del Rio Formation as part of the Edwards aquifer and is the interval modeled in this study.

Other research used for subsurface interpretation for conceptual model development includes stratigraphic descriptions (Rose, 1972; Hanson and Small, 1995; Moore, 1996; and Small and others, 1996) and structural interpretations of Garner and Young (1976) and Collins and Woodruff (2001). A number of differences in interpretation among previous researchers are noted. Moore (1996) emphasized the lateral facies variation in dominant lithology and nomenclature in response to genetic sequences and paleogeography. The nomenclature derived from Rose (1972) and developed for the San Antonio segment uses a stratigraphic approach, recognizing eight named and numbered, lithologically defined hydrostratigraphic units that were applied in the Barton Springs segment by Hauwert and others (1997) and Small and others (1996).

Similarly, variations in fault interpretation are noted. The mapping of Collins and Woodruff (2001) employs a relay-ramp conceptual model (Collins, 1996; Ferrill and Morris, 2001). In this model, the vertical displacement varies laterally along each fault strand. As displacement decreases on one strand, the strain is taken up on adjacent strands. The fault strands form an en echelon pattern, with each strand dying out along strike. Between the fault strands, the rocks are folded to accommodate deformation, forming structures described as a relay ramps. The mapping of Hauwert and others (1997), Small and others (1996), and Hanson and Small

(1995) follows a conceptual model in which faults generally continue until they intersect another fault. Rather than folds commonly interpreted in the relay-ramp model, changes in elevation of formation or member contacts are commonly interpreted as the result of cross-faulting between major fault strands.

Hydrostratigraphy

The Edwards aquifer is an interval containing carbonates that have numerous intervals of intercrystalline high porosity, as well as petrophysical properties that make the carbonates subject to development of karst conduits. Underlying and, to a lesser extent, overlying stratigraphic intervals also serve as aquifers and can develop karst conduits.

Conventionally the lower boundary of the Edwards aquifer is defined as the top of the Glen Rose Formation (fig. 6). The Glen Rose Formation is the uppermost unit in the Trinity aquifer (Mace and others, 2000). In the study area, supratidal and paleosol deposits at the top of the Glen Rose Formation are overlain by marly, nodular limestones and calcareous shales (Moore, 1996, Molineux, 2001). These onlapping transgressive systems tract deposits are classified as the Walnut Formation (Rose, 1972; Moore, 1996) or the basal nodular member of the Kainer Formation, Edwards Group (Rose, 1972; Small and others 1996; Hauwert and others 1997). Irrespective of stratigraphic complexity, in many areas these units limit vertical permeability. Evidence of limited vertical permeability includes (1) numerous springs and seeps that discharge at this contact in outcrop and (2) an increase in salinity in the subsurface below the Glen Rose contact evident on resistivity logs. Regionally, however, there is cross-formational interconnection across the Edwards-Glen Rose contact. Both units are karstic limestones, and large caves that cross the contact are interpreted as evidence that cross-formational flow occurs through karst systems in at least parts of the San Antonio segment of the Edwards aquifer. Likewise, modeling of flow in the Trinity aquifer (Mace and others, 2000) concludes that cross-formational flow of significant volumes of water occurs from the Trinity into the Edwards in the San Antonio segment, illustrating connection between the aquifers.

The carbonates in the Edwards aquifer are laterally and vertically heterogeneous. This heterogeneity reflects the complex interactions among (1) paleogeography, (2) sea-level variation, (3) carbonate accumulation (productivity and transport), (4) siliciclastic transport, (5), early diagenesis, and (6) subsidence. The study area was on the north flank of a broad, low-relief

positive area known as the Texas Platform and San Marcos Arch (Rose, 1972). Stratigraphic units deposited on the platform include the Walnut Formation/basal nodular member of the Kainer Formation, and the Kainer and Person Formations. These units collectively are described as the Edwards Group (Rose, 1972). A regionally traceable transgressive unit, known as the Regional Dense Member of the Person Formation, separates the Kainer and Person. Slightly deeper water in the North Texas Basin toward the north is interpreted from facies changes. Time-equivalent units recognized in North Central Texas include the Walnut, Comanche Peak, Kiamichi, and Duck Creek Formations (Rose, 1972; Moore, 1996). Sea-level variation is reflected in regionally correlated sequences (Immenhauser and Scott, 1999) and patterns of stacked high-frequency cycles. High-frequency cycles have been described in the Walnut Formation (Moore, 1996). Inspection of outcrop and log data suggests that the same type of high-frequency upward-shoaling cyclicity recognized in the San Antonio segment (Hovorka, 1996) is a dominant pattern in the Barton Springs segment; however, no detailed stratigraphic studies have been done in units younger than the Walnut. In the San Antonio segment of the Edwards aquifer, interaction between lithologies and structure was observed to influence distribution of karst conduits (Hovorka and others, 1998). Karst conduits developed preferentially where fractures intersect subtidal dolomites. Beds of calcitized and dissolved evaporites may also focus karst dissolution. The relationship between lithofacies and structure within the Edwards aquifer of the Barton Springs segment will most likely impact flow within the aquifer similarly; however, the relationships have not been documented.

The Edwards Group is overlain by transgressive carbonates of the Georgetown Formation. The contact is at least locally unconformable, with development of pre-Georgetown karst (Rose, 1972). The Georgetown Formation is generally of a lower porosity than the Edwards Group. It is commonly included within the Edwards aquifer because (1) there is no barrier to hydrologic connection between the Edwards and Georgetown, (2) karst features are at least locally developed in the Georgetown, and (3) it is difficult to separate the carbonates of the Edwards Group consistently from the carbonates of the Georgetown using the gamma-ray logs or driller's reports commonly available from the subsurface.

The thick and regionally extensive shale of the Del Rio Formation forms a significant aquitard at the top of the Edwards aquifer. This contact can be recognized reliably on almost any type of log. Locally fracture systems may allow interconnection between the Edwards aquifer

and overlying fractured or karsted carbonates; however the high clay content and plasticity of the Del Rio suggest that in most places it will function as an effective barrier to vertical flow.

## Structure

For this study, we developed three maps covering the area of the Barton Springs segment: faults and structure contour on top of the Edwards aquifer (base Del Rio) in the confined aquifer (fig. 9), faults and structure contour on the base of the Edwards aquifer (top Glen Rose) throughout the aquifer (fig. 10), and an isopach map of the Edwards aquifer (fig. 11).

The procedure for creating digital maps was designed to reduce the frequency of errors and artifacts in this structurally complex area. A table of subsurface depths to stratigraphic formation tops prepared by Nico Hauwert (unpublished digital data, 1998) was reviewed and compared with the source log data from which it was derived. Many tops were reported from driller's logs and other data sources and could not be checked. Four hydrostratigraphic units were initially isopached and the isopach maps digitized: the Georgetown, Person, and Kainer (without basal nodular member) Formations and the Walnut Formation/Basal Nodular Member. Isopachs reflect stratigraphic thickness, not a reduction in thickness as a result of normal faulting. A combination of low density of subsurface information for the lower units and apparent inconsistencies in unit identification resulted in low confidence in interpretation of isopach maps. Therefore, the digital isopachs were summed, giving a net aquifer thickness (fig. 11).

The elevation of picks (in feet, sea-level datum) was posted on a paper plot for two contacts at each subsurface data point (fig. 12). In the unconfined section, the top Glen Rose/base Edwards aquifer (Walnut/basal nodular) was mapped. In the confined section, the top Edwards aquifer (top Georgetown)/base Del Rio contact was mapped. A match line generalized from the downdip edge of the Edwards outcrop was selected to control merging of the two maps. Data density on the surface geologic map is much higher than in the subsurface. In order to increase control and assure a good match between the subsurface and surface mapping, the surface geologic mapping was used to estimate the geometry of the aquifer in the subsurface. Faults mapped at the surface were extrapolated vertically into the subsurface (fig. 7). Although we know that most Balcones faults are high angle but nonvertical, this simplification is necessary because we have little control on fault-plane dip. In addition, some refraction and possibly change in fault abundance are likely because faults intersect units with different mechanical

10

properties (Collins and Woodruff, 2001). Generalized isopach maps of map units were prepared. Then, within each fault block, the depth to the selected subsurface mapping horizon was calculated at several points from the elevation of the mapped contacts and the unit thickness. Because of the structural complexity, we elected to hand contour the resulting data using an irregular contour interval. This allows geologic intuition to be used to guide interpolation through areas with few data. In most fault blocks, regional dip was required to accommodate the mapped outcrop pattern and subsurface data, supporting a relay-ramp geometry, so this concept was used throughout the mapping. Integration of data and comparison of one structure map with another suggested some revision and downdip extension of the fault and outcrop patterns, which were modified to match the revised interpretation in ARC/EDIT.

The hand-contoured structure maps were digitized, attributed, and imported into ARC/INFO. The resulting contours for the top of the Edwards aquifer in the confined zone and the bottom of the Edwards aquifer in the unconfined zone were imported into GeoQuest CPS3 gridding software. This software was selected for its fault-handling capabilities. Several iterations of the grid were created until all fault blocks were completely populated with elevation data and artifacts removed.

We subtracted the gridded aquifer thickness map from the gridded top of the Edwards aquifer in the confined zone to create a grid for the base of the Edwards aquifer structure in the confined aquifer. This procedure is preferred over creation of two structure maps in structurally complex areas because it eliminates artifacts that impact the isopach used in the model. Thinning of the aquifer because of fault offset was not incorporated into the isopach. The impact of faults with greater than 250 ft of throw were represented as flow barriers in the model as discussed later in this paper. Grids for the base of the aquifer in the confined and unconfined zones were then merged along the merge line to create a base aquifer grid. The gridded top of the Edwards aquifer in the confined zone was merged with the grid for land surface in the unconfined zone to create a grid for the aquifer top.

Structure in the aquifer can be described in terms of a regional eastward dip created by faulting on north-northeast-trending normal faults and graben systems. Faulting impacts the flow in the aquifer by limiting cross-fault flow because of reduced aquifer thickness or enhancing fault-parallel flow through fracture zones associated with faults (Hovorka and others, 1998).

Water Levels and Regional Groundwater Flow

A generalized water-level map was developed for the Barton Springs segment of the Edwards aquifer by using water levels measured in July/August 1999 (fig. 13). This time period was chosen because it includes the largest compilation of synoptic water-level measurements. Water levels generally follow the topography and the groundwater flow direction is generally to the east in the west part of the aquifer and to the northeast in the east part of the aquifer, toward Barton Springs.

Water-level fluctuations vary throughout the aquifer. Unlike many of the aquifers in the state, such as the Ogallala aquifer, where there is a continual decline in groundwater levels in response to pumping, water levels in the Barton Springs aquifer do not show a long-term decline as a result of pumping. The Barton Springs aquifer is dynamic, and water levels generally respond to temporal variations in recharge and local areas of pumping. Although water levels decline during long periods of drought, they recover rapidly in response to recharge. Slade and others (1985) noted that maximum water-level fluctuations range from 1 to 10 ft in the west area, 10 to 50 ft in the central area, and 40 to 119 ft in the east area. Water-level fluctuations are greatest in the confined section of the aquifer.

Water levels are continuously monitored in eight wells in the study area (figs. 14, 15). A variety of factors impact the range of water levels recorded by various wells, including penetration of fractures and/or conduits and location near major pumping centers. It is difficult to compare the range in water-level fluctuations among the monitoring wells because the record lengths are quite variable. In wells with the longest monitoring record, the range in water levels was from 96 ft (58-58-123; fig. 15c) to 164 ft (58-50-216; fig. 14b). Minimal water-level fluctuations in well 58-50-411 (range 28 ft; fig. 15a) are attributed to penetration of conduits during well construction. Most of the monitoring wells demonstrate large seasonal fluctuations in water levels. Senger and Kreitler (1984) indicated that water-level fluctuations in many of the wells in the confined section of the aquifer correlated with variations in spring discharge. For example, well 58-58-301, which is just east of the bad-water line, correlated with spring discharge, indicating a hydraulic connection between the "bad-water" zone and the fresh-water aquifer. Short-term fluctuations in water levels were also recorded in several wells. Hauwert and Vickers (1994) noted that well 58-50-801 showed rises of 10 to 20 ft in response to 1- to 2-inch rainfall events in early 1992. Similarly well 58-58-123 showed an 8-ft rise in water level in

response to rain in May 1994. These large water-level fluctuations represent the movement of pressure pulses through the aquifer and indicate that the wells are hydraulically connected to the recharge area.


## Rivers, Streams, Lakes, and Springs

Five major drainage basins traverse the study area (fig. 1). The drainage basins include a catchment area where the groundwater discharges to the streams and the streams are gaining. When the streams reach the outcrop area of the Edwards, they become losing streams and recharge the aquifer. The catchment area of the streams is 264 mi$^2$, whereas the recharge zone is about 90 mi$^2$. Stream flow is recorded in nine gaging stations in the study area (figs. 16 through 24). Stream-gaging stations are located upstream and downstream of the outcrop zone on Onion Creek (fig. 25). The other creeks have gaging stations on the upstream edge of the outcrop zone. Most of the streams are ephemeral and oftentimes record no flow during the summer (July, August, September) or during winter months (December, January, February) (figs. 16 through 24).

Most flow in the aquifer discharges in Barton Springs (figs. 1, 26). The mean spring discharge is 53 cfs (1917 through 1998). Discharge ranged from 13 cfs at the end of the drought in the 1950's (1956) to 106 cfs (1992). Barton Springs consists of five major springs (Senger and Kreitler, 1985). The Main Springs consists of three springs in the pool area and constitutes about 80 percent of the discharge; Concession Springs, just north of the pool, and Old Mills Springs discharge from a small pool downstream from Main Springs on the south bank of Barton Creek. Cold Springs, located northwest of Barton Springs, discharges into the Colorado River and is flooded by Town Lake.


## Recharge

The primary source of recharge is provided by seepage from streams crossing the outcrop area. Flow losses from the creeks are sufficient to account for groundwater discharge in springs and through wells. Five major creeks (Barton, Williamson, Slaughter, Bear, and Onion) provide most of the recharge to this area (fig. 1, table 1). The creek watersheds can be subdivided into contributing and recharge zones. The contributing zone (264 mi$^2$) is west of the recharge zone,

and the streams are gaining streams as they flow over low-permeability Glen Rose limestone. The recharge zone (90 mi$^2$) coincides with the outcrop area of the Edwards aquifer, where the streams become losing streams. About 15 percent of the total recharge also occurs in interstream regions, where rainfall infiltrates the soil (Slade and others, 1985).

Calculation of stream recharge was described in detail by Barrett and Charbeneau (1996) and Slade and others (1985). Procedures developed in these earlier studies were followed in this study. Hourly flow records from gaging stations located upstream and downstream of the recharge zone were downloaded from the U.S. Geological Survey Web site (http:\\tx.usgs.gov). Recharge was calculated by subtracting daily average flow downstream of the recharge zone from that upstream of the recharge zone for Onion Creek. With the exception of Barton Creek, recharge increases linearly with flow in the upstream gaging station until a threshold flow is exceeded. These threshold values were determined by Slade and others (1985) and were used in this study (table 1). All flow in the upstream gaging station less than the threshold value was therefore assigned to recharge. Once the threshold value was reached, recharge was assumed constant at that value. Barrett and Charbeneau (1996) calculated recharge values by using data from 1979 through 1995. These recharge calculations were extended to December 31, 1998, in this study. Surface runoff from interstream areas to streams in the recharge zone was ignored in the recharge calculations because such runoff generally only occurs during very large storms, when recharge is already maximized. In the case of Barton Creek, the downstream gaging station is located within the recharge zone; therefore, recharge from this creek may be underestimated. A new gaging station was installed 110 ft upstream of Barton Springs on October 1, 1998, and a low-flow rating curve was developed for this station (Mike Dorsey, U.S. Geological Survey, personal communication, 2000). Additional data are required to develop rating curves for higher flows. Various relationships were used to assign recharge to Barton Creek. For low flows ($\leq$ 30 cfs in Lost Creek), recharge is equal to stream loss. Between 30 and 250 cfs, a quadratic relationship developed by Barrett and Charbeneau (1996) was used. Flows greater than 250 cfs were assigned this value for recharge because this was the highest measured recharge. Average annual recharge was calculated for the 20-yr period (1979 through 1998). The percentage of total recharge represented by each creek is similar to values found by Barrett and Charbeneau (1996) (table 2). Diffuse interstream recharge was assumed to equal 15 percent of total recharge on the basis of studies conducted by Barrett and Charbeneau (1996) and is similar to the estimate provided by Slade and others (1985).

<center>Hydraulic Properties</center>

Although hydraulic property data from aquifer tests are not very useful in estimating zonal properties for equivalent porous media models, information on hydraulic properties from the literature was compiled to estimate the range in measured hydraulic parameters. On the basis of aquifer tests in the Edwards and associated limestones in Travis County (north of the Colorado River), Brune and Duffin (1983) reported a range of transmissivities from 400 to 300,000 gal/d/ft (53.6 to 40,200 $ft^2$/d). Senger and Kreitler (1984) calculated transmissivity using recession-curve analyses from wells near Barton Springs. Values range from 0.1 $m^2$/s (93,000 $ft^2$/d) to 0.4 $m^2$/s (372,003 $ft^2$/d).

To determine a range of values of hydraulic properties in the BSEACD, aquifer-test reports and analyses were compiled. Aquifer tests are required as part of the application process for commercial and public water-supply wells in the Barton Springs Edwards Aquifer Conservation District. Data from 24 aquifer tests conducted within the study area from 1982 through 2001 were compiled. Several hydraulic conductivity values, or a range of values, were averaged for each aquifer test. Hydraulic conductivity values range from 0.40 to 75.3 ft/d. Hydraulic conductivity values appear to be log-normally distributed, although the limited number of data may not adequately define the distribution (fig.27). The geometric mean hydraulic conductivity is 0.6 ft/d (table 3).

Brune and Duffin (1983) estimated the range of specific yield to be 0.04 to 0.06 and specific storage to be 0.00025 to 0.00045 $ft^{-1}$. Senger and Kreitler (1984) estimated storativities using recession-curve analyses from wells near Barton Springs. Values range from 0.001 to 0.023. Slade and others (1985) calculated a mean specific yield of 0.017 and estimated the storativity (0.00003 to 0.00006 $ft^{-1}$) taken from aquifer compressibility analyses by Maclay and Small (1984). Specific yield and storativity values were estimated for 10 of the 24 aquifer tests compiled from the study area. Specific yield ranged from 0.005 to 0.06 (n=5), and storativity ranged from $1 \times 10^{-6}$ to $2.9 \times 10^{-2}$ $ft^{-1}$ (n=5).


<center>Discharge</center>

Groundwater discharge occurs primarily at Barton Springs, which consists of a series of springs in the Barton Springs Pool area in Barton Creek close to where it enters the Colorado River. Barton Springs discharge is calculated from a rating curve that relates water levels in well

<center>15</center>

YD-58-42-903 to spring discharge. Discharge at Barton Springs was highly erratic during the winter and spring of 1992, as a result of a large flood in December 1991. Barton Springs Pool was drained for repairs as a result of the flood (Barrett and Charbeneau, 1996). The lower water level in the pool resulted in underestimation of spring discharge because of its effect on the water level in the well used to estimate spring discharge. During the spring of 1992, several large storms caused the pool to fill, resulting in large increases in estimated spring discharge. Although a separate rating curve has been developed for periods when the pool is empty (Slade, personal communication, 2001), the reported decrease in spring discharge is questionable. Accurate discharge estimates are available from when the pool was refilled in the summer of 1992. Long-term discharge at Barton Springs is 53 cfs (1918 through 1999). Cold Springs, northwest of Barton Springs, discharges into the Colorado River but is not gaged because it is flooded by Town Lake. A limited number of flow data are available from Cold Springs. Discharge from Cold Springs of 3.7 cfs was measured on 8/10/1918 when discharge at Barton Springs was 14 to 15 cfs (N. Hauwert, BSEACD, personal communication, 2000), suggesting that discharge at Cold Springs is about 25 percent of that at Barton Springs. This value is considered the most accurate total measurement of flow at Cold Springs. Other measurements, considered partial measurements for Cold Springs, indicate that flow at Cold Springs ranges from 3 to 4 cfs when the corresponding flow at Barton Springs ranges from 14 to 84 cfs. These data suggest that discharge at Cold Springs may be as low as 4 percent of the discharge at Barton Springs.

Groundwater is also discharged through pumping wells. Monthly pumpage data are collected by the BSEACD and are available from 1989 through present. Pumpage data are also available from the Texas Water Development Board (TWDB); however, the data from the BSEACD are considered more reliable for later years because the district requires discharge reporting and meters have been installed in a number of wells, whereas the TWDB reporting is voluntary. The number of reported users ranged from 100 in 1989 to 142 in 1998 (table 4). The location of the major pumping areas is shown in fig. 28. Values for unreported pumpage were calculated from countywide estimates obtained from the TWDB and percentage of the county in the study area (~ 5%). This pumpage was uniformly distributed among all the active cells in the model. Annual pumpage ranged from 3.9 cfs (1990, 1991) to 6.3 cfs (1998). The years with lowest pumpage (1991 and 1992) correspond to years with highest precipitation. Annual pumpage ranges from 3 percent (1991, 1992) to 138 percent (1996) of recharge (table 4).

Other potential discharge areas include subsurface flow from the Edwards to other underlying aquifers (that is, the Glenrose Limestone); however, Slade and others (1985) concluded that such flow is negligible.

## CONCEPTUAL MODEL OF GROUNDWATER FLOW

Development of a conceptual model of groundwater flow is a prerequisite for numerical modeling of any aquifer. This conceptual model describes our understanding of how the aquifer works. Precipitation falling on the contributing zone generally moves into streams, which recharge the aquifer as they traverse the outcrop. There are five major stream drainages in the study area. Recharge increases linearly with stream flow to a threshold stream flow and remains uniform after further increases in stream flow. Approximately 15 percent of the recharge in the study area results from infiltration of precipitation on the outcrop. Groundwater generally flows from areas of higher to lower topography (west to east) in the west part of the aquifer and then flows north in the east part of the aquifer toward Barton Springs and Cold Springs. Most of the aquifer discharges to the springs. Discharge to wells represents about 10 percent of long-term average discharge at Barton Springs. The aquifer is unconfined in the outcrop zone and in the adjacent area, where the Edwards limestone is overlain by the Del Rio Clay. Farther to the east the aquifer is confined (fig. 1). The east boundary of the region is marked by the bad-water line, where the TDS of the water exceeds 1,000 mg/L. The aquifer is dynamic and responds rapidly to recharge events. This rapid response is attributed to the high degree of karstification, as evidenced by caves. Additional evidence of karstification is provided by the results of dye tracer tests, which indicate that water travels long distances within hours.Groundwater levels fluctuate to as much as 90 ft in some areas. Because of the dynamic nature of the aquifer, it will also respond quickly to drought conditions, and flow at Barton Springs could decrease rapidly in response to severe droughts. The aquifer should recover fairly rapidly after drought, however, and cumulative effects of drought should be negligible.

## MODEL DESIGN

Model design includes information on the code and processor, aquifer discretization, and model parameter assignment.

## Code and Processor

MODFLOW-96 (Harbaugh and McDonald, 1996), a modular finite-difference groundwater flow code developed by the U.S. Geological Survey, was used for the simulations. This code was chosen because (1) it is the most widely used and tested code for groundwater resource evaluation, (2) it is well documented (McDonald and Harbaugh, 1988), and (3) it is in the public domain. A variety of pre- and postprocessors have been developed to facilitate data entry and allow analysis of model output. In this study we used the Processing MODFLOW for Windows (PMWIN) version 5.0.54 (Chiang and Kinzelbach, 1998). The model was run on Dell Latitude with a  Pentium II Processor and 64 MB RAM running Windows NT.

## Grid

The model consists of 1 layer that has 120 rows and 120 columns and a total of 14,400 cells. The cell size was chosen to be small enough to reflect the availability of input data, to provide appropriate details in the output, and to be manageable. Model rows were aligned parallel to the strike of the Edwards; the grid was therefore rotated 45° from horizontal. Rectangular cells were 1,000 ft long parallel to the strike of the faults and 500 ft wide (fig. 29). This discretization is much finer than that previously used by Slade and others (1985; minimum cell spacing was 1,500 ft). The zone of active cells was defined on the basis of the hydrologic boundaries as described previously. The north boundary is the Colorado River. The east boundary is the bad-water line that was obtained from the BSEACD. The south boundary is a hydrologic divide located along Onion Creek in the Edwards aquifer recharge zone and between the cities of Buda and Kyle in the confined part of the aquifer, as determined by Stein (1995). The west boundary is the Mount Bonnell fault, which acts as a hydrologic (no-flow) barrier (Senger and Kreitler, 1984). Cells with layer thickness of less than 20 ft were assigned as inactive. Cells outside the model area were made inactive, resulting in 7,043 active cells.

## Model Parameters

Model parameters include (1) elevations of the top and bottom of the layer, (2) horizontal hydraulic conductivity, (3) specific yield, and (4) specific storage. Specific yield and specific storage are required only for the transient simulations.

The structure of the top of the aquifer was based on ground-surface elevation in the unconfined recharge zone. A digital elevation map of the ground surface was downloaded from the U.S. Geological Survey Web site. East of the outcrop zone, the top of the aquifer corresponds to the base of the Del Rio Clay. The base of the aquifer corresponds to the base of the Walnut Formation, determined from recent studies by Small and others (1996). The location of faults was also based on interpretations by Small and others (1996). The contoured structure surfaces and faults were digitized and gridded using CPS3 for input to the model. Structure surfaces were interpolated to model cell centers using GIS software (ARC/INFO).

The model layer was assigned as confined/unconfined. The model was set up to calculate transmissivity and storativity on the basis of saturated thickness. The length unit was feet, and the time unit was days for all model input. Initial head for the steady-state simulations was the top of the aquifer.


MODEL BOUNDARIES

We assigned model boundaries for (1) recharge, (2) pumping, (3) springs, and (4) initial conditions. Recharge values were assigned to stream cells on the basis of analysis of flow losses in the streams. Recharge was uniformly distributed in each stream where the stream intersects the outcrop. Interstream recharge was 15 percent of the total stream recharge and was assigned to all active cells.

Pumping was assigned to cells on the basis of the location of pumping wells reported to the BSEACD. Unreported domestic (rural) pumpage was calculated from countywide estimates and was assigned to all active cells.

We used the Drain Package of MODFLOW to represent Barton Springs and Cold Springs. The drain elevation is the spring elevation (432 ft for Barton Springs and 430 ft for Cold Springs), and a high drain conductance value was used (1,000,000 $ft^2$/d) to allow unrestricted discharge of water.


Modeling Approach

Three basic steps were followed in modeling the aquifer: (1) a steady-state model was developed to determine the spatial distribution of hydraulic conductivity, (2) a transient model

was run for a 10-yr period (1989 through 1998) by using monthly recharge and pumpage, and (3) a predictive model was developed to evaluate effects of increased pumpage and potential future droughts on groundwater availability. The steady-state model was developed because it is much more readily calibrated (because specific yield or storage coefficient data are not required) and the simulations run much faster. The calibration process involved matching simulated and measured water levels. Water levels measured during July/August 1999 were used for the steady-state calibration because spring discharge (66 cfs) was close to average conditions (53 cfs) during this time and water levels measured during this time represent the most extensive survey conducted in the aquifer. Trial and error and automated procedures were used to estimate the zonal distribution of hydraulic conductivity during model calibration. Sensitivity analyses were conducted to assess the impact of varying recharge and hydraulic properties on the model results. We quantified the calibration, or goodness of fit between the simulated and measured water-level values, using the root mean square (RMS) error, where $n$ is the number of calibration points, $h_m$ is the measured hydraulic head at point $i$, and $h_s$ is the simulated hydraulic head at point $i$.

$$RMS = \left[ \frac{1}{n} \sum_{i=1}^{n} (h_m - h_s)_i^2 \right]^{0.5}$$

(1)

The framework of the steady-state model was used to develop a transient model for the years 1989 through 1998, using monthly time steps. The zonal distribution of hydraulic conductivity developed from the calibrated steady-state model was used in the transient model. Hydraulic heads simulated in the steady-state model were used as input to the transient model. The 10-yr time period was chosen because pumpage records were only available for this time period, detailed synoptic water levels were measured during this time, transient water-level monitoring records correspond to this time period, and this record includes a range of hydrologic conditions from dry (1996 drought) to wet (1991, 1992). Very little calibration was required for the transient model.

The transient model was then used to predict how water levels and spring discharge might change during the next 50 yr in response to increases in pumping and potential future droughts.

STEADY-STATE MODEL

Calibration

Measured water levels in July and August (1999) were used to evaluate the steady-state model calibration because the number of measured water levels (99) was greatest for this time and spring discharge was close to average conditions (~ 66 cfs). The spatial distribution of recharge among the streams and in the interstream settings was based on the average recharge for a 20-yr record (1979 through 1998; table 2). The total amount of recharge was reduced to equal the average spring discharge for Barton and Cold Springs of 55 cfs and pumpage for 1989 of 5 cfs. Recharge was assumed to be known and was not changed during calibration. The distribution of hydraulic conductivity was estimated using a combination of trial and error and automated inverse approaches. The trial-and-error calibration involved the following steps:

- Horizontal hydraulic conductivity was adjusted during successive steady-state runs. Initial simulations used a uniform distribution of hydraulic conductivity that ranged from 5 to 50 ft d$^{-1}$.

- The next set of simulations used a zonal distribution of hydraulic conductivity, with conductivities ranging from 5 to 40 ft d$^{-1}$ in the recharge zone and 200 ft d$^{-1}$ outside the recharge zone. A zone of high conductivity (~ 1,000 ft d$^{-1}$) was then set adjacent to Barton Springs. Either the simulations did not converge or the simulated heads were much too high.

- We then imported the spatial distribution of hydraulic conductivities used by Slade and others (1985); however, almost the entire model region went dry when these conductivity values were used.

- We simulated faults with the greatest amount of offset as horizontal flow barriers (Hsieh and Freckleton, 1993). Input data required for this module include the hydraulic conductivity divided by the aquifer thickness; values of 0.01 d$^{-1}$ (southwest fault) and 0.05 d$^{-1}$ (other faults) were used in the simulations. Three faults were used in the simulations.

- The final approach that was used to achieve a calibrated model involved increasing the complexity of the hydraulic conductivity distribution from the

simple three-zone model based on calibrated hydraulic conductivities determined by Slade and others (1985) and variations in the hydraulic gradient. Steep hydraulic gradients in the southwest part of the model suggested low hydraulic conductivities, and shallow hydraulic gradients near Barton Springs suggested high hydraulic conductivities. The structure of the base of the aquifer was adjusted in some of the steady-state simulations to achieve convergence.

The results of the trial-and-error calibration indicated that there are 10 zones of hydraulic conductivity that range from 1 to 1,000 ft/d. Monthly pumpage at 1989 rates was also included in the final steady-state model and represents approximately 6 percent of the discharge at Barton Springs. Including this amount of pumpage did not significantly alter water levels or spring discharge in the model.

The results of the trial-and-error calibration generally reproduced the spatial distribution of water levels. Comparison of measured and simulated water levels resulted in an RMS error of 35 ft. The RMS error indicates that, on average, the simulated water levels differ from the measured water levels by about 35 ft. We also evaluated the use of automated inverse modeling to estimate the zonal distribution of hydraulic conductivity. Initial attempts to use automated inverse modeling in the early stages of calibration suggested that this procedure could not be used to determine reasonable values of hydraulic conductivity. Once the trial-and-error calibration was completed, we wanted to determine whether automated procedures could further improve the calibration and reduce the RMS error. The automated inverse code UCODE (Poeter and Hill, 1998) was used for this process. The hydraulic conductivity estimates from the trial-and-error calibration were used as initial estimates of the zonal hydraulic conductivity for UCODE. Log transformation of the hydraulic conductivity was used. Initially all 10 zones were included in the automated fitting; however, best results were obtained when only 4 of the 10 zones were fitted. Use of automated inversion reduced the RMS error to 24 ft. This error represents 7 percent of the total head drop across the model. The primary difference between the trial-and-error and automated zonal hydraulic conductivity estimates was in the confined section to the southeast, where hydraulic conductivity was increased from 1 to 39 ft/d. The final distribution of hydraulic conductivity is shown in fig. 30. The steady-state model generally reproduced the potentiometric surface developed from water-level measurements in July/August 1999 (fig. 31). The scatter plot of simulated versus measured heads indicates that there is very little bias in the simulation results (fig. 32). The RMS error reflects both uncertainties in

22

measured and simulated hydraulic heads. The heads were measured over a 2-mo period. Synoptic water-level measurements over a 2-mo period is generally considered very short for most porous media aquifers but is fairly long for this karst aquifer, which is dynamic, and spring discharge decreased from 80 to 60 cfs during this time.Therefore, the measured heads may not reflect the average discharge of Barton Springs (~53 cfs).  Most of the head data were based on well locations and elevations obtained from 1:250,000 topographic maps, whereas some head data were based on global positioning system measurements. Errors were generally low throughout the model area with the exception of the southwest area, where heads are underpredicted by up to 60 ft (fig. 33). Simulated discharge was 52 cfs at Barton Springs, 2.8 cfs at Cold Springs, and 5 cfs from pumping wells.

Sensitivity Analysis

Once the steady-state model was calibrated, the sensitivity of water levels in the model to different aquifer parameters was evaluated. Sensitivity analysis quantifies the uncertainty of the calibrated model to uncertainty in the estimates of the aquifer parameters, stresses, and boundary conditions (Anderson and Woessner, 1992, p. 246). Sensitivity analysis is used to evaluate the nonuniqueness of the calibrated model. The hydrologic parameters that have the greatest impact on simulated water levels and spring discharge can be identified through sensitivity analyses.

Sensitivity analyses were conducted on hydraulic conductivity, recharge, spring conductance, and pumpage. Each parameter was varied systematically, and the change in simulated water levels from the base case was calculated (1) at the location of the calibration wells and (2) in each active cell in the model. Any bias in the sensitivity analysis and the calibration between the calibration points and the entire model layer could be identified by comparing the results at the well locations and the active cells. The change in water levels was quantified by calculating the mean difference:

$$MD = \frac{1}{n} \sum_{i=1}^{n} \left( h_{sen} - h_{cal} \right)$$

(2)

where $n$ is the number of points, $h_{sen}$ is the simulated water level for the sensitivity analysis, and $h_{cal}$ is the calibrated water level. Positive values indicate that simulated water levels are higher than calibrated values, and negative values indicate that simulated water levels are lower than calibrated values.

Simulated water levels in the model were most sensitive to recharge and hydraulic conductivity and insensitive to pumpage and drain conductance (fig. 34). The mean differences calculated at the calibration locations and at each active cell in the model are similar, indicating that the calibration points probably do not bias the sensitivity analysis and represent the aquifer well. Higher values of recharge resulted in higher simulated water levels. The model failed to converge for reductions in recharge of 25 and 50 percent of the calibrated value. Higher values of hydraulic conductivity resulted in lower simulated water levels, whereas lower values of hydraulic conductivity resulted in higher water levels. The sensitivity to hydraulic conductivity was slightly asymmetric in that the simulated water levels were more sensitive to lower than to higher hydraulic conductivities.

## TRANSIENT MODEL

Simulated heads and the calibrated distribution of horizontal hydraulic conductivity from the steady-state model were used as input for the 10-yr transient model, which was from 1989 through 1998. Annual precipitation during this time ranged from 26 inches in 1989 to 52 inches in 1991 (fig. 35; table 4). Monthly stress periods were used for the transient simulations, with 12 time steps in each stress period. This setup resulted in a total of 120 stress periods for the 10-yr simulation (1989 through 1998). A stress period is a time interval in MODFLOW during which all inflow, outflow, properties, and boundary conditions are constant. Recharge and pumpage were changed for each stress period (fig. 35a, b). Recharge rates were estimated from stream-loss studies, as discussed previously. Annual recharge was highest in 1992 (169 cfs) and lowest in 1996 (4 cfs) (table 4). Monthly recharge was much more variable and ranged from 0.3 to 500 cfs (fig. 35b). Pumpage was assigned on the basis of data from the BSEACD. Annual pumpage ranged from 3.9 cfs (1990, 1991) to 6.3 cfs (1998) (table 4). Because recharge varied greatly from year to year, the percentage of recharge represented by pumpage varies from 3 percent during 1991 and 1992 to 138 percent during 1996. Initial estimates of specific yield (0.005) and specific storage ($5 \times 10^{-5}$ ft$^{-1}$) were based on data from Slade and others (1985).

Initial transient simulations did not converge because of cells near the west-central portion, in which the simulated hydraulic head oscillated between iterations. These cells were located in a zone where the base of the Edwards aquifer was much higher than surrounding areas. By lowering the base of some of these cells to values similar to those in adjacent areas, we

24

achieved convergence. This lowering assumes that the underlying Glen Rose Formation is locally permeable and connected to the Edwards aquifer.

The transient simulation was evaluated using three different criteria: (1) Simulated and measured spring discharge were compared (figs. 36, 37). (2) Simulated hydraulic heads were compared with hydrographs for eight monitoring wells (figs. 38 and 39). (3) Scatter plots were developed for simulated and measured heads during low (1994, 1996) and moderately high (1998) flow conditions (fig. 40).

Generally good agreement was obtained between measured and simulated discharge at Barton Springs (figs. 36, 37). Simulated discharge at Barton Springs was calculated by subtracting discharge at Cold Springs (6 percent of total discharge) from total discharge listed in the output file. The RMS error between measured and simulated discharge for the distributed model is 12 cfs, which represents 11 percent of the discharge fluctuations measured at Barton Springs during that time. Data from an 8-mo period, December 1991 through July 1993, were omitted from the error calculations because of uncertainties related to the measured discharge data as a result of flooding. One of the main objectives of the model is to accurately simulate low flows in Barton Springs. The scatter plot suggests that on average there is no bias in the results (fig. 37); however, this plot masks underpredictions and overpredictions at different times. Overprediction of low spring flows in 1989 and early 1990 is attributed to the initial conditions (hydraulic head from steady-state model) not being in equilibrium with the boundary conditions (recharge and discharge) for the transient simulation. Good correspondence between measured and simulated discharge was found for 1990 through1991. Simulated spring discharge generally underestimates measured discharge during the 1994 low flow period; however, both measured and simulated discharges have the same minimum value. In contrast, simulated discharge overestimates measured discharge during the 1996 low flow period. The slope of the simulated recession is more gradual than that of the measured recession, which is U shaped, and the timing of the minimum simulated discharge is later than that of the measured data. Peak discharges are underestimated in some cases (1990 through 1991), simulated accurately in other cases (1989, 1993, 1995), and overestimated in other cases (1991 - 1992, 1997, 1998). During high flows, some of the discharge may be diverted to an ungaged spring and other smaller springs along Barton Creek, which is unaccounted for in the model.

The transient model generally reproduces water levels monitored continuously in many of the continuously monitored water levels (figs. 38, 39). Water levels in the north part of the

aquifer are reproduced more accurately than those to the south. The RMS error ranged from 3.8 ft (58-42-8TW) to 31 ft (58-50-221) in the four wells in the north, and these errors represent 16 to 63 percent of the range in water-level fluctuations. RMS errors increase in wells to the south and range from 37.5 ft (58-50-411) to 83.7 ft (58-58-123). Because well 58-50-411 is located adjacent to a cave (N. Hauwert, BSEACD, personal communication, 2000), its water levels remain fairly constant. These water levels are not reproduced in the simulation, which cannot represent flow in caves.

Scatter plots between measured and simulated water levels were developed for different times during the transient simulation (fig. 40). The scatter plot for March/April 1994 shows that the model generally simulated the water levels during low-flow conditions (fig. 40a). The RMS error of 29 ft represents 11 percent of the head drop in the model area. Comparison of measured and simulated water levels for July and August 1996 (fig. 40b) indicates that simulated water levels underestimate measured water levels by 37 ft (10 percent of the head drop across the model area) on average for this low-flow period. It is difficult to compare measured and simulated water levels during high flow periods because spring discharge is generally changing rapidly and synoptic water-level measurements over 2-mo time periods generally span large changes in spring discharge. The scatter plot for July and August 1998 generally represents the end of the transient simulation (fig. 40c). The RMS error of 64 ft (22 percent of the head drop in the model) is much higher than the other RMS errors and is attributed, in part, to the dynamic nature of the aquifer during high flow conditions. In general, the model provides reasonable simulations of water levels for different times.

Sensitivity analyses were conducted to assess the impact of varying groundwater recharge, pumpage, specific yield, and specific storage on simulated spring discharge and water levels in monitoring wells (figs. 41 through 45). In many cases, we could not evaluate the effect of reducing the various parameters by 50 percent because the simulations did not converge in most cases. Therefore, the evaluation is limited to the range of −10 to + 50 percent. Groundwater recharge had the greatest impact on spring discharge and water levels in monitoring wells. Increasing recharge by 50 percent resulted in increasing the mean spring discharge by about the same amount (table 5; fig. 41a). Increasing recharge had a greater impact on high spring flows than on low flows, and spring discharge was more variable, as shown by the range and coefficient of variation of spring discharge (table 5). Simulated water levels in monitoring wells displayed a similar response to variations in recharge as spring discharge (fig. 42). Decreasing

recharge had the opposite effect of increasing recharge. Simulated spring discharge and water levels in wells were much less sensitive to variations in pumpage, specific yield, and specific storage (figs. 41b, c, d; 43, 44, 45; table 5). Increasing pumpage by 50 percent had a negligible effect on spring discharge and water levels in wells. Increasing specific yield and specific storage by 50 percent resulted in 1.6 and 0.7 percent increase in mean spring discharge, respectively, compared with 50 percent increase in response to recharge. Uncertainties in specific storage are greater than those of specific yield; therefore, an additional simulation was conducted to evaluate the impact of varying specific storage by a factor of 10. Increasing specific storage by 10 decreased the mean spring discharge slightly but greatly reduced the range in spring discharge (table 5). The increased specific storage does not simulate the low spring discharges which are critical for groundwater manaagement. Increasing specific storage by 10 had a similar effect on the simulated water levels in the monitoring wells, which better replicate the measured water-level fluctuations in the monitoring wells (fig. 45). However, the emphasis of the study on simulating low spring discharges over accurately simulating water levels in monitoring wells precludes using the higher specific storage in the final simulations.

## PREDICTIONS

The calibrated model was used to evaluate the future availability of groundwater in the Barton Springs segment of the Edwards aquifer under average recharge and drought-of-record conditions. Senate Bill 1 requires water planning under drought-of-record conditions to ensure that future water needs are met during times of severe drought. The drought of record was evaluated for the study area.

### Future Pumpage

The future simulations were initiated with pumpage data from BSEACD for 2000. Estimates of future groundwater demands were based on demand numbers from the Regional Water Planning Group (Region K). Future pumpage was estimated on the basis of projections made by the Region K Water Planning Group and the Capital Area Metropolitan Planning Organization (CAMPO). Estimates of future population and water usage have been made by these groups for cities and counties in and around the District; however, none of these

projections could be applied directly to the District. On the basis of estimated total pumpage in the District (permitted and exempt wells), a multiplier of 2.1 was used to calculate pumpage in 2050 from current pumpage (2000). This multiplier is higher than estimates for rural areas, but lower than for towns. Starting with current (year 2001) total pumpage of 6,754 acre-ft/yr (equivalent to 9.3 cfs), pumpage in 2050 was estimated to be 14,183 acre-ft/yr (19.6 cfs). Monthly pumpage used in the future simulations was linearly interpolated between 2001 and 2050. The regional planning groups included the implementation of conservation measures as a part of projected water usage but did not consider substitution of surface water for groundwater. Because we do not have any information on the seasonal distribution of pumpage, we used the monthly data from the transient simulation from 1989 through 1998 and simply multiplied by the factors required to increase the annual pumpage to the values for 2001 through 2050.

Drought of Record

A drought of record is the most severe drought during the period of record in terms of duration and lack of rainfall. The drought of record for the study area occurred between 1950 and 1956 according to the 140-yr record of precipitation (1860 through 2000) (fig. 46). Precipitation ranged from 25.8 inches in 1950 to 11.4 inches in 1954. The mean annual precipitation during the 7-yr drought period (23.1 inches) was about two-thirds of the long-term annual precipitation (33.5 inches). The mean annual precipitation during the last 3 yr of the drought (16.5 inches) was about half the long-term average precipitation.

We tried to estimate the recharge that would correspond to the 1950's drought by relating precipitation to recharge for the period of record (1989 through 1998), but the relationship was very poor. We then tried to relate recharge to Barton Springs discharge for the same period, but the scatter plot indicated very poor relationships. Comparison of the time series nevertheless suggested a much stronger relationship, with some lag between recharge and discharge. Therefore, we finally decided to assume that recharge equals discharge, although doing so may slightly overestimate recharge during low recharge conditions because it might include discharge from storage in the aquifer. Annual discharge values for Barton Springs were obtained from Slade and others (1986) for the period 1950 through 1956 (fig. 26) and were increased by 5 percent to account for discharge from Cold Springs. Recharge for normal climatic conditions was based on long-term average discharge at Barton Springs and Cold Springs of about 55 cfs. The

monthly distribution of recharge from the transient simulation (1989 through 1998) was used for the future simulations of drought conditions, and these values were reduced to average recharge of 55 cfs for the first 3 yr and reduced by the amount required to obtain the recharge for the 1950's drought for the remaining 7 yr. Future simulations of average recharge (55 cfs) with increased pumpage used evenly distributed recharge for each month of the year and not the seasonal distribution from the transient simulation from 1989 through 1998. The latter approach was used because the simulated potentiometric surfaces from future simulations with the seasonal distribution of recharge varied markedly, making it difficult to estimate drawdowns when comparing different potentiometric surfaces. The baseline potentiometric surface was developed by simulating average recharge (55 cfs) evenly distributed throughout the year and current pumpage conditions (2000) (fig. 47).

Predicted Groundwater Availability

Predictive simulations were conducted with the calibrated model: baseline run with average recharge (55 cfs) evenly distributed throughout the year and future pumpage for each 10-yr period (2001 through 2010; 2011 through 2020; 2021 through 2030; 2031 through 2040; 2041 through 2050); simulations with future pumpage and drought conditions for each 10-yr period (3 yr of average recharge followed by 7 yr of drought) (Table 6).

We calculated the water-level declines at the end of the first and last decades (2010 and 2050) by subtracting the predicted water levels at the end of these decades from the baseline water levels. The predictive simulations indicate that water-level declines in response to increased groundwater pumpage are small: ≤ 5 ft in 2010 and ≤ 35 ft in 2050 (figs. 48a, 49a). In contrast, water-level declines in response to increased pumpage and drought-of-record conditions were much greater: ≤ 200 ft in 2010 and ≤270 ft in 2050 (figs. 48b, 49b). These results are consistent with the sensitivity analyses for the transient simulation, which indicate that the model is much more sensitive to recharge than to pumpage.

Average discharge at Barton Springs in response to average recharge and current pumpage (9 cfs) is about 43 cfs (fig. 50a). The sum of discharge at Barton Springs (43 cfs), Cold Springs (3 cfs), and pumpage (9 cfs) equals the average recharge of 55 cfs. The model predicts that Barton Springs discharge will decrease to 41 cfs in 2010 and to 33 cfs in 2050, which is directly proportional to increased pumpage (~ 2 cfs per decade and 10 cfs over 50 yr). The model

predicts that spring discharge should decline much more in response to potential drought-of-record conditions. Predicted spring discharge at the end of 2010 is 7.5 cfs and 0 cfs in 2050 under drought-of-record conditions (fig. 50b). The results for spring discharge are similar to those for water levels and emphasize the significance of recharge and potential droughts in controlling water availability in the future.

## MODEL LIMITATIONS

All numerical groundwater models are simplifications of the real system and therefore have limitations. Limitations generally result from assumptions used to develop the model, limitations in the input data, and the scale at which the model can be applied.

Use of a distributed, porous media model to simulate flow in a karst system is a simplification, and the model will not be able to simulate some aspects of flow accurately in this system, particularly the effects of conduits on groundwater flow. This simplification is not critical for water-resources management, and the study showed that the model was able to predict variations in spring flow over time, as well as fluctuations in water levels in monitoring wells. However, this model was not able to simulate very low water-level fluctuations in one of the monitoring wells that was located adjacent to a cave. The model will not be able to simulate traveltimes for contaminants in the system and should not be used for this purpose. The bad-water line to the east was simulated as a no-flow line. This representation may not be entirely accurate, particularly during low flow periods when low gradients may induce flow from the east. Further studies should evaluate this process. The current model did not include the underlying Glen Rose Limestone, which in some areas may be sufficiently permeable and may contribute to flow in the Edwards aquifer.

There are also limitations associated with input data. Recharge data for this model are generally considered much more accurate than are available for many other regions. Stream recharge was distributed uniformly along the outcrop areas because of lack of information on spatial focusing of recharge in particular locations. This assumption may affect flow to Cold Springs because the line of recharge along Williamson Creek generally forms a divide, minimizing flow south of this creek to Cold Springs. Future studies should spatially distribute recharge along the streams. Because recharge data are not available for the 1950's drought, we approximated recharge during this time by assuming that recharge equals discharge. More

studies should be conducted to develop better estimates of recharge during this time. Water-level data for drawing potentiometric surfaces may affect our evaluation of the goodness of fit of the model because comparisons of simulated and measured water levels are restricted to areas where water levels have been measured.

The model also predicts drying in certain zones, such as in the south-central region.Such dry zones may be an artifact of the model as a result of steep gradients in the base of the Edwards and may or may not be realized in the future. Such drying may also depend on the conductivity of the underlying Glen Rose and the hydraulic connectivity of the units at the base of the Edwards units. The model also predicted unrealistically high water levels in the western fringe of the model, particularly in the southwest region. Overestimation of water levels in this zone may result from the aquifer being very thin in this region, and future modeling studies should evaluate whether this region should be included in the model. The high water levels may also be an artifact of the uniform distribution of recharge along streams in the model. This situation should also be evaluated in future studies.

This model was developed to evaluate variations in spring discharge and aquiferwide water-level declines over the next 50 yr. The model is not considered appropriate for local issues, such as water-level declines surrounding individual wells, because of the coarse grid size (500 × 1,000 ft) and limitations described earlier.

CONCLUSIONS

The Edwards aquifer is a critical source of water to about 45,000 residents in Travis and Hays Counties. We developed a numerical groundwater flow model for the Barton Springs segment of the Edwards aquifer to predict water levels and spring discharge under future pumping and potential future drought conditions. The model has 1 layer and 7,043 active cells and incorporates recent information on the geology and hydrology of the Edwards aquifer in this region. Recharge to the system was calculated by using stream-gage data. A steady-state model was calibrated to determine the distribution of hydraulic conductivity in the model, and a transient model simulated flow for a 10-yr period from 1989 through 1998. Future simulations included various projected pumpage scenarios and 3 yr of average recharge, followed by 7 yr of drought conditions similar to that of the 1950's drought.

Good agreement was found between measured and simulated water levels for the steady-state model (RMS error is 24 ft, 7 percent of the hydraulic head drop across the study area). The steady-state model predicted that 6 percent of the discharge was through Cold Springs and the remainder through Barton Springs. The transient simulation generally reproduced measured spring discharge for 1989 through 1998. The RMS error was 12 cfs, which represents 11 percent of the discharge fluctuations measured at Barton Springs during that time.

To assess the future availability of groundwater in the Barton Springs segment of the Edwards aquifer, we used the calibrated model to predict future water levels under drought-of-record conditions using estimates of future groundwater demands that were based on demand numbers from the Regional Water Planning group. The model predicts that water-level declines in response to increased pumpage under average recharge conditions are small ($\leq$35 ft), whereas water-level declines in response to increased pumpage and drought-of-record conditions are much greater ($\leq$270 ft). Declines in spring discharge in response to increased pumpage are also small and proportional to the increased pumpage ($\sim$ 10 cfs in the next 50 yr), whereas the model predicts that spring discharge will decrease to 0 in response to drought-of-record conditions by as early as 2030. The extreme sensitivity of water levels and spring discharge to recharge and drought conditions indicates that aquifer management under drought conditions should consider enhanced recharge in addition to groundwater conservation.


ACKNOWLEDGMENTS

(U.S. Geological Survey) who conducted previous modeling studies of the aquifer.  Figures were drafted by Jason West (BSEACD) and Pat Alfano (Bureau of Economic Geology).

# REFERENCES

Anderson, M. P., and W. W. Woessner, 1992, Applied groundwater modeling, simulation of flow and advective transport:  New York, Academic Press, 381 p.

Barrett, M. E., and Charbeneau, R. J., 1996, A parsimonious model for simulation of flow and transport in a karst aquifer: Technical Report Center for Research in Water Resources, Report No. 269, 149 p.

Chiang, W. H., Kinzelbach, W., and others, 1998, Aquifer simulation model for Windows—groundwater flow and transport modeling, an integrated program: Berlin, Stuttgart, Gebruder Borntraeger, ISBN 3-443-01029-3.

Collins, E. W. and Woodruff, C. M., 2001, Faults in the Austin, Texas, area—defining aspects of the local structural grain, *in* Woodruff, C. M., and Collins, E. W., trip coordinators, Austin, Texas, and beyond, geology and environment: Austin Geological Society Guidebook 21, p. 15–26.

Collins, E. W., 1996, San Antonio relay ramp; area of stratal continuity between large-displacement barrier faults of the Edwards aquifer and Balcones Fault Zone, Central Texas: Gulf Coast Association of Geological Societies Transactions, v. 46, p. 455–456

Ferrill, D. A., and Morris, A. P., 2001, Displacement gradient and deformation in normal fault systems: Journal of Structural Geology, v. 23 no. 4, p. 619–638.

Garner, L. E., and Young, Keith, 1976, Environmental geology of the Austin area: an aide to urban planning: The University of Texas at Austin, Bureau of Economic Geology Report of Investigations No. 86, 39 p.

Guyton, W. F., and Associates, 1958, Recharge to the Edwards reservoir between Kyle and Austin: report prepared for the City Water Board, San Antonio, Texas, 9 p.

Hanson, J. A., and Small, T. A., 1995, Geologic framework and hydrogeologic characteristics of the Edwards aquifer outcrop, Hays County, Texas: U.S. Geological Survey, Water-Resources Investigations Report 95-4265, 10 p. (1 sheet).

Harbaugh, A. W., and McDonald, M. G., 1996, User's documentation for MODFLOW-96, an update to the U.S. Geological Survey modular finite-difference ground-water flow model: U.S. Geological Survey Open-File Report 96-485, 56 p.

Hauwert, Nico, Hanson, John, Small, Ted, and Liang, Shu, 1997, Geologic map of the Barton Springs segment of the Edwards aquifer: Barton Springs/Edwards Aquifer Conservation

district in co-operation with the U.S. Geological Survey: unpublished ARC/INFO Geographic Information System database and map plot.

Hauwert, N., and Vickers, S., 1994, Barton Springs/Edwards aquifer hydrogeology and groundwater quality: Austin, TX, Barton Springs/Edwards Aquifer Conservation District, report prepared for Texas Water Development Board under contract no. 93483-346, 92 p.

Hovorka, S. D., 1996, High-frequency cyclicity during eustatic sea-level rise: Edwards Group of the Balcones Fault Zone: Gulf Coast Association of Geological Societies Transactions, v. 46, p. 179–184.

Hovorka, S. D., Mace, R. E., and Collins, E. W., 1998, Permeability structure of the Edwards aquifer, South Texas—implications for aquifer management: The University of Texas at Austin, Bureau of Economic Geology Report of Investigations No. 250, 55 p.

Hsieh, P. A., and Freckleton, J. R., 1993, Documentation of a computer program to simulate horizontal-flow barriers using the U.S. Geological Survey's modular three-dimensional finite-difference ground-water flow model U.S. Geological Survey, Open-File Report 92-477, 32 p.

Immenhauser, Adriana, and Scott, R. W., 1999, Global correlation of Middle Cretaceous sea-level events: Geology, v. 27, no. 6, p. 551–554.

Larkin, T. J., and Bomar, G. W., 1983, Climatic atlas of Texas: Austin, Texas, Department of Water Resources, 151 p.

Mace, R. E., Chowdhury, A. H., Anaya, R., and Way, S. C., 2000, Groundwater availability of the Trinity Aquifer, Hill Country Area, Texas: numerical simulations through 2050: Texas Water Development Board Report 353, 117 p.

Maclay, R. W., and Small, T. A., 1976, Progress report on geology of the Edwards aquifer, San Antonio area, Texas, and preliminary interpretation of borehole geophysical and laboratory data on carbonate rocks: U.S. Geological Survey Open-File Report 76-627, 65 p.

McDonald, M. G., and Harbaugh, A. W., 1988, A modular three-dimensional finite-difference ground-water flow model: U.S. Geological Survey, Techniques of Water Resources Investigations, Book 6, Chapter A1.

Moore, C. H., 1996, Anatomy of a sequence boundary—Lower Cretaceous Glen Rose/Fredericksburg, Central Texas Platform: Gulf Coast Association of Geological Societies Transactions, v. 46, p. 313–320.

Poeter, E. P., and Hill, M. C., 1998, Documentation of UCODE, a computer code for universal inverse modeling: U.S. Geological Survey Water-Resources Investigations Report 98-4080, 116 p.

Rose, P. R., 1972, Edwards Group, surface and subsurface, Central Texas: The University of Texas at Austin, Bureau of Economic Geology Report of Investigations No. 74, 198 p.

Senger, R. K., and Kreitler, C. W., 1984, Hydrogeology of the Edwards aquifer, Austin area, Central Texas: The University of Texas at Austin, Bureau of Economic Geology Report of Investigations No. 141, 35 p.

Slade, R. M., Jr., Dorsey, M. E., and others, 1986, Hydrology and water quality of the Edwards aquifer associated with Barton Springs in the Austin area, Texas: U.S. Geological Survey, Water-Resources Investigations Report 86-4036, 96 p.

Slade, R. M., Ruiz, L., and others, 1985, Simulation of the flow system of Barton Springs and associated Edwards aquifer in the Austin area, Texas: U.S. Geological Survey, Water Resources Investigations Report 85-4299, 49 p.

Small, T. A., Hanson, J. A., and Hauwert, N. M., 1996, Geologic framework and hydrogeologic characteristics of the Edwards aquifer outcrop (Barton Springs segment), northeastern Hays and southwestern Travis Counties, Texas: U.S. Geological Survey, Water-Resources Investigations WRI 96-4306, 15 p. (1 sheet).

Stein, W. G., 1995, Edwards aquifer ground-water divides assessment, San Antonio region, Texas: Edwards Underground Water District Report 95-01 prepared by LBG-Guyton Associates, variously paginated.

Trescott, P. C., Pinder, G. F., and others, 1976, Finite-difference model for aquifer simulation in two dimensions with results of numerical experiments: U.S. Geological Survey, Techniques of Water Resources Investigations, Book 7, Chapter C1, 116 p.
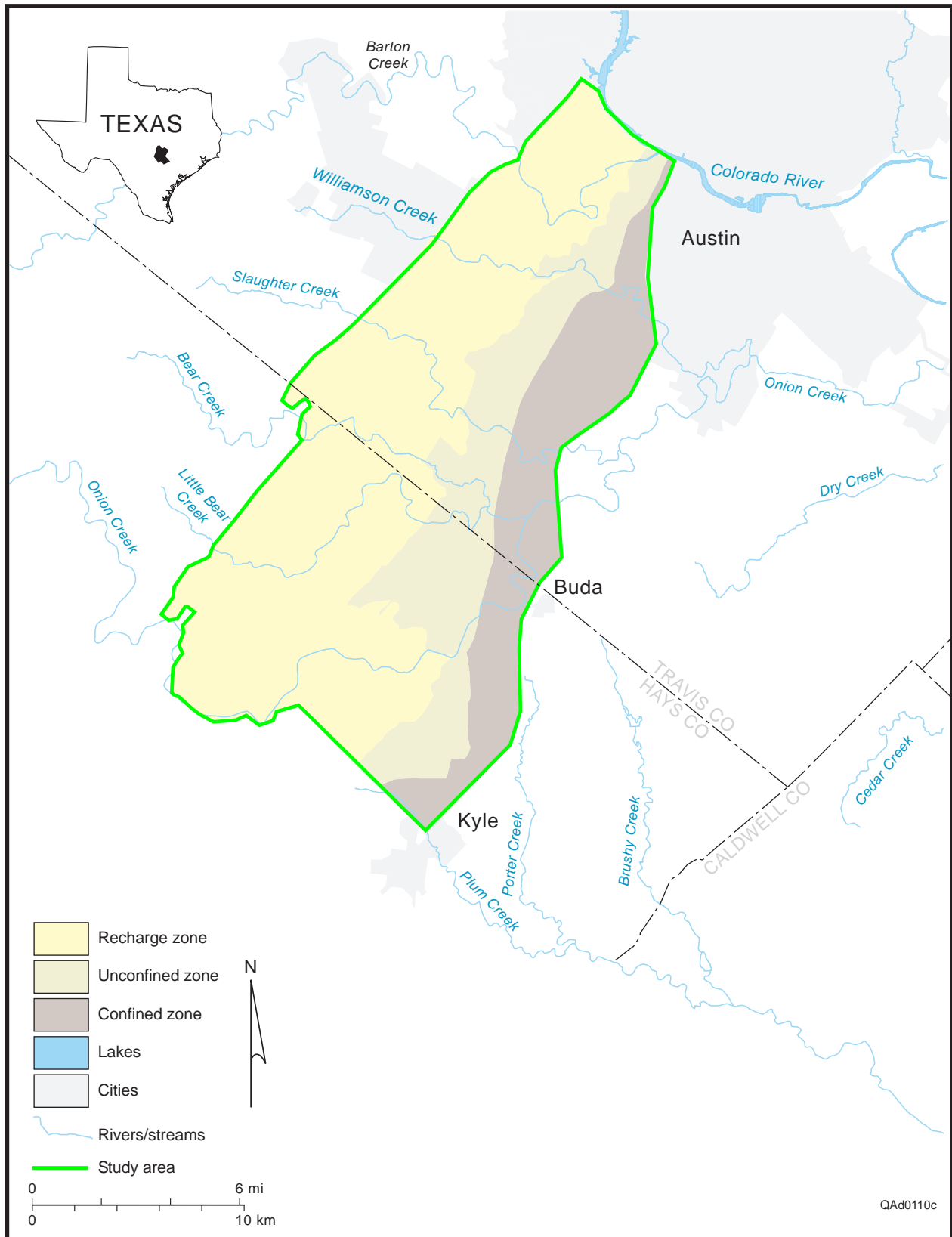
Figure 1. Location of the study area relative to cities, towns, roads, and rivers.

TEXAS

Hays Trinity Groundwater
Conservation District

Barton Springs/Edwards
Aquifer Conservation District

TRAVIS CO
HAYS CO

CALDWELL CO

Edwards Aquifer Authority

N

—— Study area

0                    6 mi

0                    10 km

QAd0111c
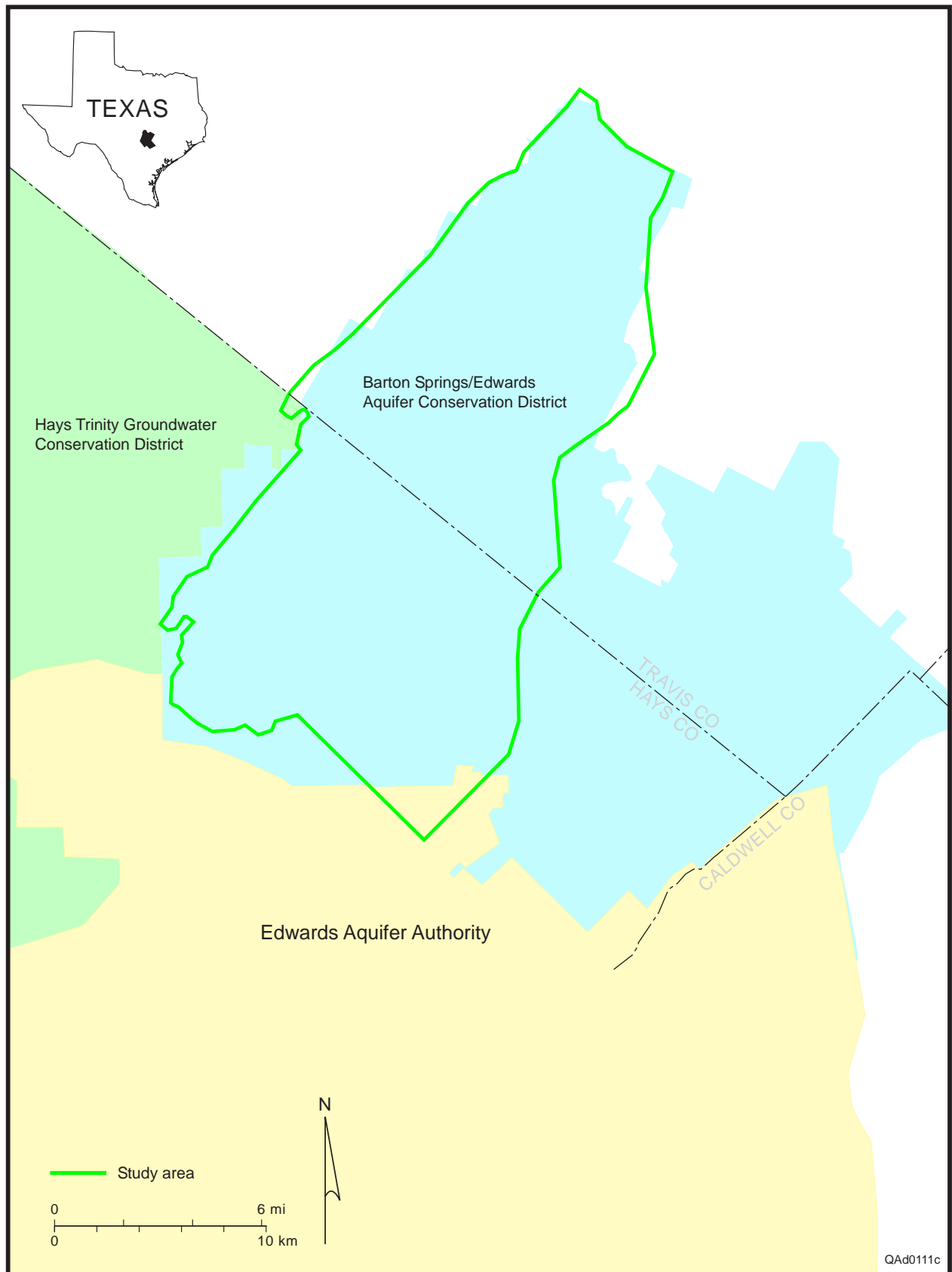
Figure 2.  Location of Groundwater Conservation Districts in the study area.
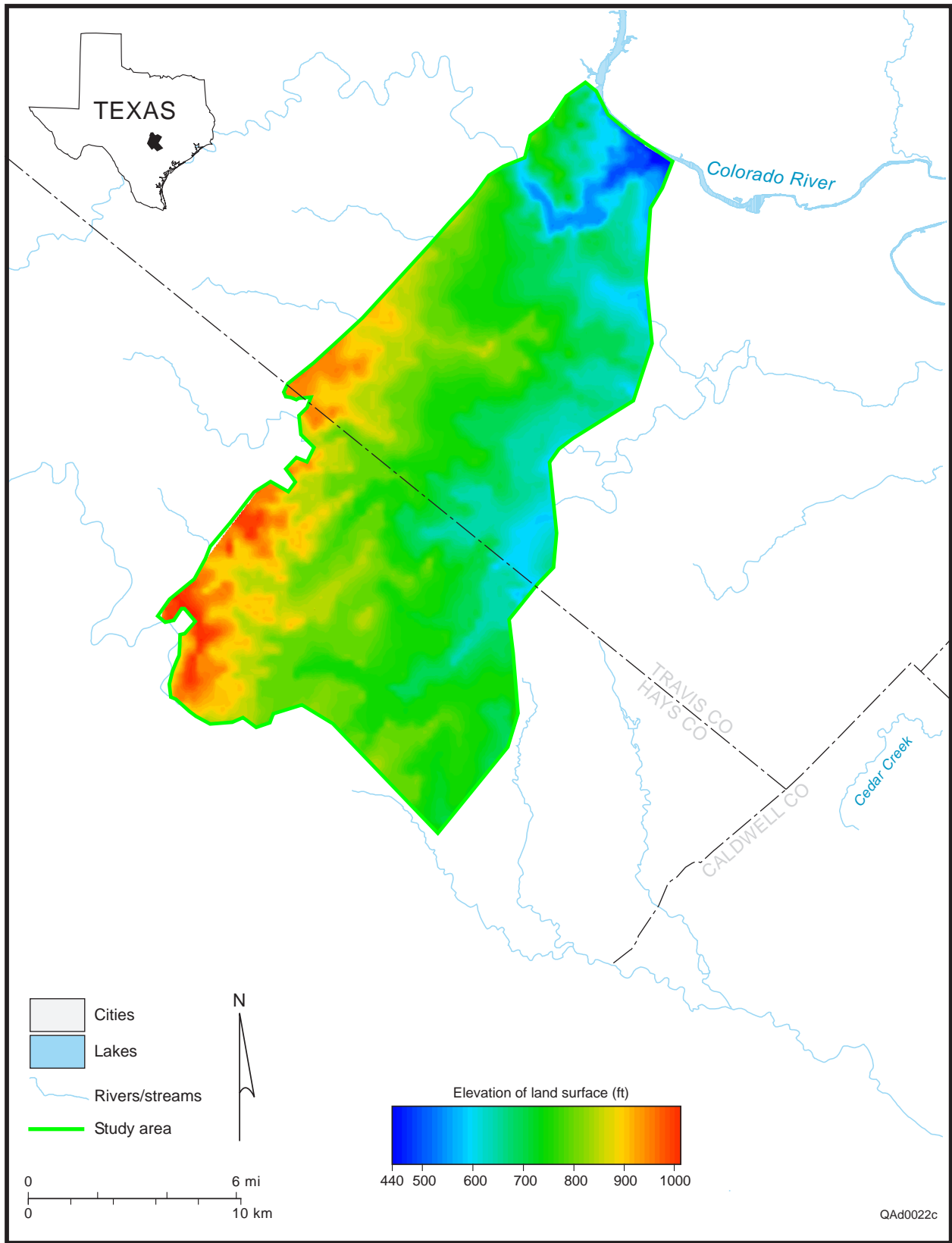
Figure 3. Land-surface elevation in the study area.
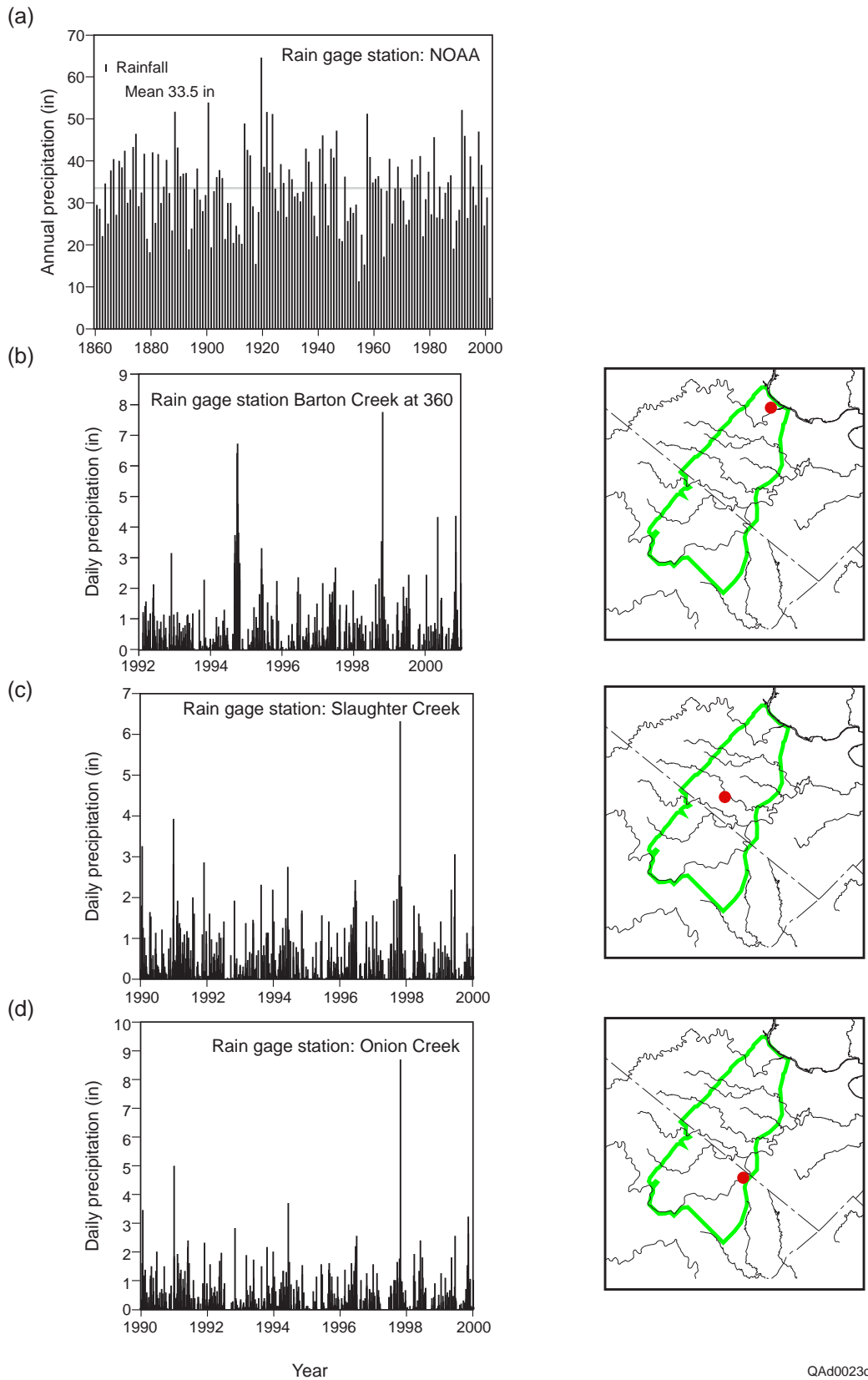
Figure 4. Historical annual precipitation for rain-gage stations at (a) Camp Mabry and Mueller Airport (NOAA station), (b) Barton Creek, (c) Slaughter Creek, and (d) Onion Creek.

QAd0023c
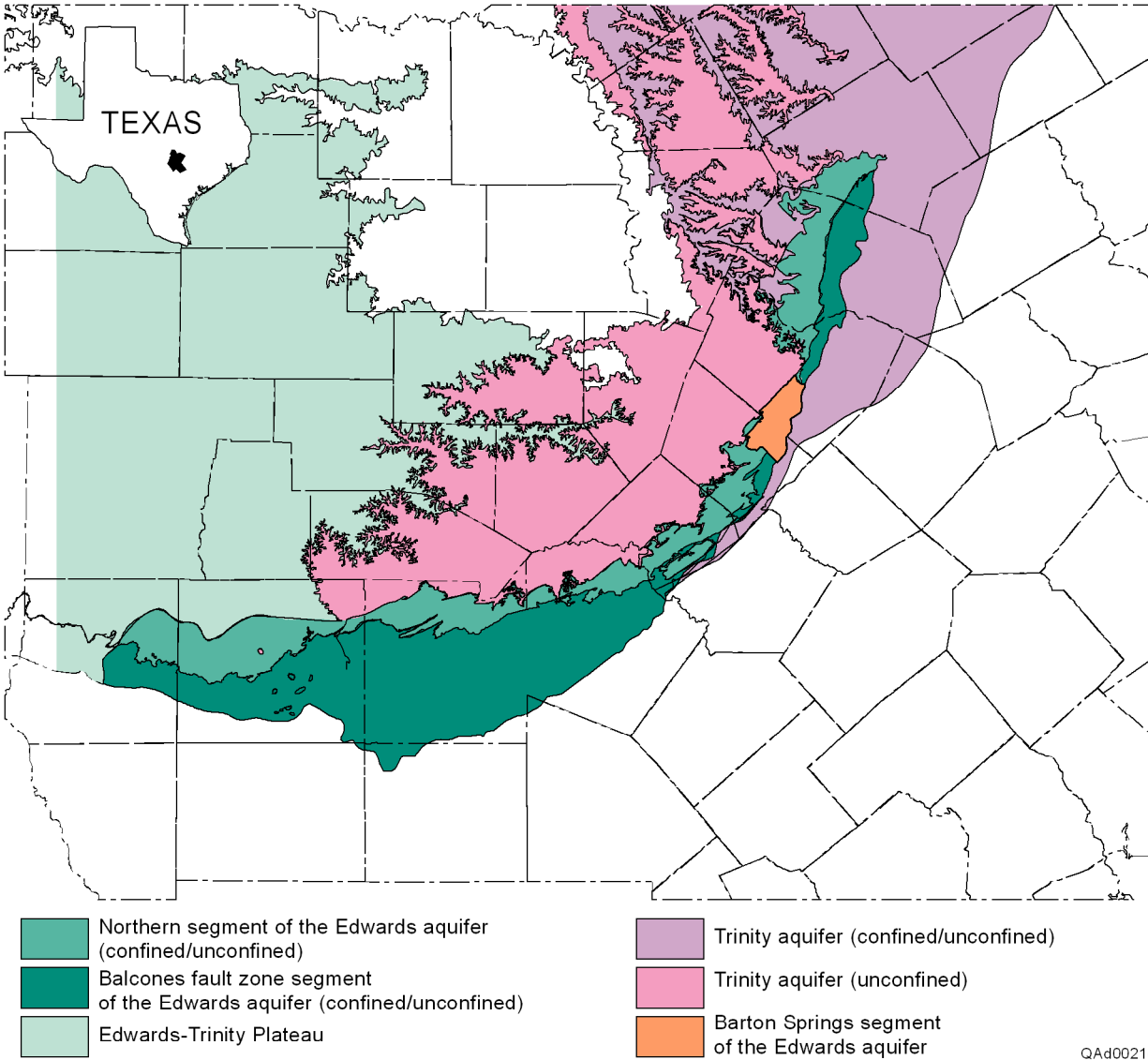
Fig. 5. Geologic setting of the Barton Springs segment of the Edwards aquifer.

Legend:

- Northern segment of the Edwards aquifer (confined/unconfined)
- Balcones fault zone segment of the Edwards aquifer (confined/unconfined)
- Edwards-Trinity Plateau
- Trinity aquifer (confined/unconfined)
- Trinity aquifer (unconfined)
- Barton Springs segment of the Edwards aquifer

TEXAS

QAd0021c
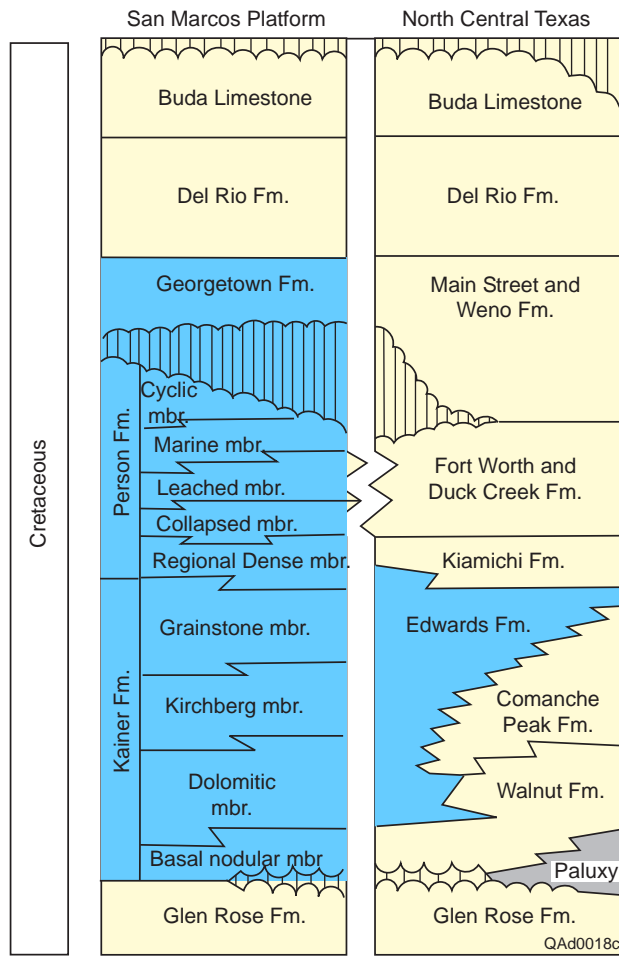
Fig. 6.  Stratigraphic and hydrostratigraphic section of the study area.

**TEXAS**

Barton Creek

Colorado River

Slaughter Creek

Onion Creek

A

Bear Creek

Little Bear Creek

Onion Creek

Dry Creek

Blanco River

Porter Creek

Plum Creek

Brushy Creek

TRAVIS CO
HAYS CO

CALDWELL CO

Cedar Creek

N

A'

0        6 mi
0        10 km

| | |
|---|---|
| Taylor Fm. | Georgetown Fm. |
| Igneous intrusives | Cyclic/marine member |
| Austin Chalk | Leached/collapsed member |
| Eagle Ford Fm. | Regional dense member |
| Buda Limestone | Grainstone member |
| Del Rio Fm. | Kirshberg Member |

Dolomite member

Basal nodular member/
Kainer Fm. Walnut Fm.

Edwards aquifer
hydrostratigraphic units

Upper Glen Rose Fm.

Lakes

Rivers/streams
Study area
Fault

QAd0019c

Fig. 7. Surface geology in the study area.

**A**
Northwest

**A'**
Southeast

ft    m
500 — 150

0 — 0

0                5 mi

0              5 km

Confining units, including Del Rio, Buda, Eagle Ford, Austin, and Taylor Formations

Edwards aquifer, including Walnut, Kainer, Person, and Georgetown Formations

Glen Rose Formation

QAd0024c
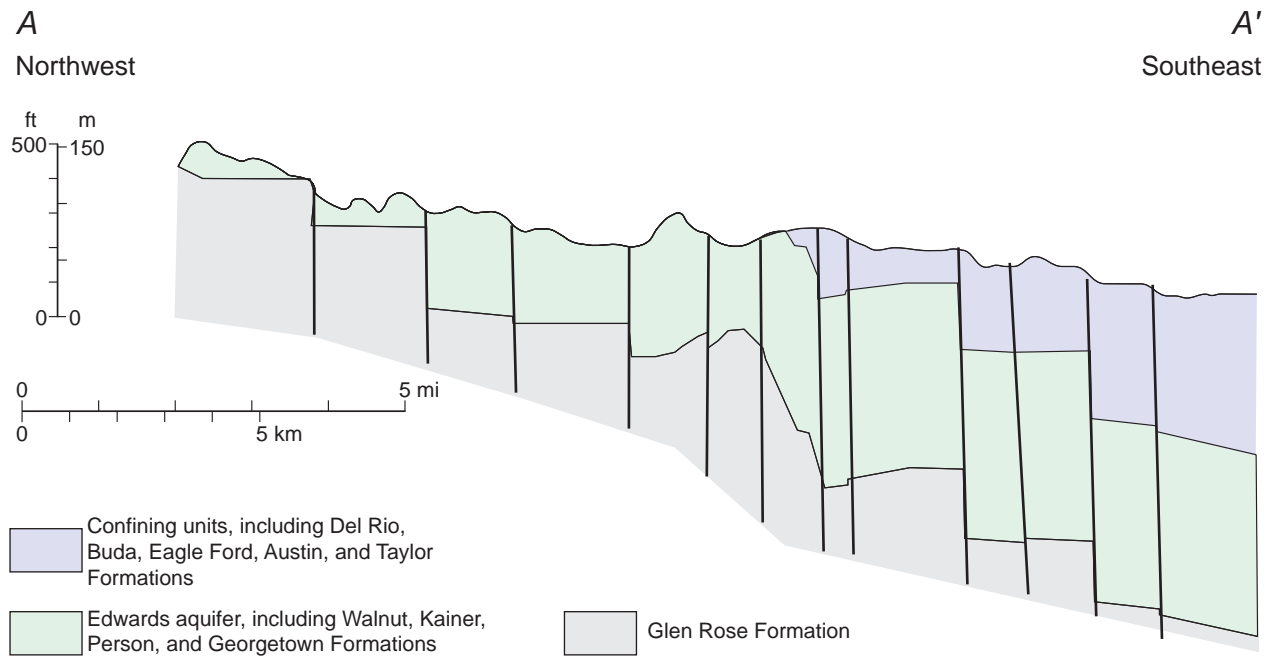
Fig. 8. Geologic cross section of the study area. Location of cross section shown in figure 7.
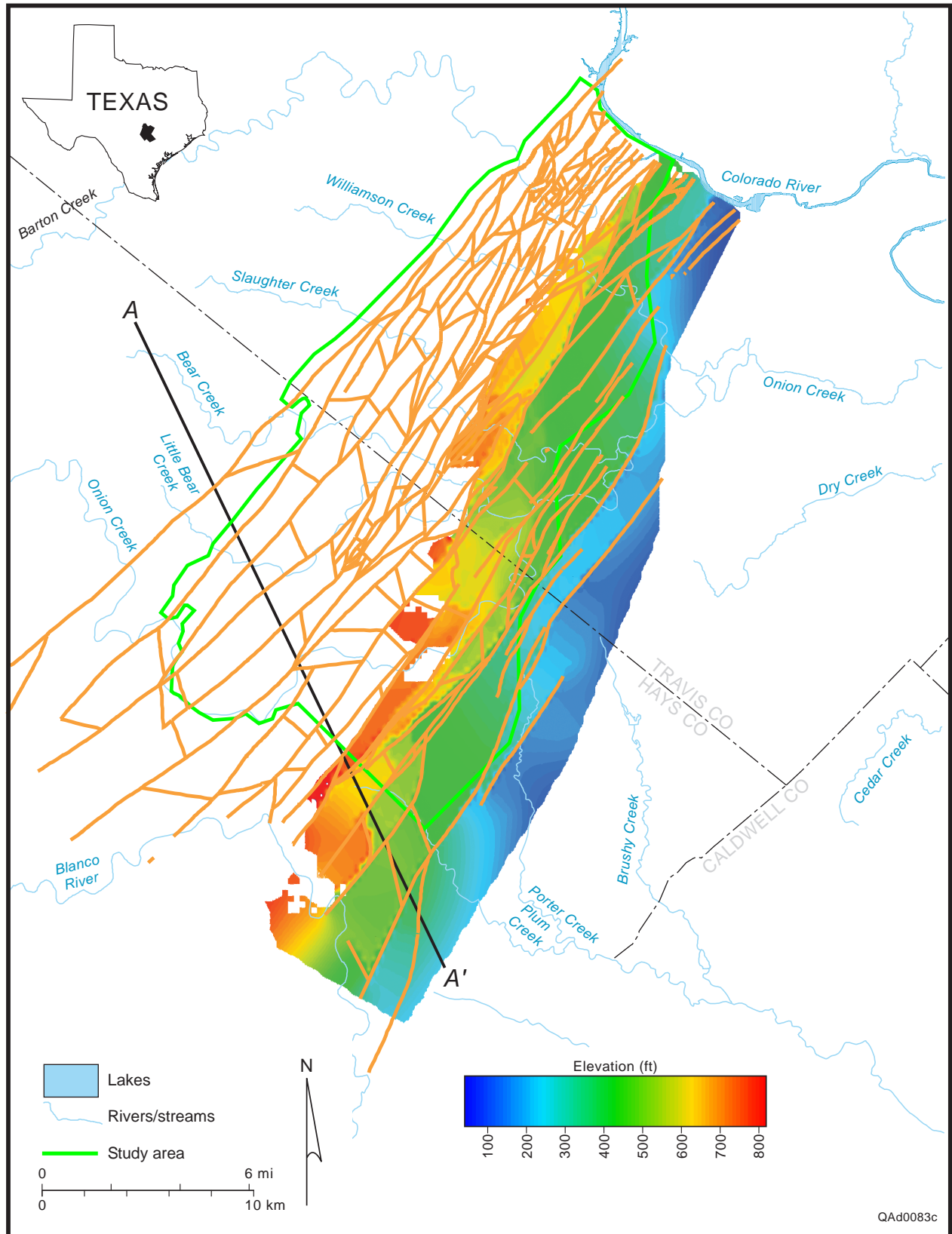
Fig. 9. Elevation of the top of the Edwards aquifer (which corresponds to the base of the Del Rio Formation). Figure 12 shows the location of the control points.
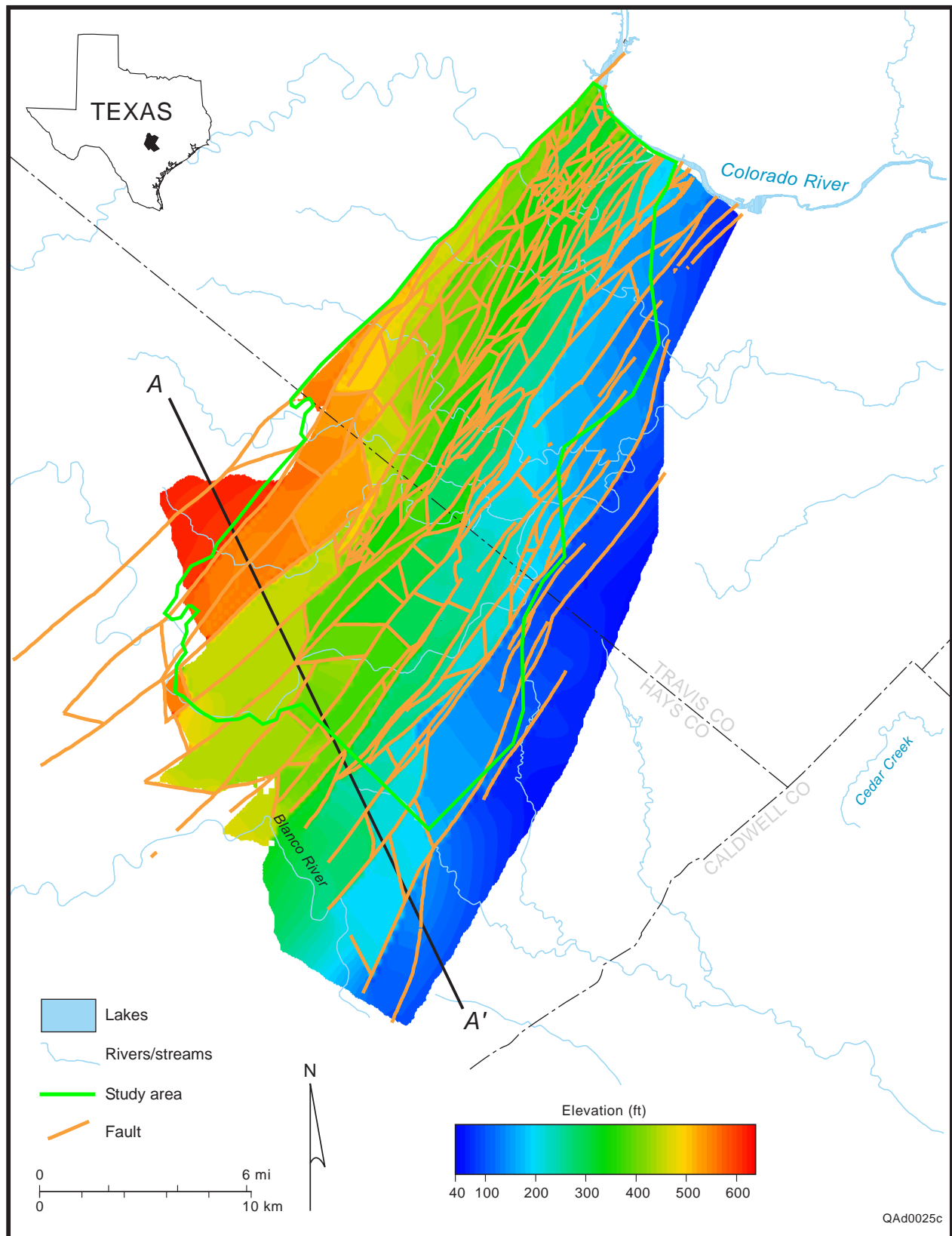
Fig. 10. Elevation of the base of the Edwards aquifer (which corresponds to the top Glen Rose Formation). Figure 12 shows the location of the control points.
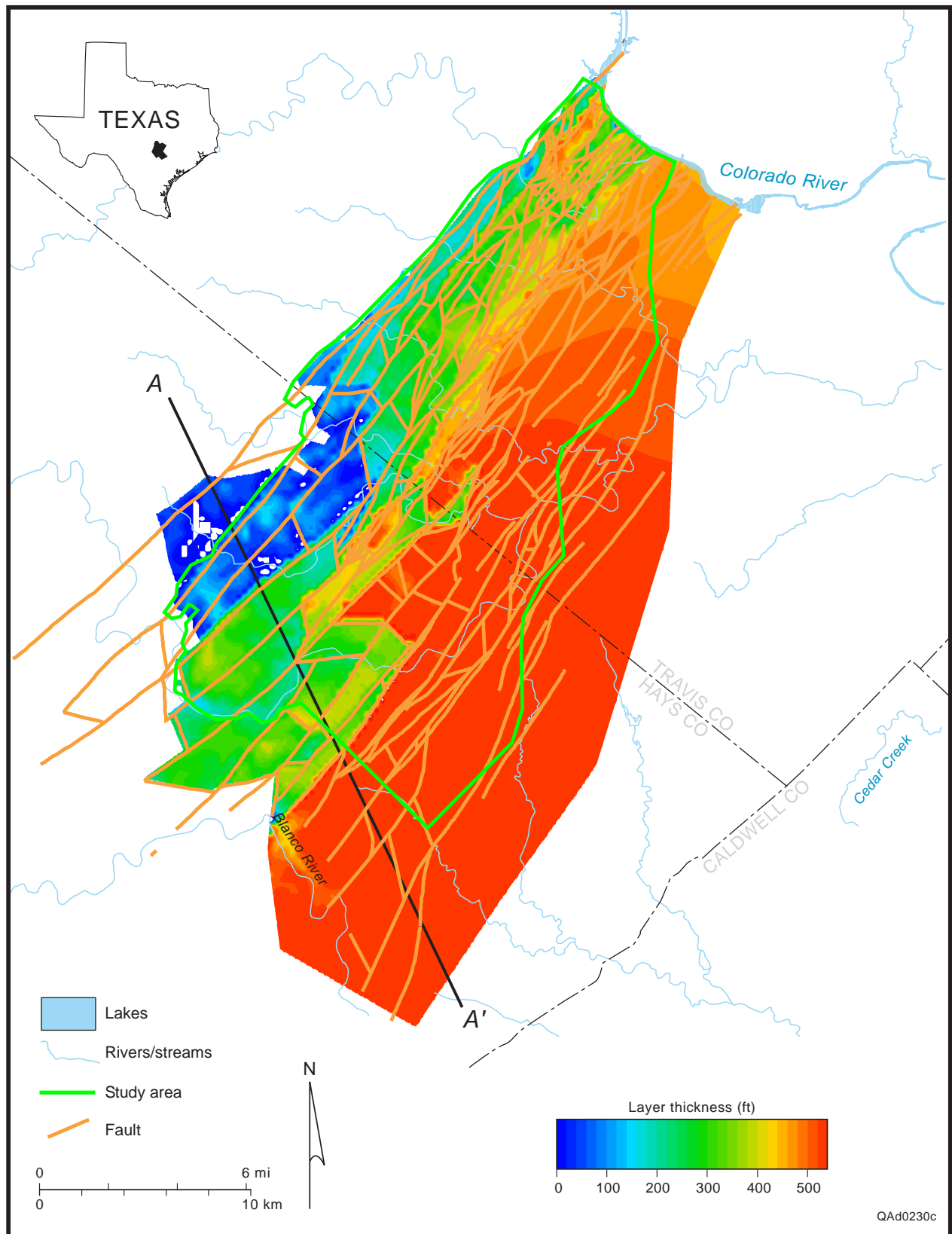
Fig. 11. Approximate thickness of the Edwards aquifer.
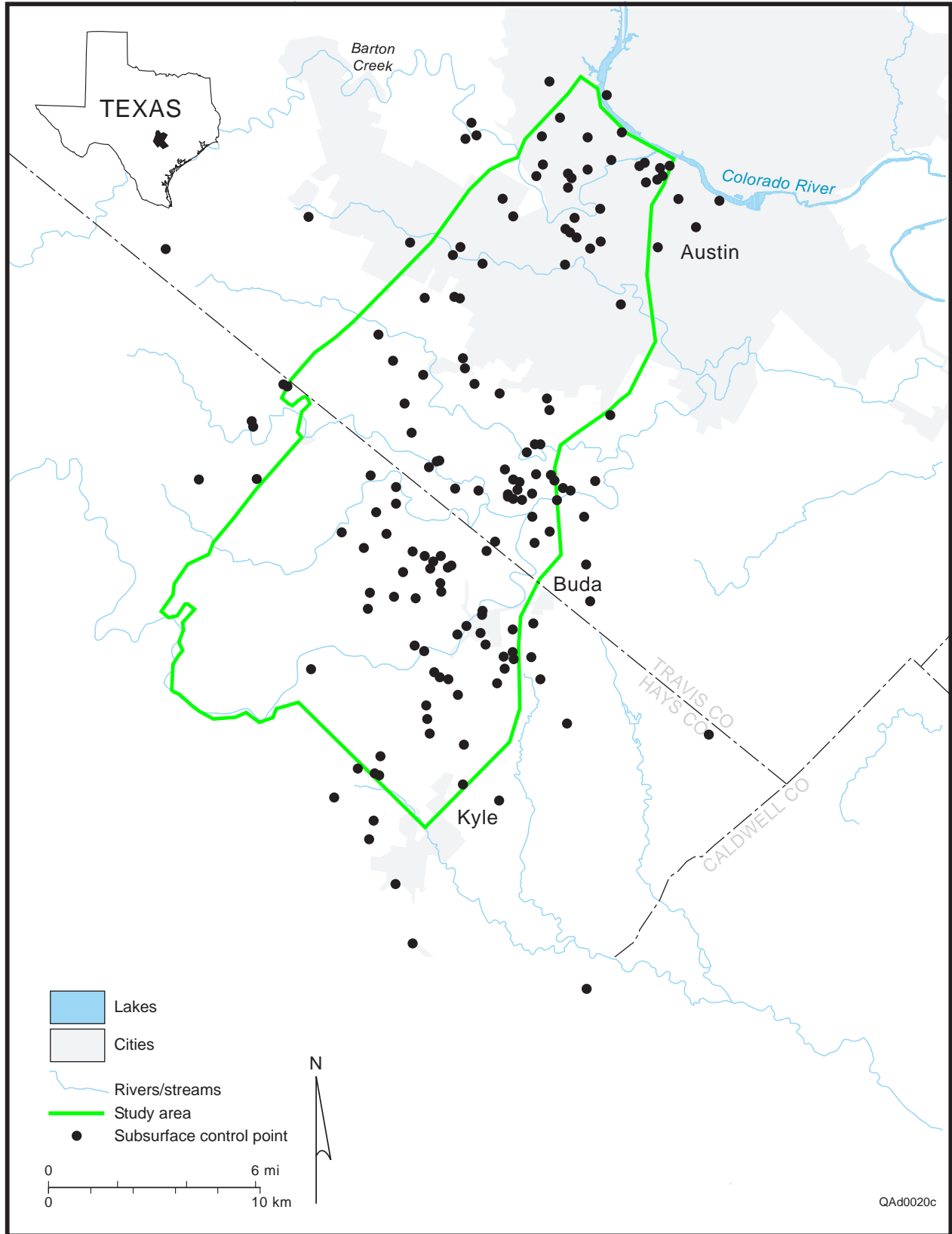
Fig. 12. Control points for the elevation of the top and the base of the Edwards aquifer.
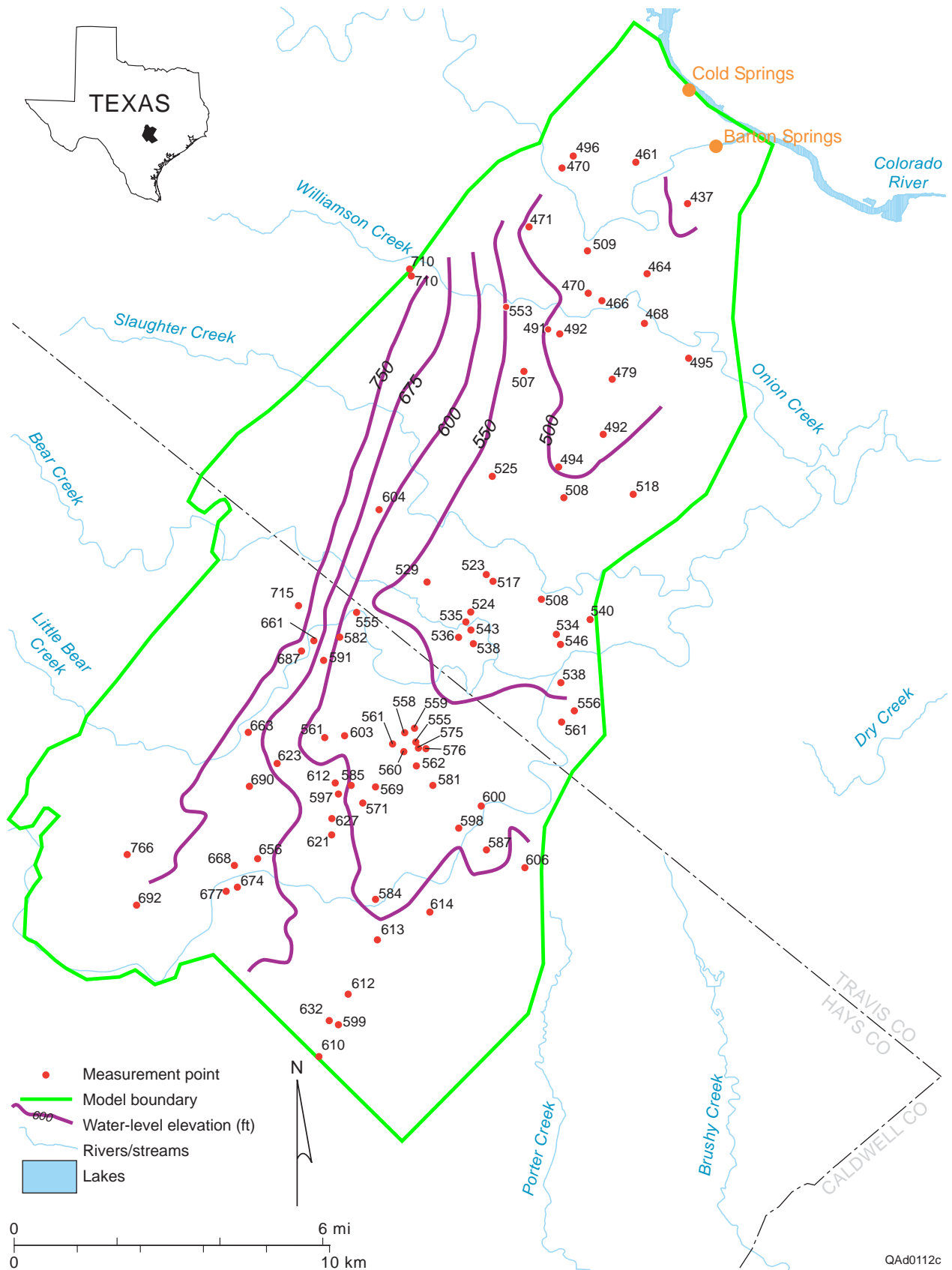
Figure 13. Water-level elevations in the aquifer (include water-level measurements in July and August 1999).
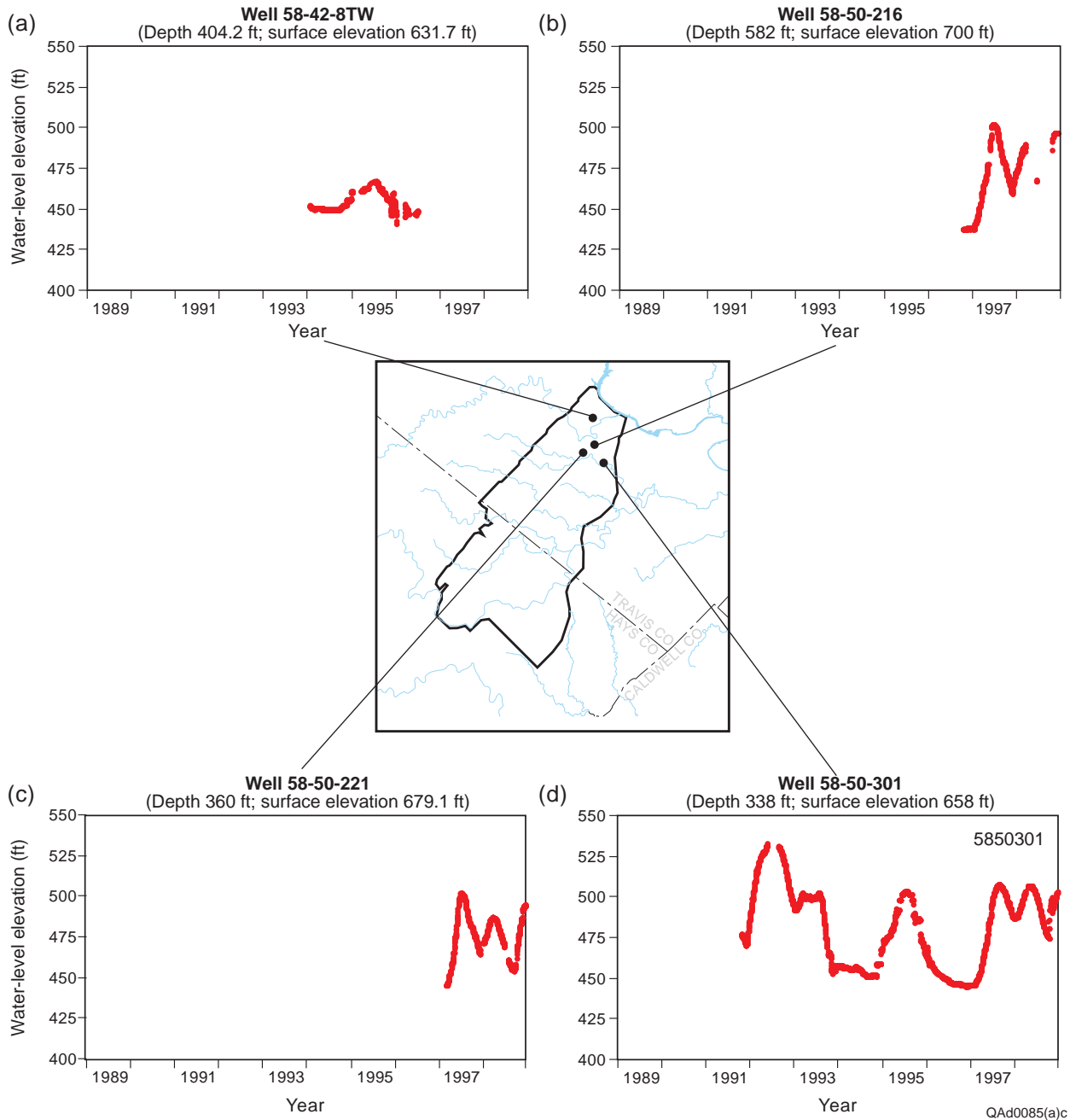
Figure 14. Hydrographs for wells (a) 58-42-8TW, (b) 58-50-216, (c) 58-50-221, and (d) 58-50-301.
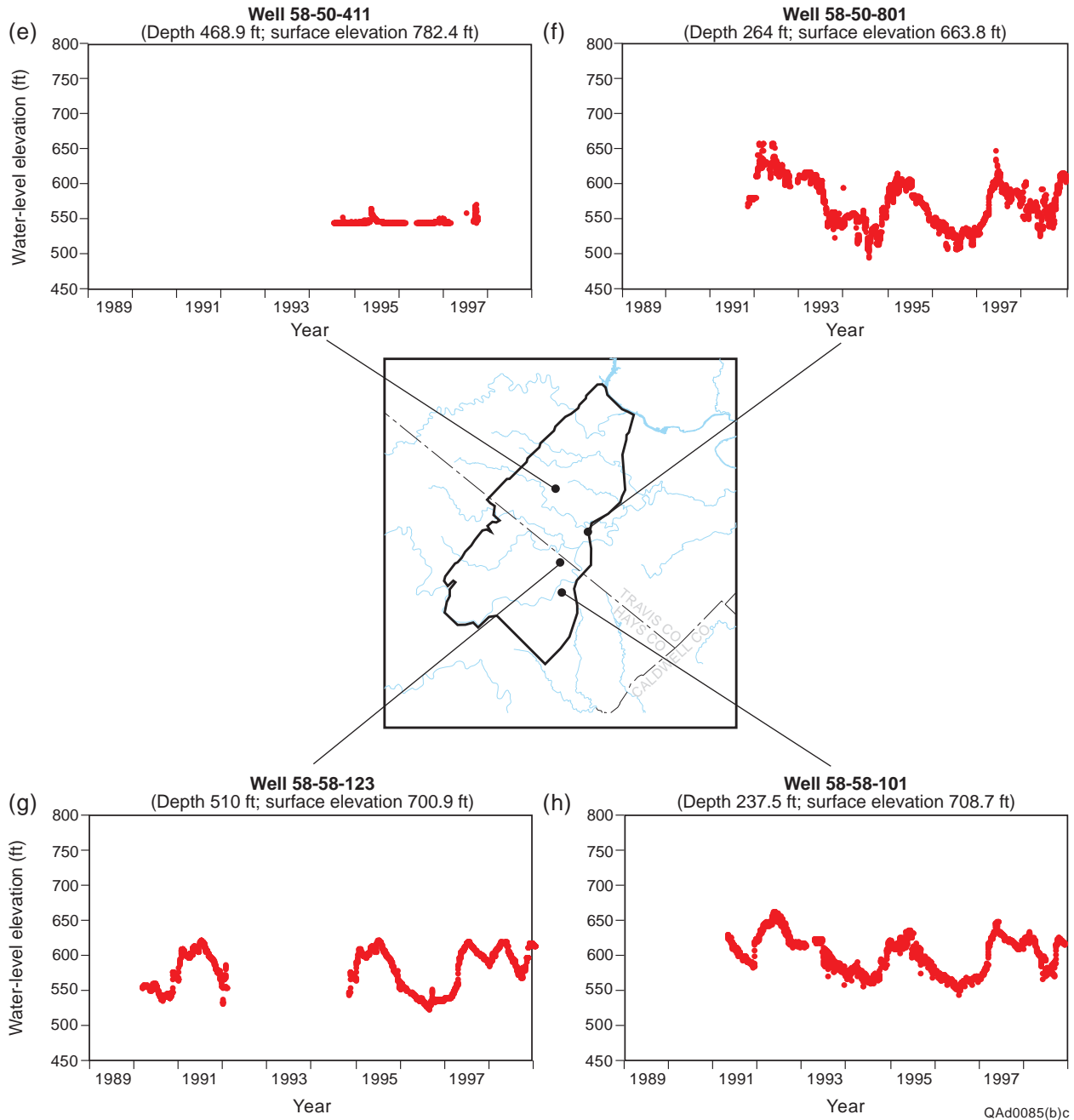
Figure 15. Hydrographs for wells (e) 58-50-411, (f) 58-50-801, (g) 58-58-123, and (h) 58-58-101.
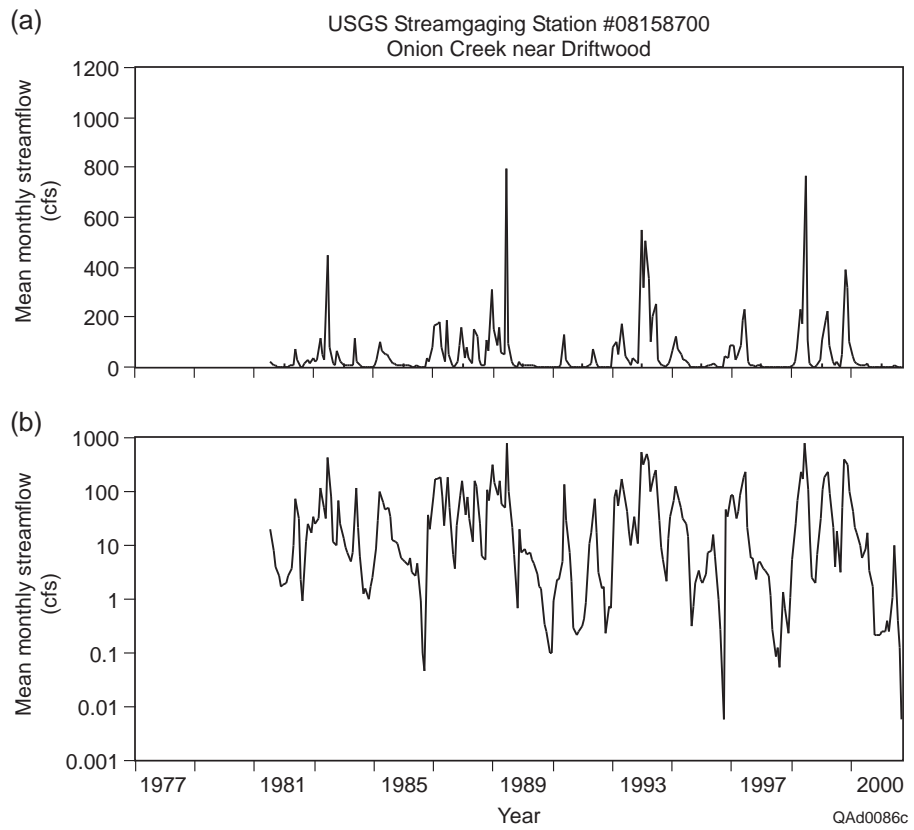
Figure 16.  Mean monthly streamflow for USGS gaging station 08158700 on Onion Creek near Driftwood for (a) linear and (b) logarithmic scales. Figure 25 shows the location of the stream gage.
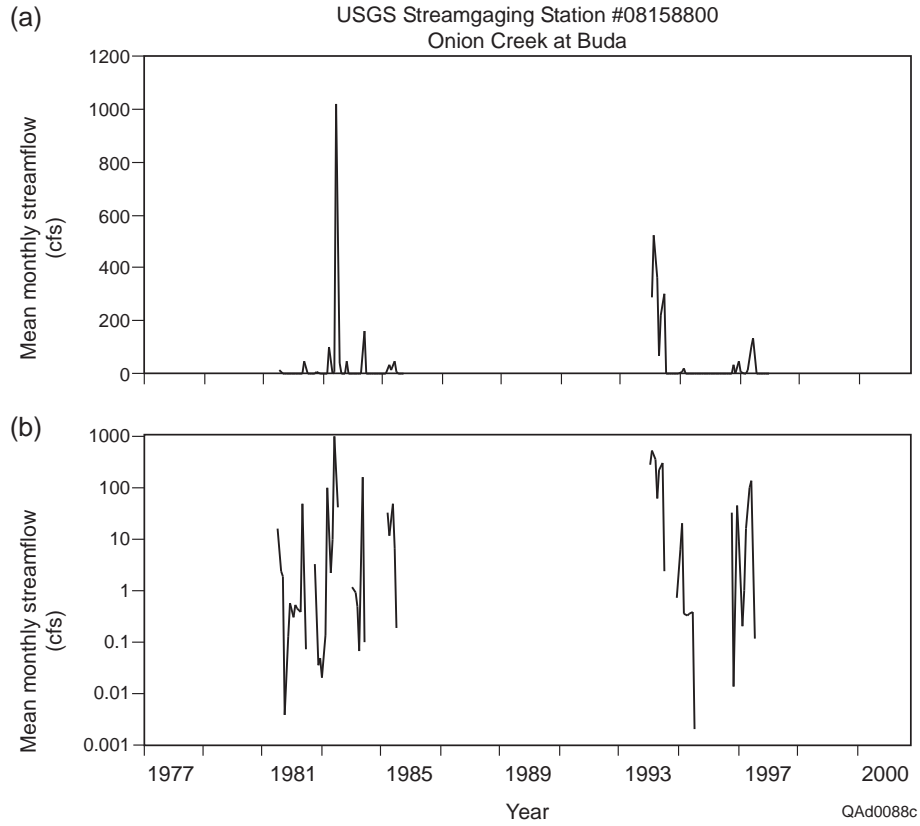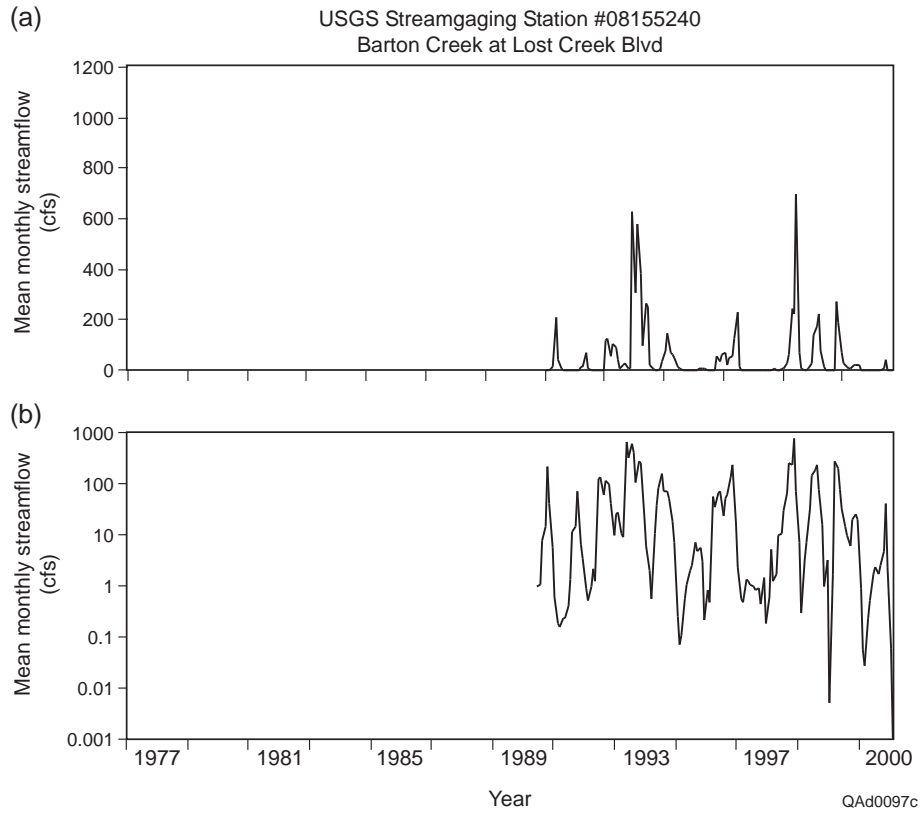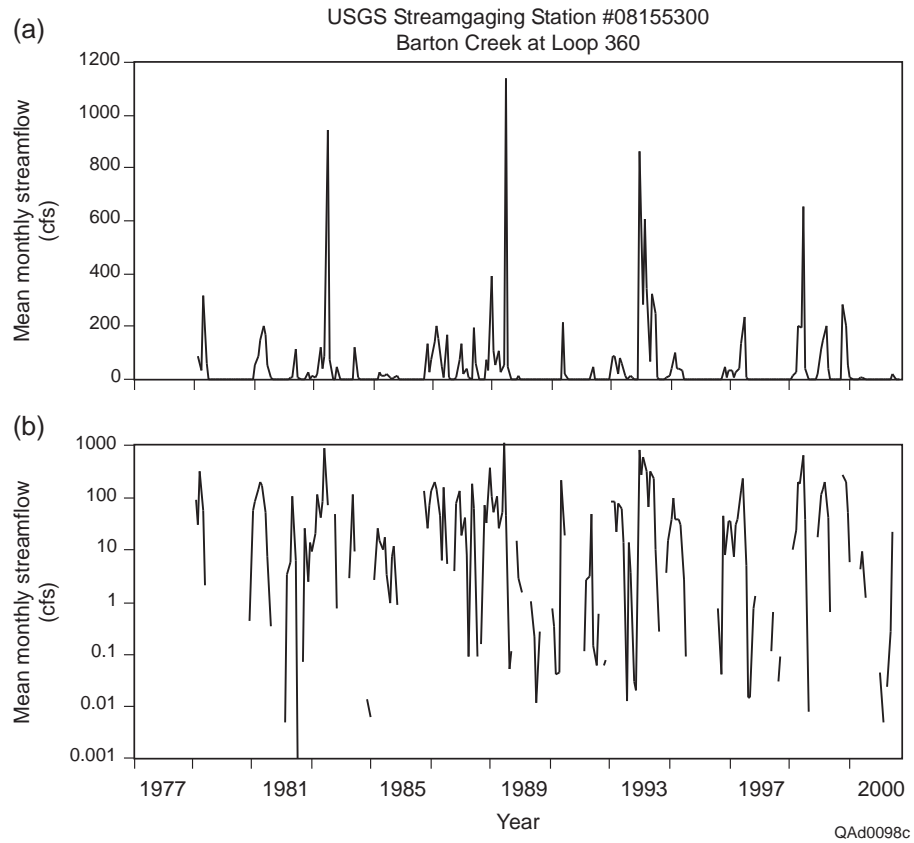
Figure 17. Mean monthly streamflow for USGS gaging station 08158800 on Onion Creek at Buda for (a) linear and (b) logarithmic scales. Figure 25 shows the location of the stream gage.

(a)

USGS Streamgaging Station #08158810
Bear Creek near Driftwood

(b)
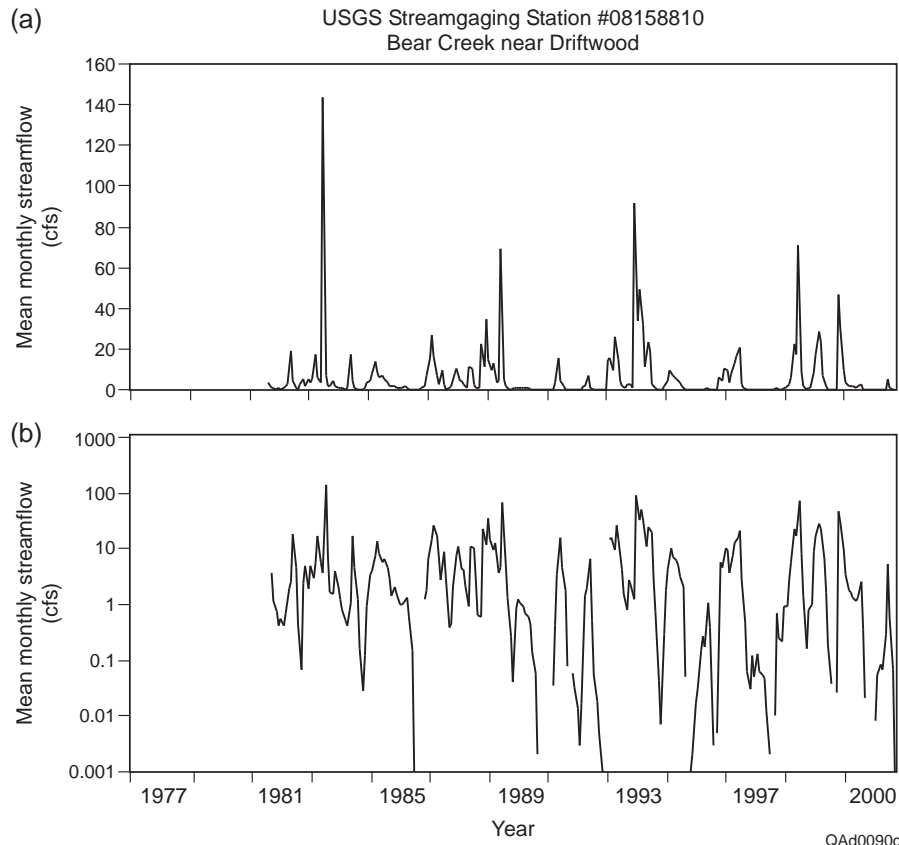
Figure 18. Mean monthly streamflow for USGS gaging station 08158810 on Bear Creek near Driftwood for (a) linear and (b) logarithmic scales. Figure 25 shows the location of the stream gage.
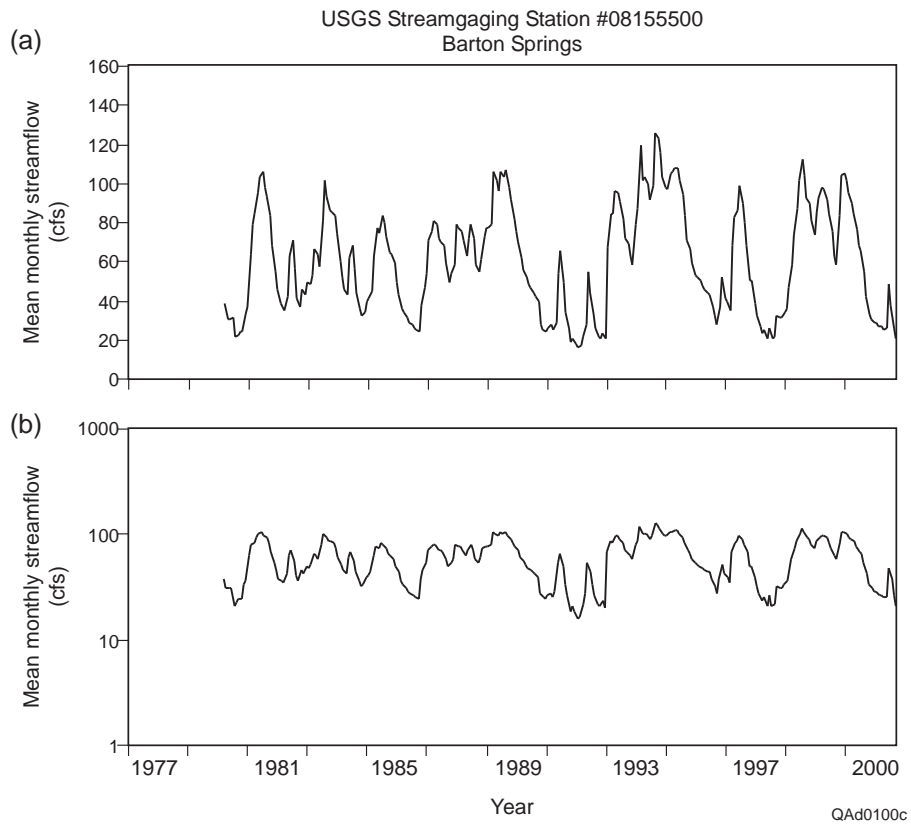
(a)

(b)
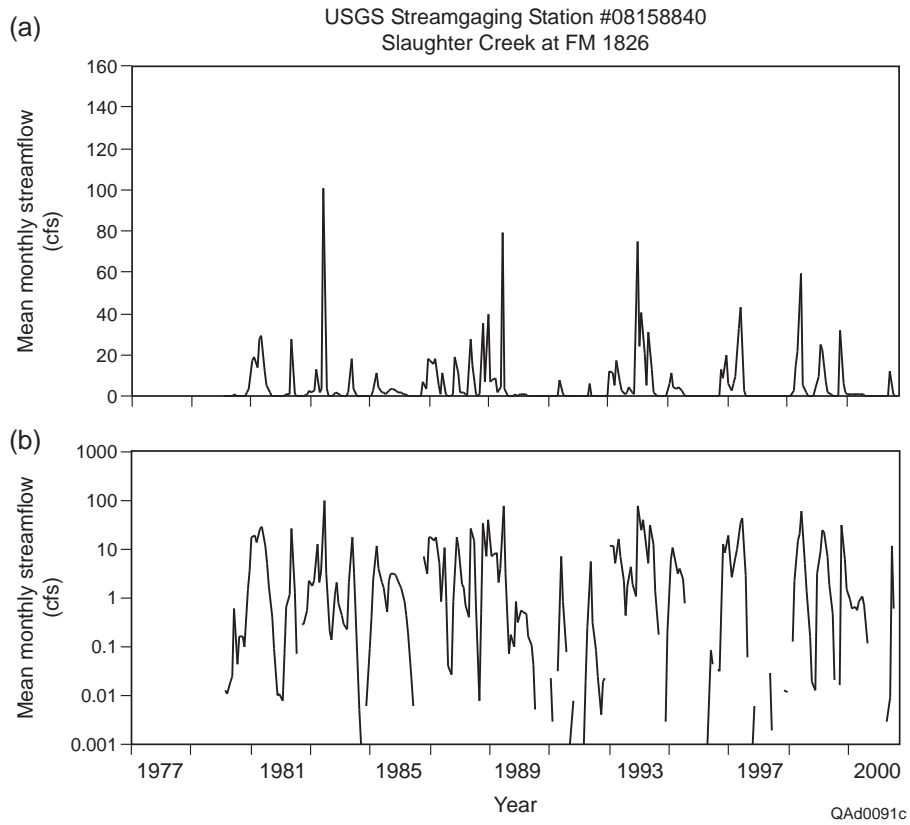
Figure 19. Mean monthly streamflow for USGS gaging station 08158840 on Slaughter Creek at FM 1826 for (a) linear and (b) logarithmic scales. Figure 25 shows the location of the stream gage.

QAd0091c

USGS Streamgaging Station #08158922
Williamson Creek at Brush Country Blvd, Oak Hill
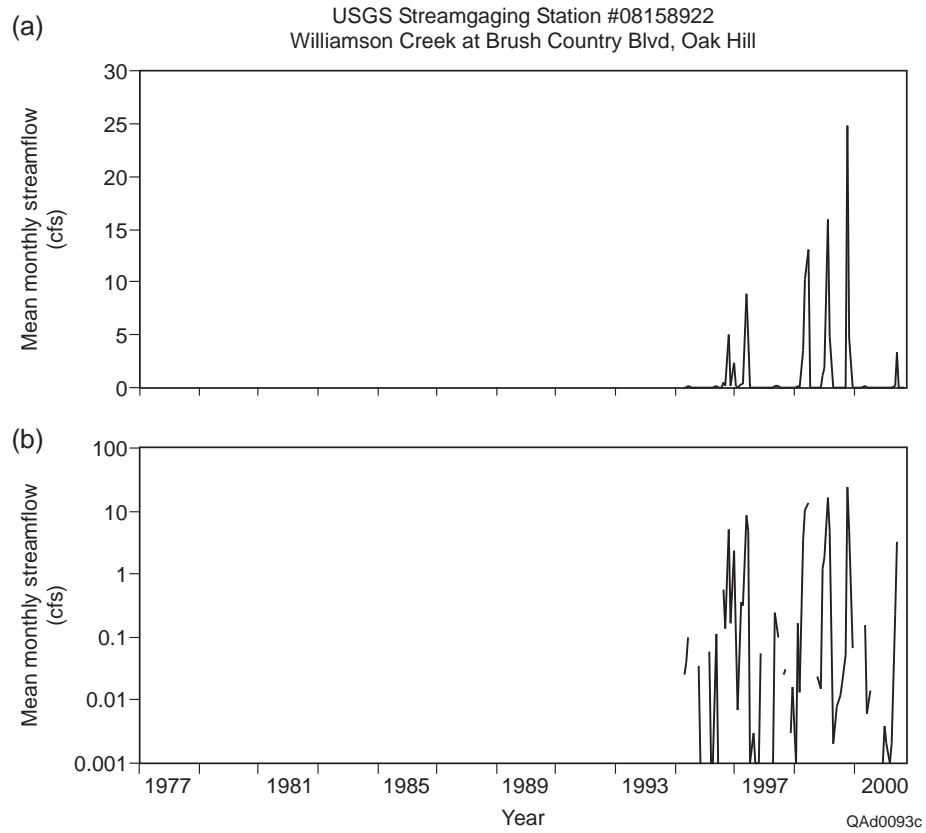
Figure 20.  Mean monthly streamflow for USGS gaging station 08158922 on Williamson Creek at Brush Country Blvd., Oak Hill, for (a) linear and (b) logarithmic scales. Figure 25 shows the location of the stream gage.
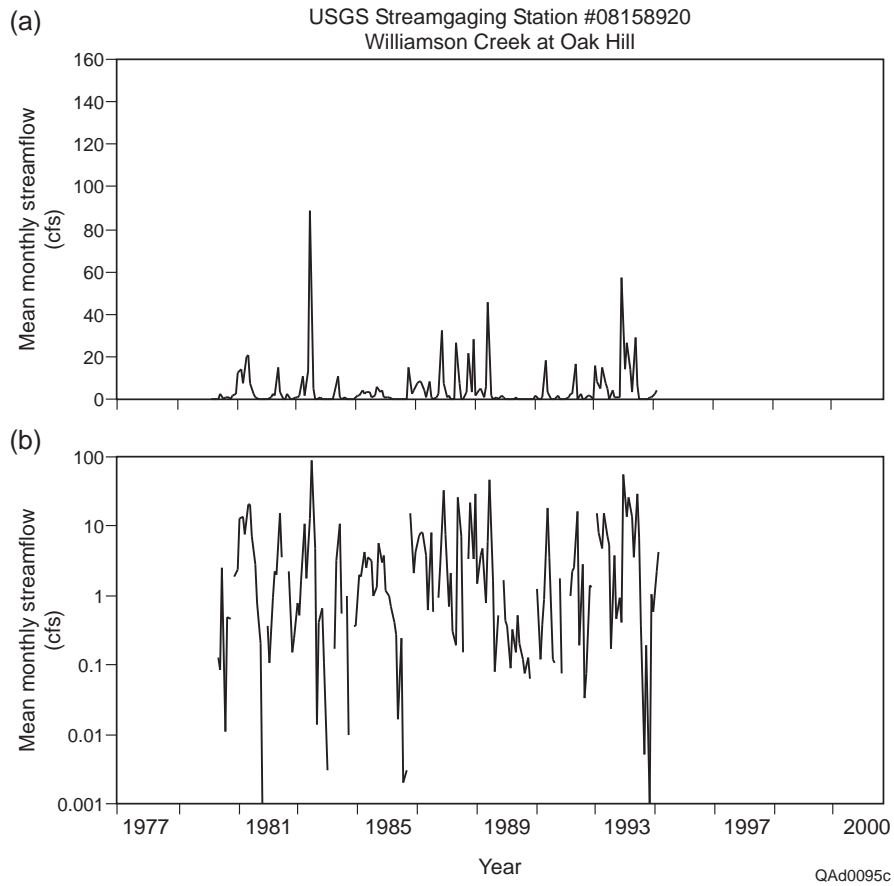
Figure 21. Mean monthly streamflow for USGS gaging station 08158920 on Williamson Creek at Oak Hill for (a) linear and (b) logarithmic scales. Figure 25 shows the location of the stream gage.

Figure 22.  Mean monthly streamflow for USGS gaging station 08155240 on Barton Creek at Lost Creek Blvd. for (a) linear and (b) logarithmic scales. Figure 25 shows the location of the stream gage.

Figure 23. Mean monthly streamflow for USGS gaging station 08155300 on Barton Creek at Loop 360 for (a) linear and (b) logarithmic scales. Figure 25 shows the location of the stream gage.

Figure 24. Mean monthly streamflow for USGS gaging station 08155500 at Barton Springs for (a) linear and (b) logarithmic scales. Figure 25 shows the location of the stream gage.
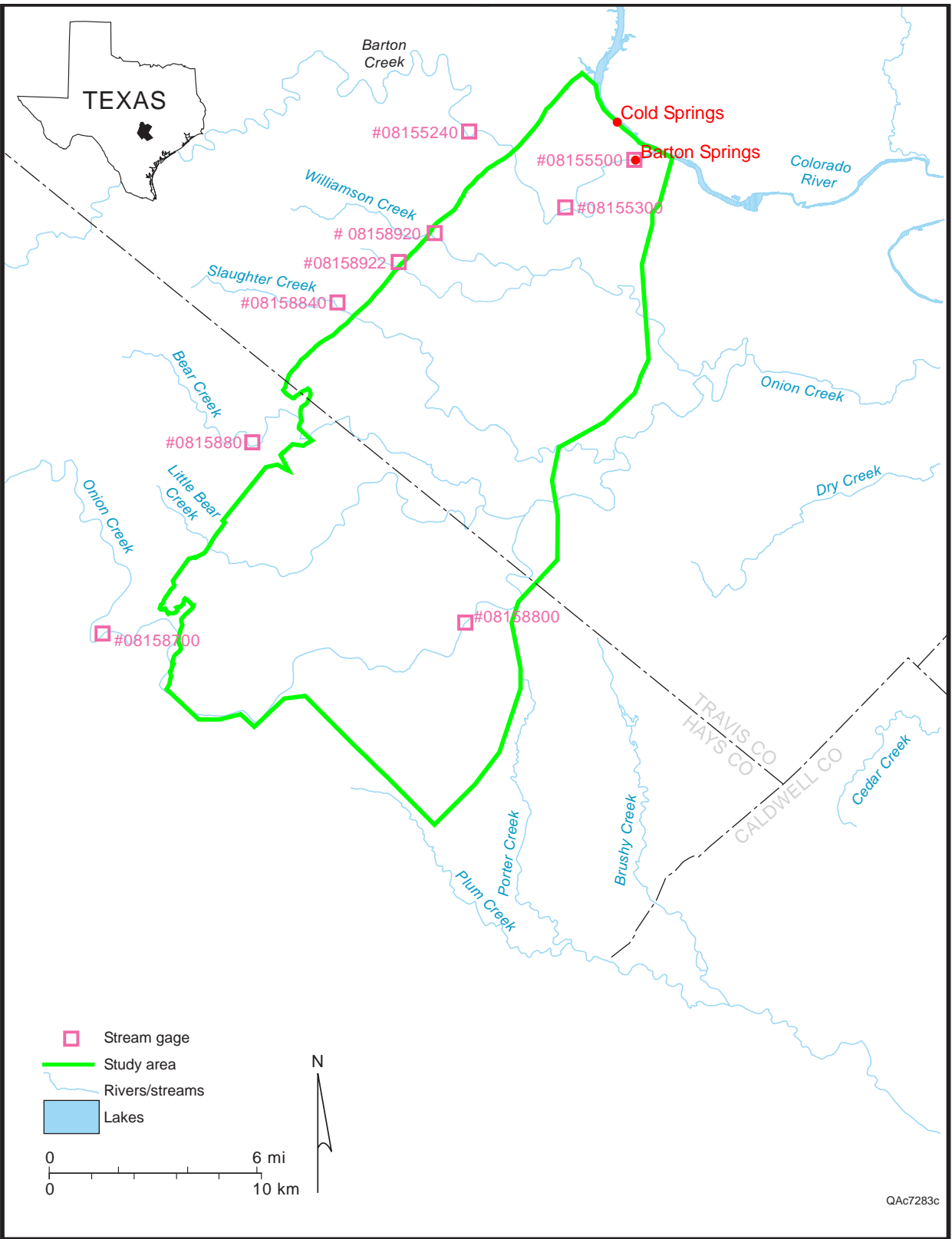
Figure 25.  Location of the stream gages for the stream-flow hydrographs shown in figures 16 through 24.
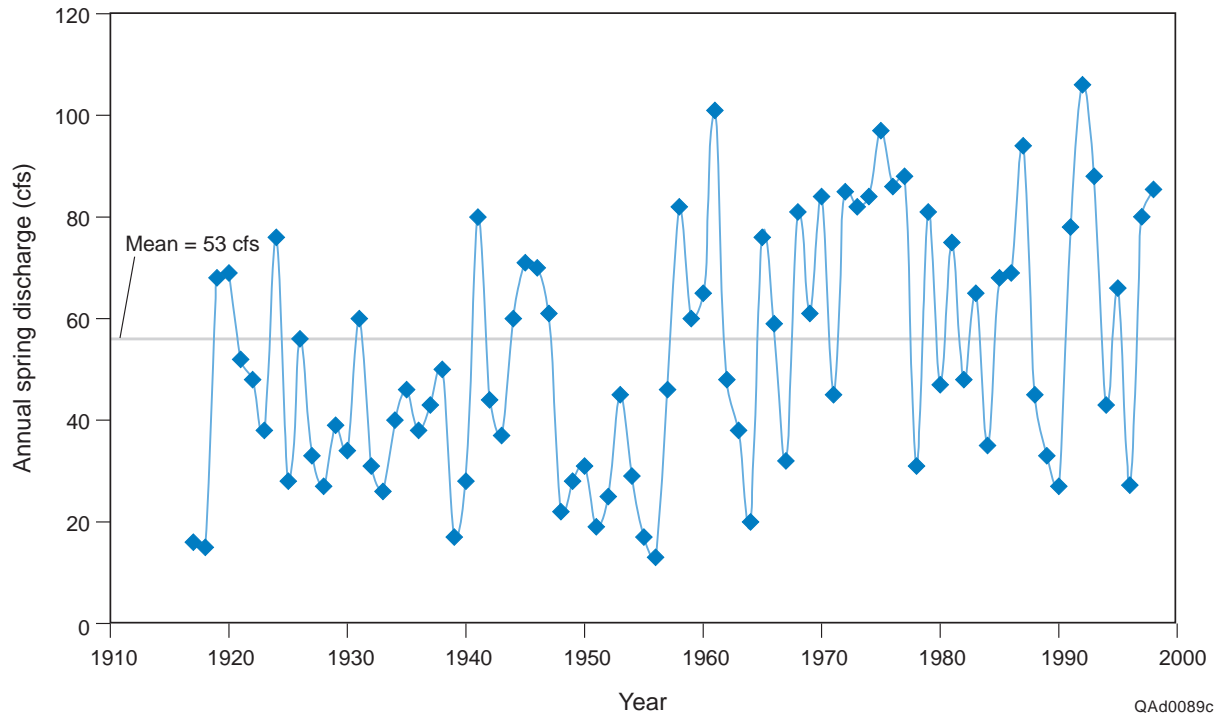
Figure 26.  Discharge at Barton Springs.
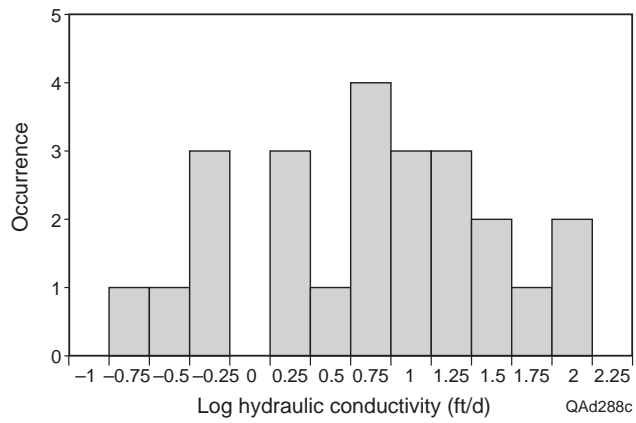
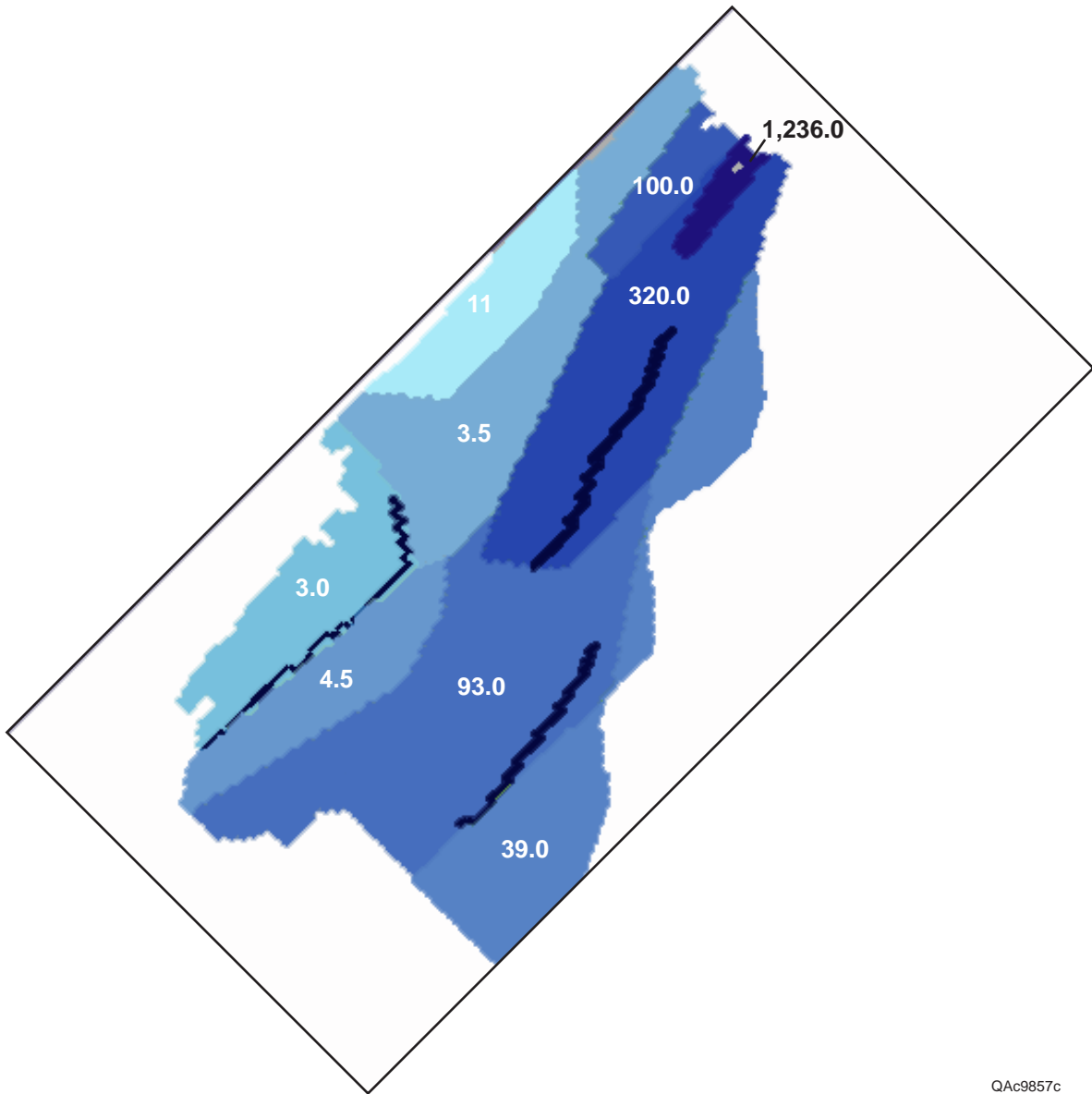Figure 27. Histogram of hydraulic conductivity from aquifer tests.

TEXAS

Barton Creek

Cold Springs

Barton Springs

Colorado River

Slaughter Creek

Stenger Ridgewood
14,502,540

City of
Sunset Valley
17,531,800

Onion Creek

The Brown School
6,321,200

Bear Creek

Little Bear Creek

Mooreland
4,844,100

Bear Creek Park
10,195,500

J. D. Malone
35,685,550

Shadow Hollow Estates
67,137,700

Onion Creek
Country Club
73,509,000

Southwest Territory
19,299,630

Onion Creek

Village of San Leanna
22,083,200

Dry Creek

Chaparral Park
26,188,088

Twin Creek PWS
12,130,000

City of Hays
9,907,610

Marbridge
26,108,870

Creedmoor-Maha
179,460,100

Mystic Oaks WSC
7,579,580

Leisurewoods
87,200,000

Arroyo Doble
48,114,300

Onion Creek Meadows
32,957,900

Huntington Utility
11,164,000

Cimarron Park
104,310,600

HCISD-Dahlstrom
2,382,800

Twin Oaks Ranch
982,940

City of Buda
69,571,600

CenTex Materials
104,587,375

TX Lehigh
62,296,295

Goforth Water Supply
Corporation
214,993,230

TX Water Services
132,564,000

Mountain City Oaks
35,832,010

HCISD-Hays
35,832,010

TRAVIS CO
HAYS CO
CALDWELL CO

Blanco River

Plum Creek

Porter Creek

Brushy Creek

Study area

Rivers/streams

Measurement points

Pumping center
(annual pumpage 2,000 gal)

N

0                    6 mi

0                    10 km

QAd0094c

Figure 28. Spatial distribution of pumping in the aquifer.
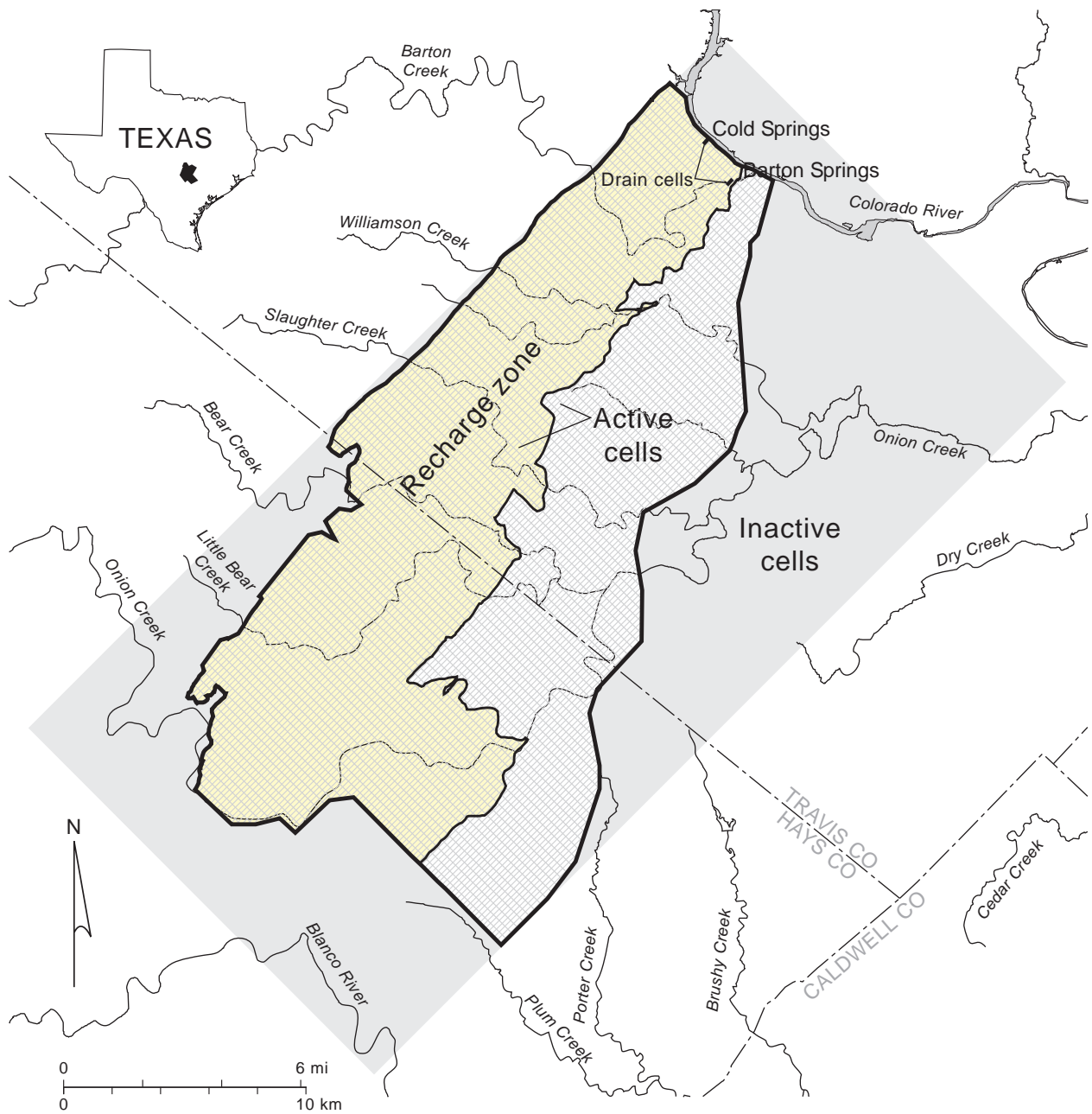
Fig. 29. Model grid, consisting of 120 cells 120 cells (14,400 cells) that ae 1,000 ft long 500 ft wide. The active zone of the model is shown by the solid line and consists of 7,043 cells.

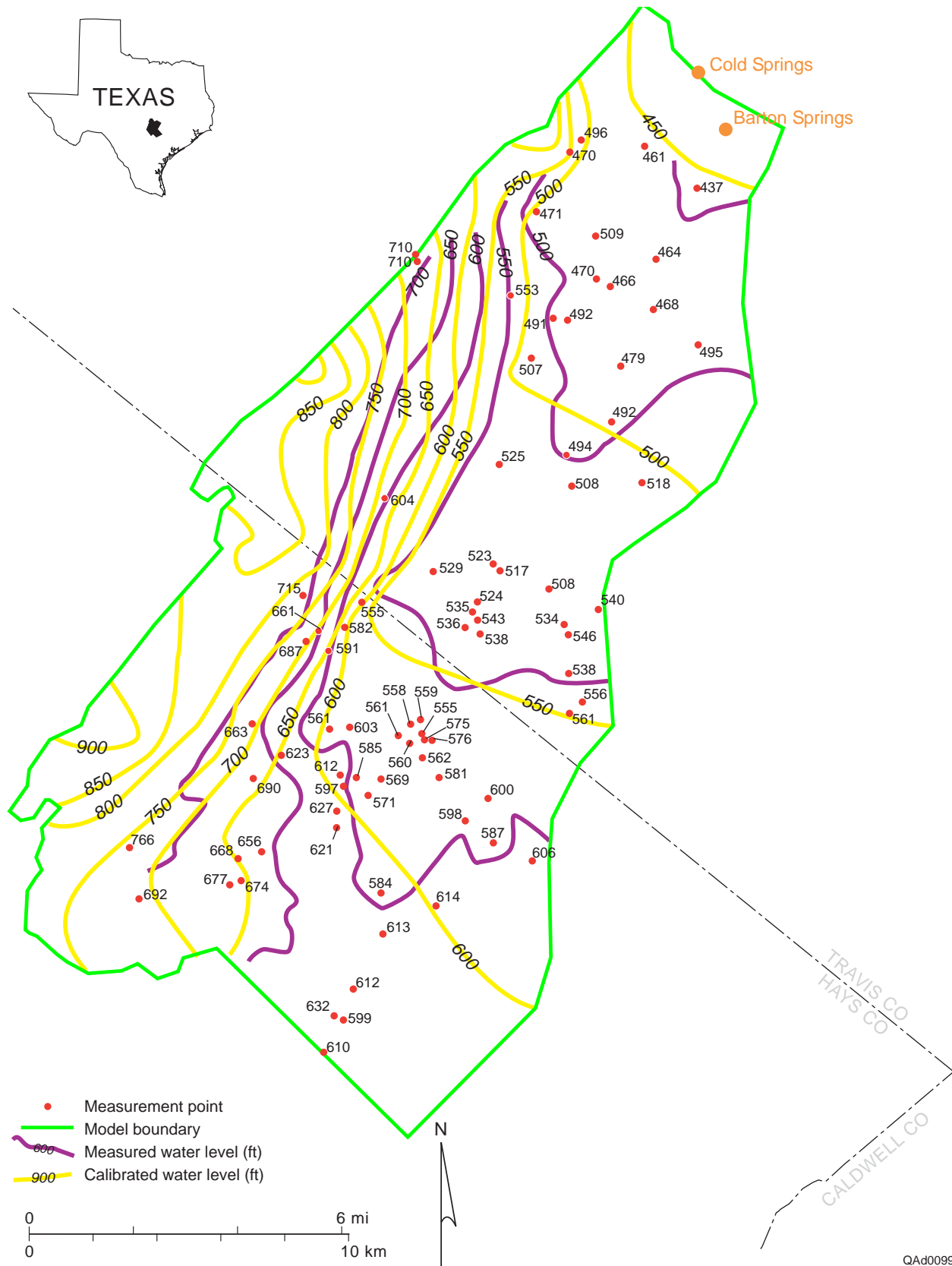Figure 30. Zonal distribution of hydraulic conductivity resulting from calibration of the steady-state model.

Figure 31. Comparison of simulated and measured (July/August 1999) water-level contours for the steady-state model.
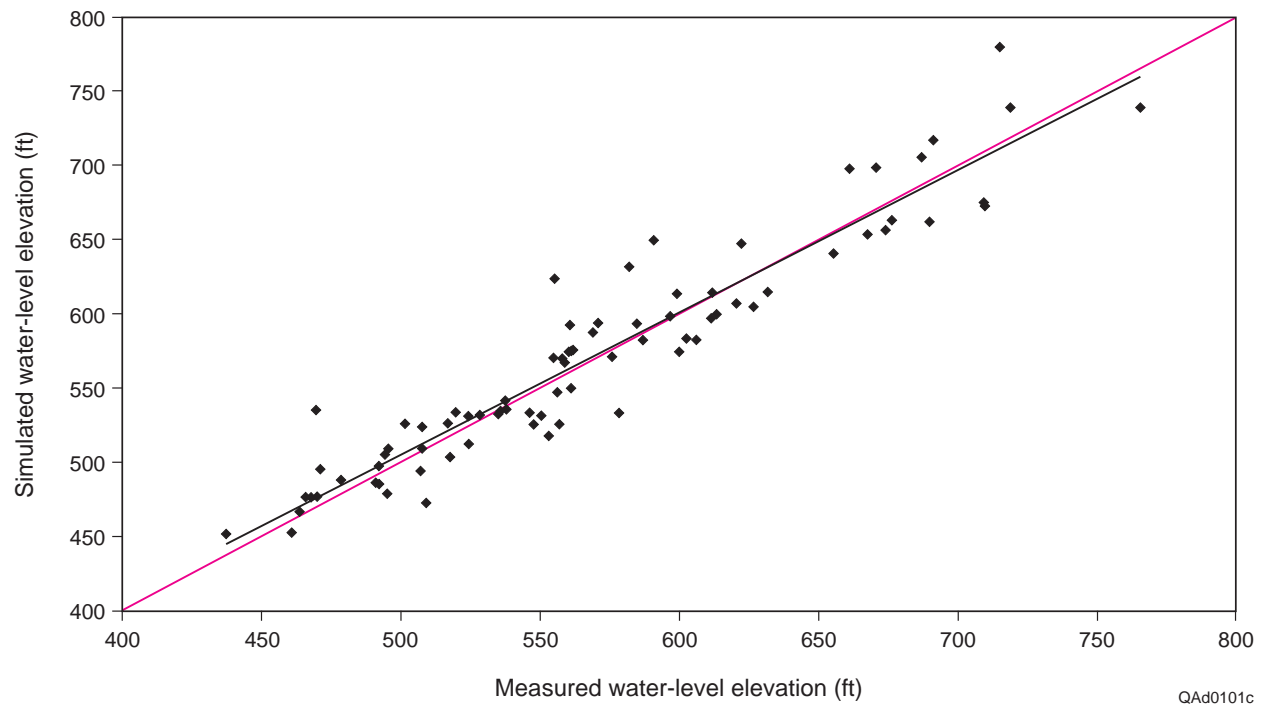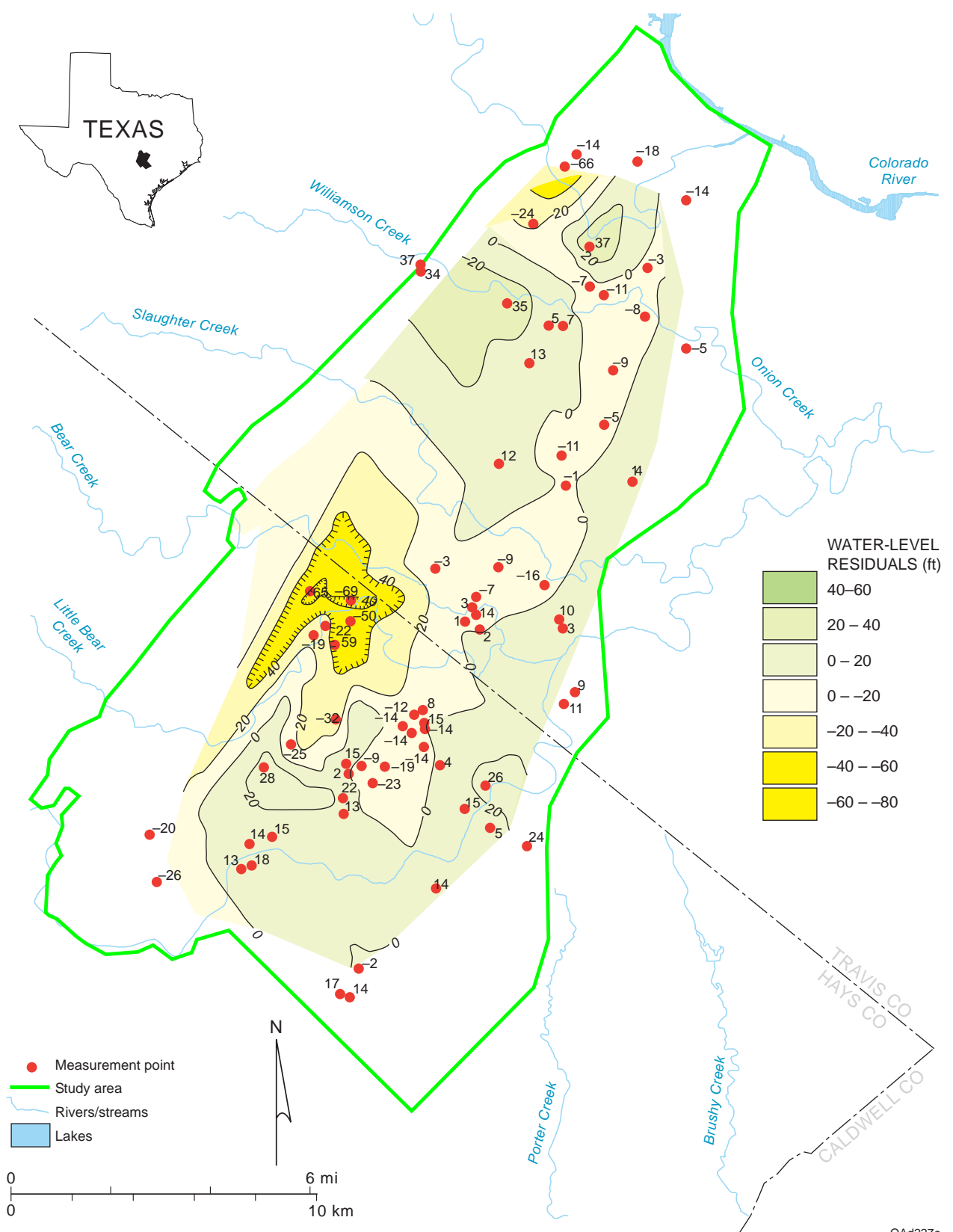
Figure 32. Scatter plot of simulated and measured (July/August 1999) water levels for the steady-state model.

Figure 33. Water-level residuals (difference between measured and simulated water-level elevations) for the calibrated steady-state model.
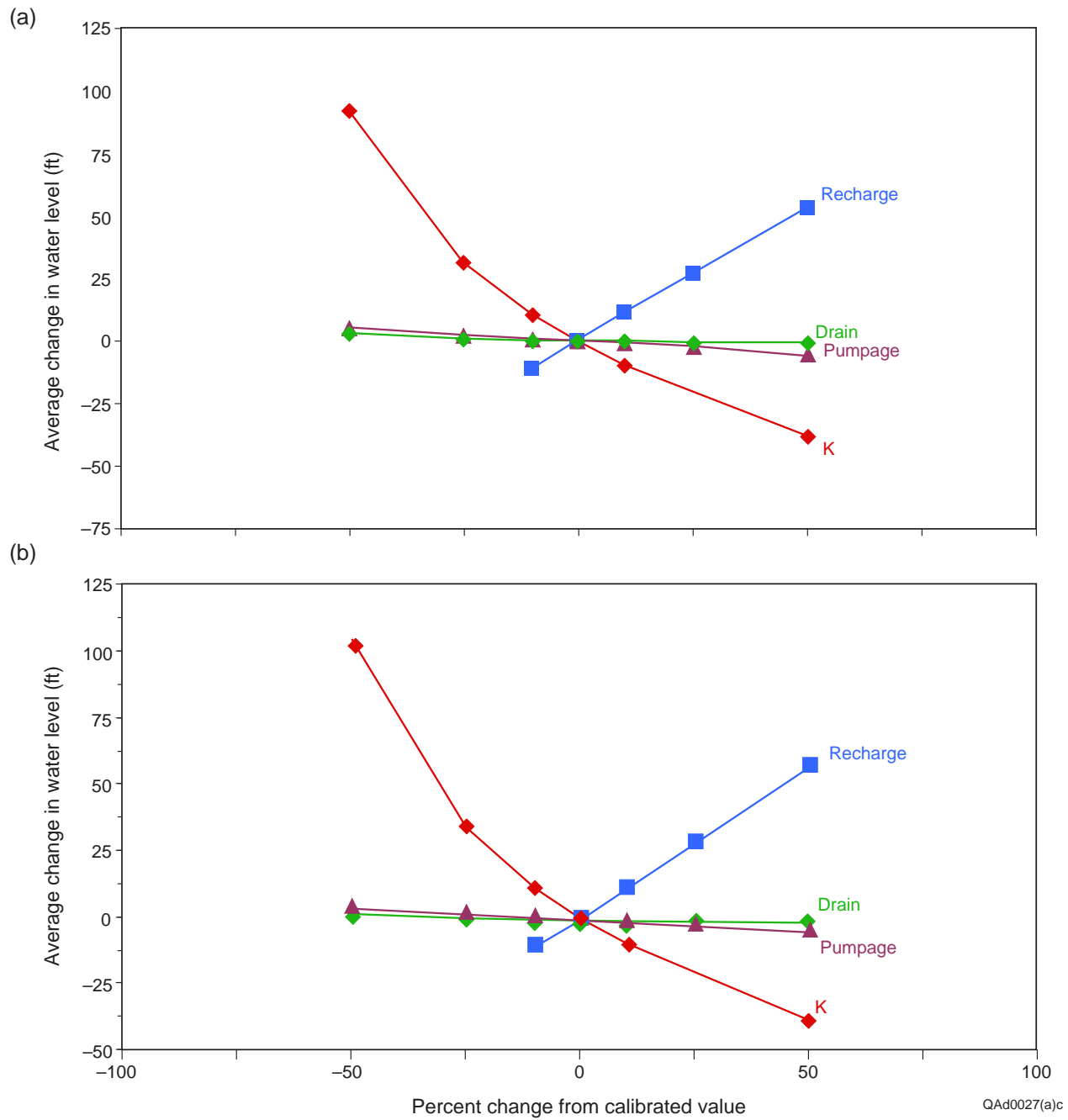
Figure 34.  Sensitivity of the numerically predicted water levels of the steady-state model to changes in model parameters at (a) calibration wells and (b) each active cell in the model.
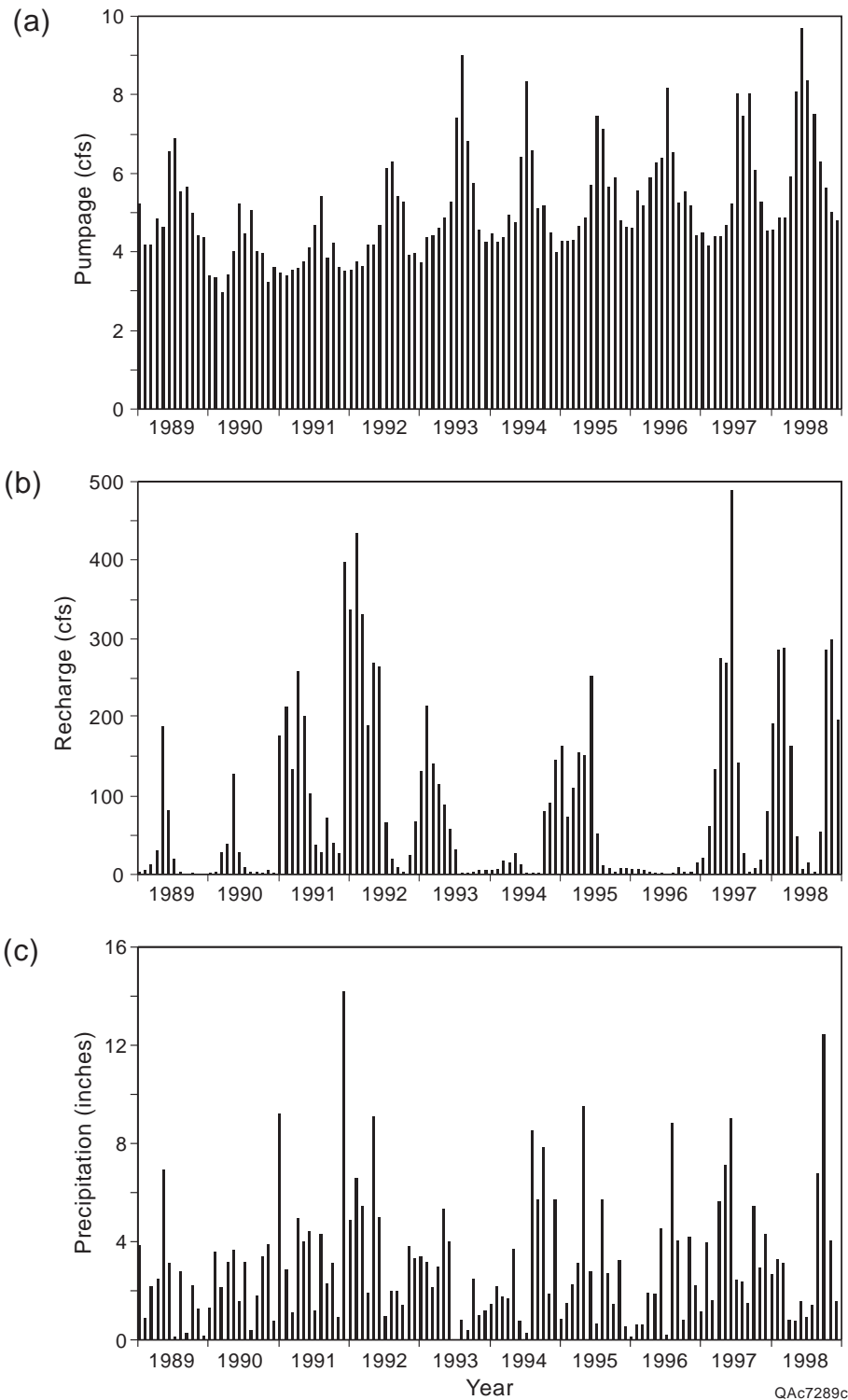
Figure 35.  (a) Monthly pumpage, (b) recharge, and (c) precipitation for the transient model (1989 through 1998).
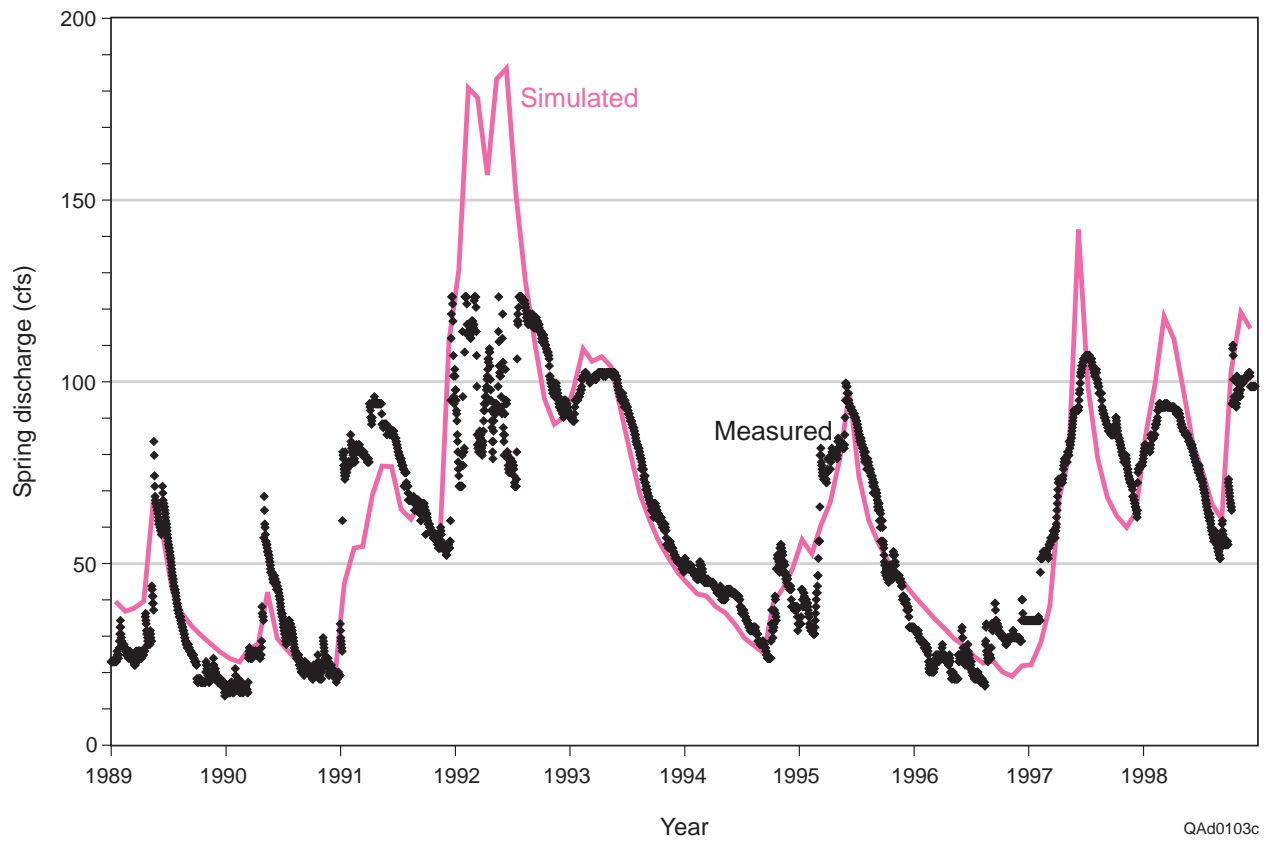
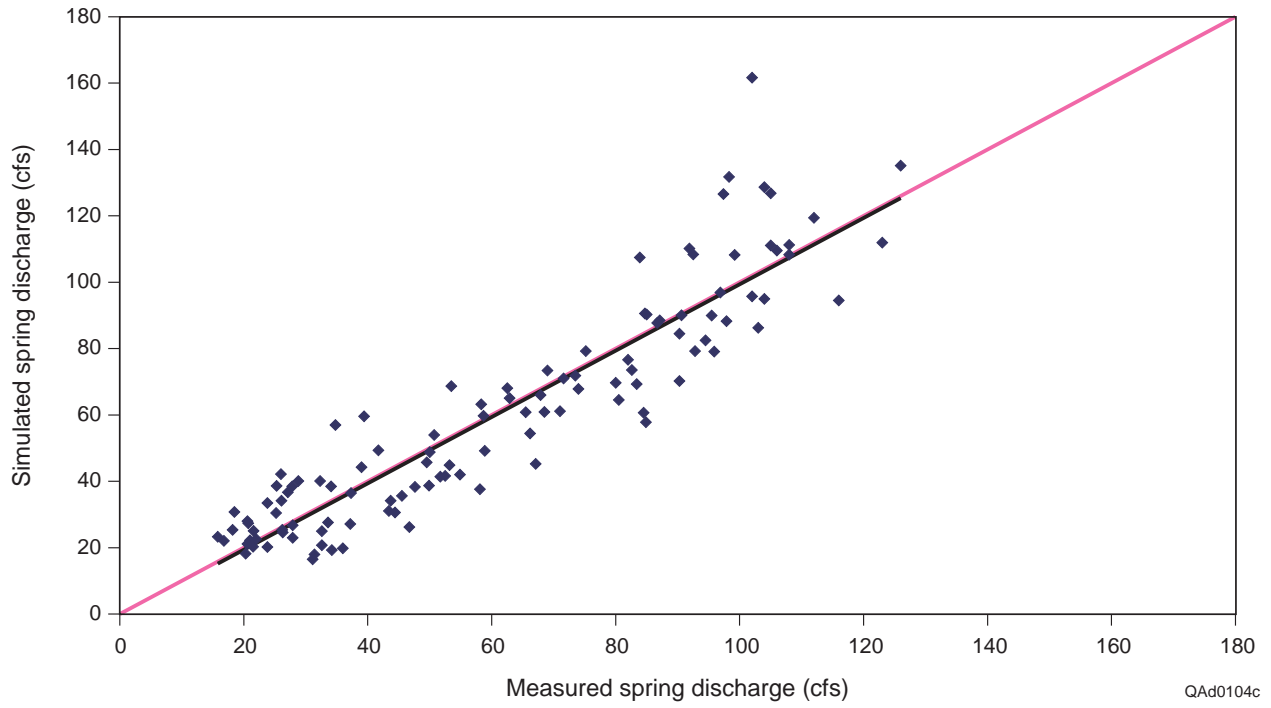Figure 36. Comparison of simulated and measured discharge at Barton Springs for 1989 through 1998.

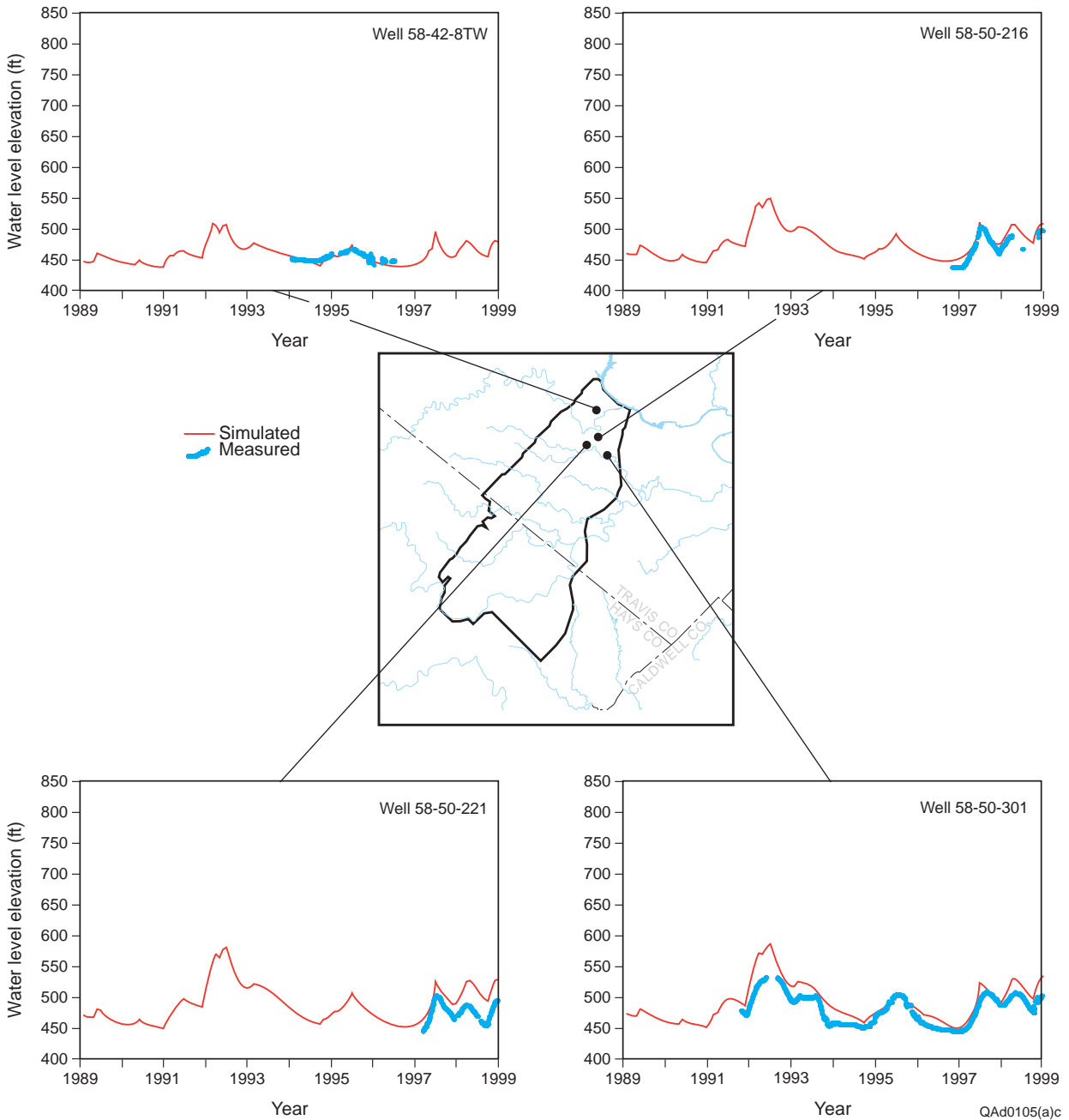Figure 37. Scatter plot of simulated versus measured spring discharge for 1989 through 1998.

QAd0104c

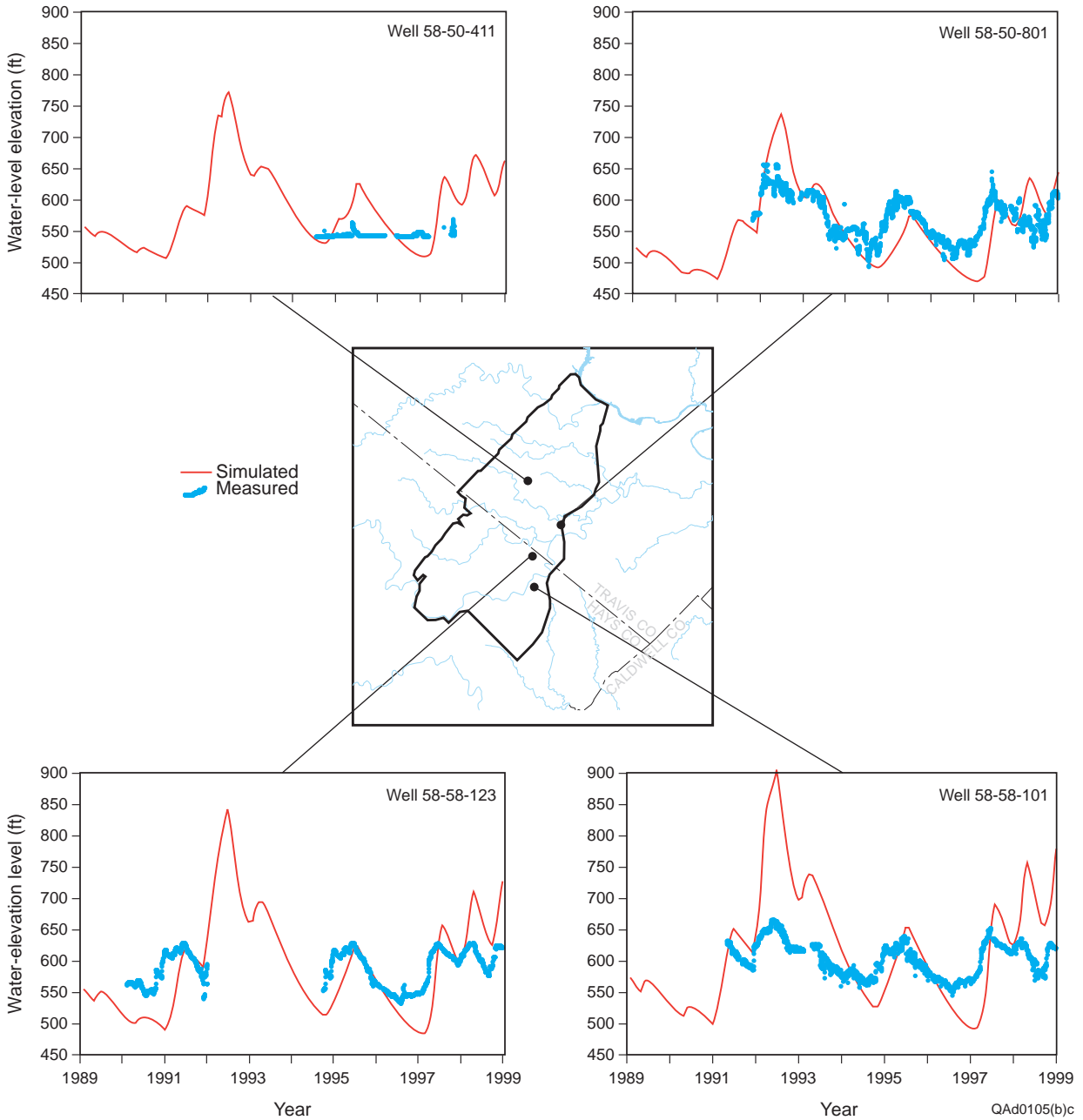Figure 38. Comparison of simulated and measured water-level elevation hydrographs in four monitoring wells, northern study area.

Figure 39. Comparison of simulated and measured water-level elevation hydrographs in four monitoring wells, central and southern study area.
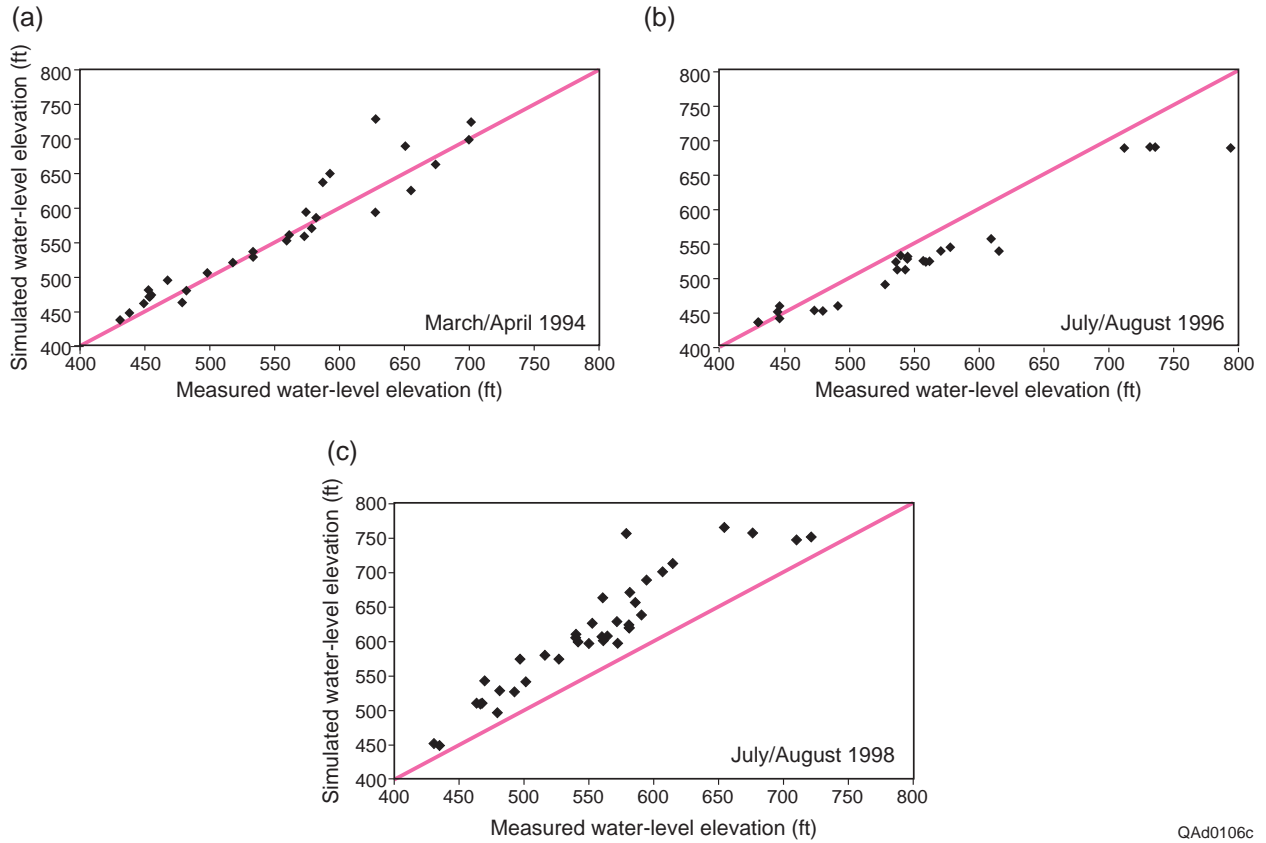
Fig. 40. Scatter plots of simulated versus measured water-level elevations for the transient simulations (a) March/April 1994, (b) July/August 1996, and (c) July/August 1998.
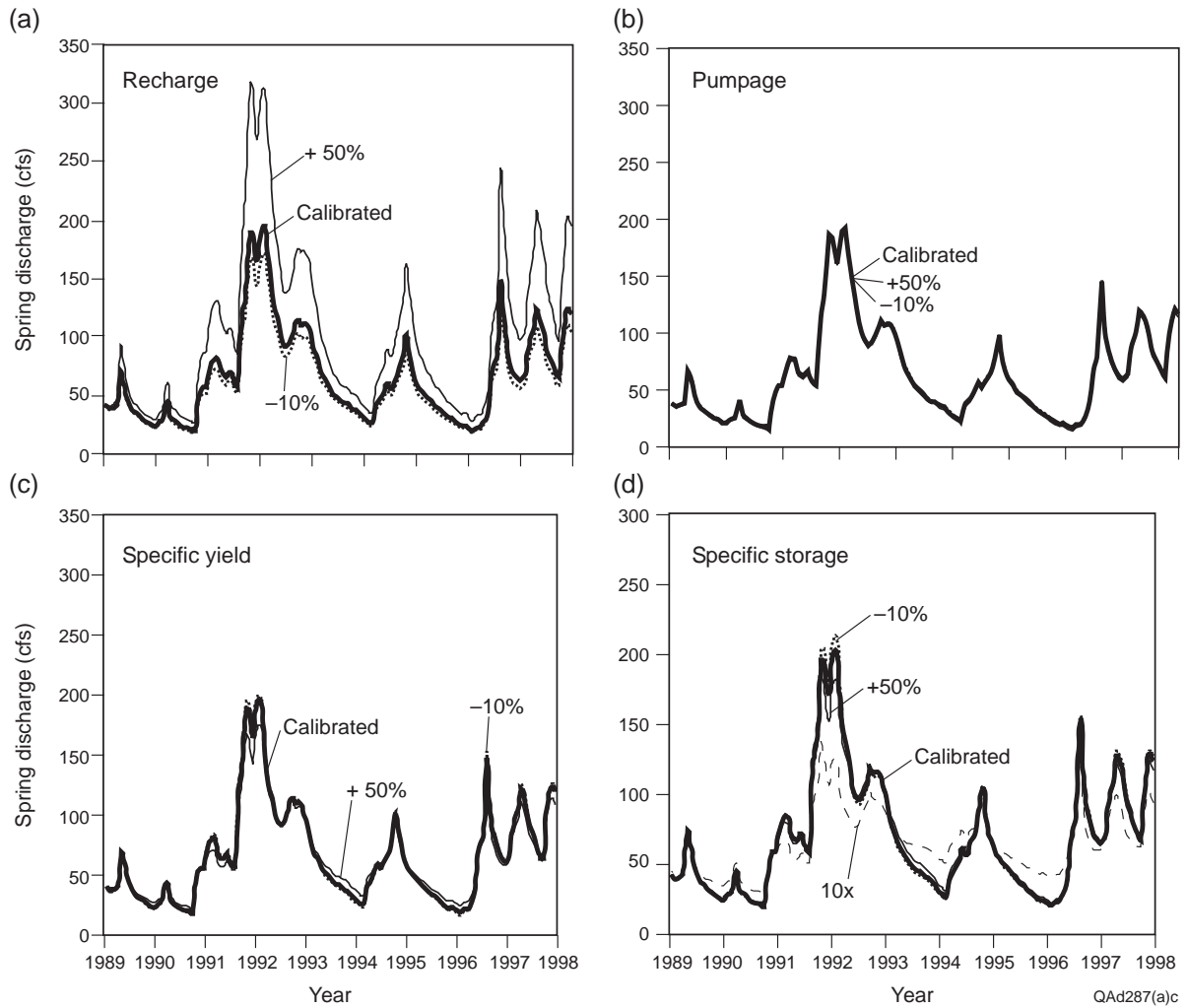
Figure 41. Sensitivity of the transient simulated spring discharge to (a) recharge, (b) pumpage, (c) specific yield, and (d) specific storage.
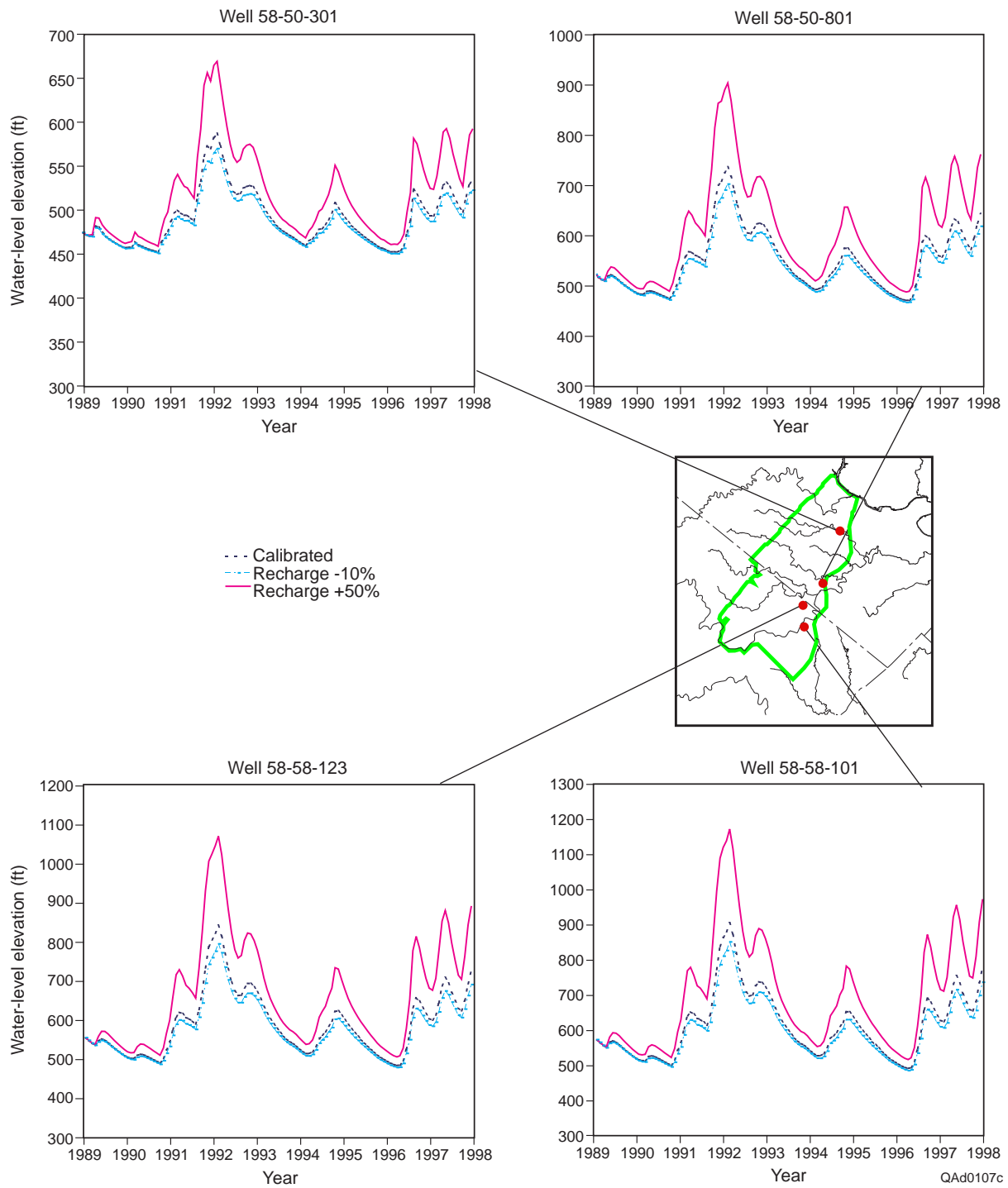
Figure 42. Sensitivity of the transient simulated water levels to recharge.
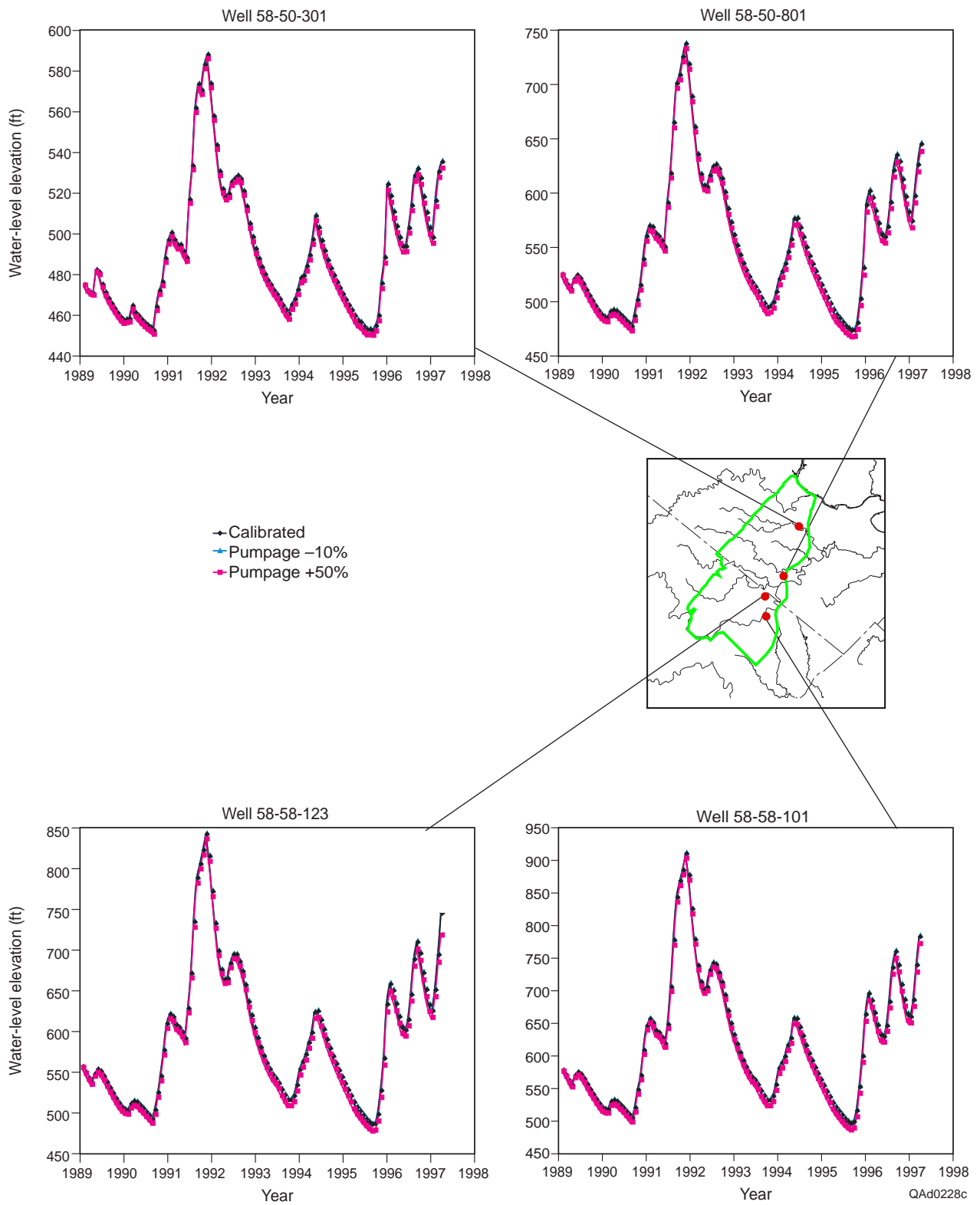
Figure 43. Sensitivity of the transient simulated water levels to pumpage.
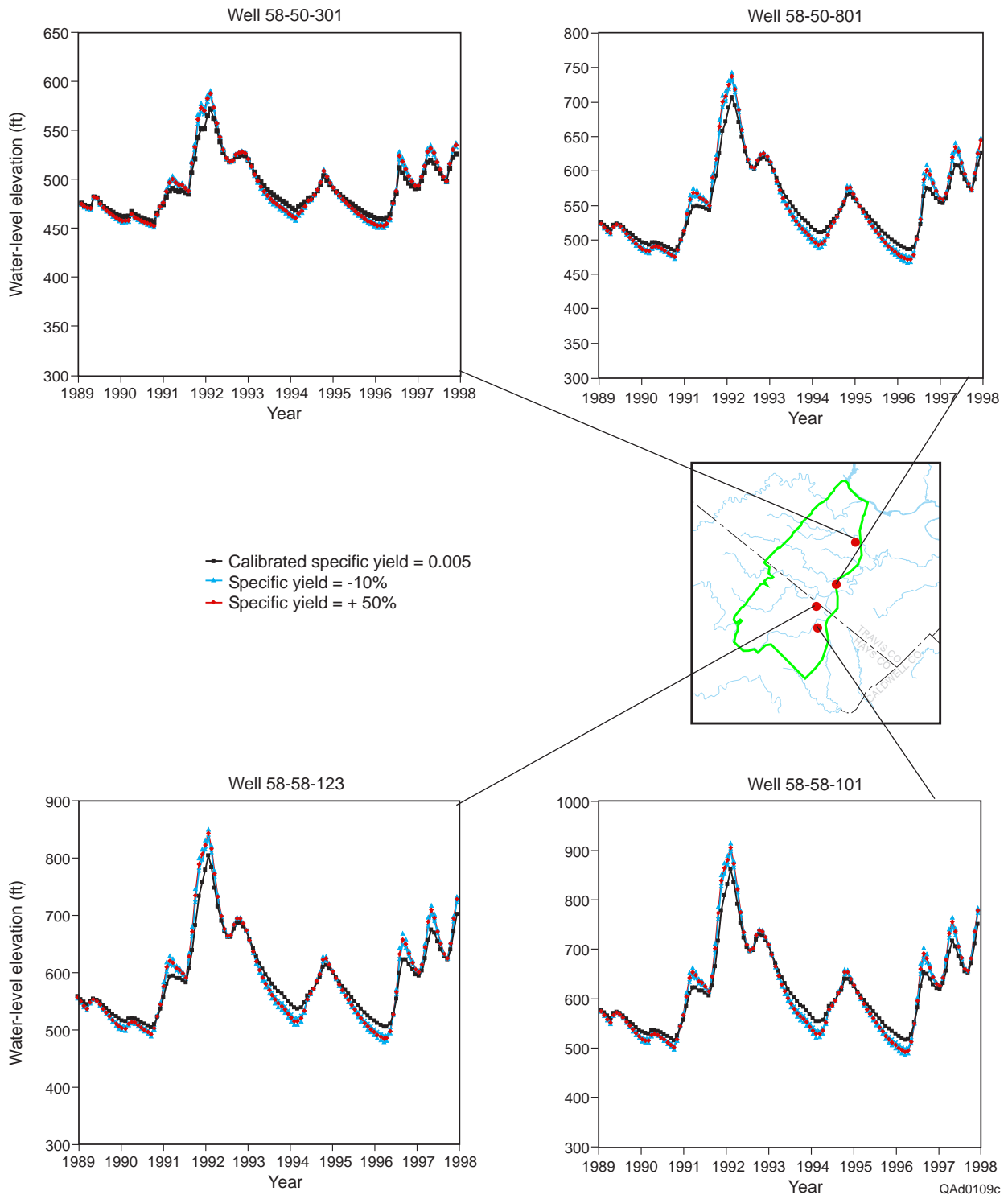
Figure 44.  Sensitivity of the transient simulated water levels to specific yield.
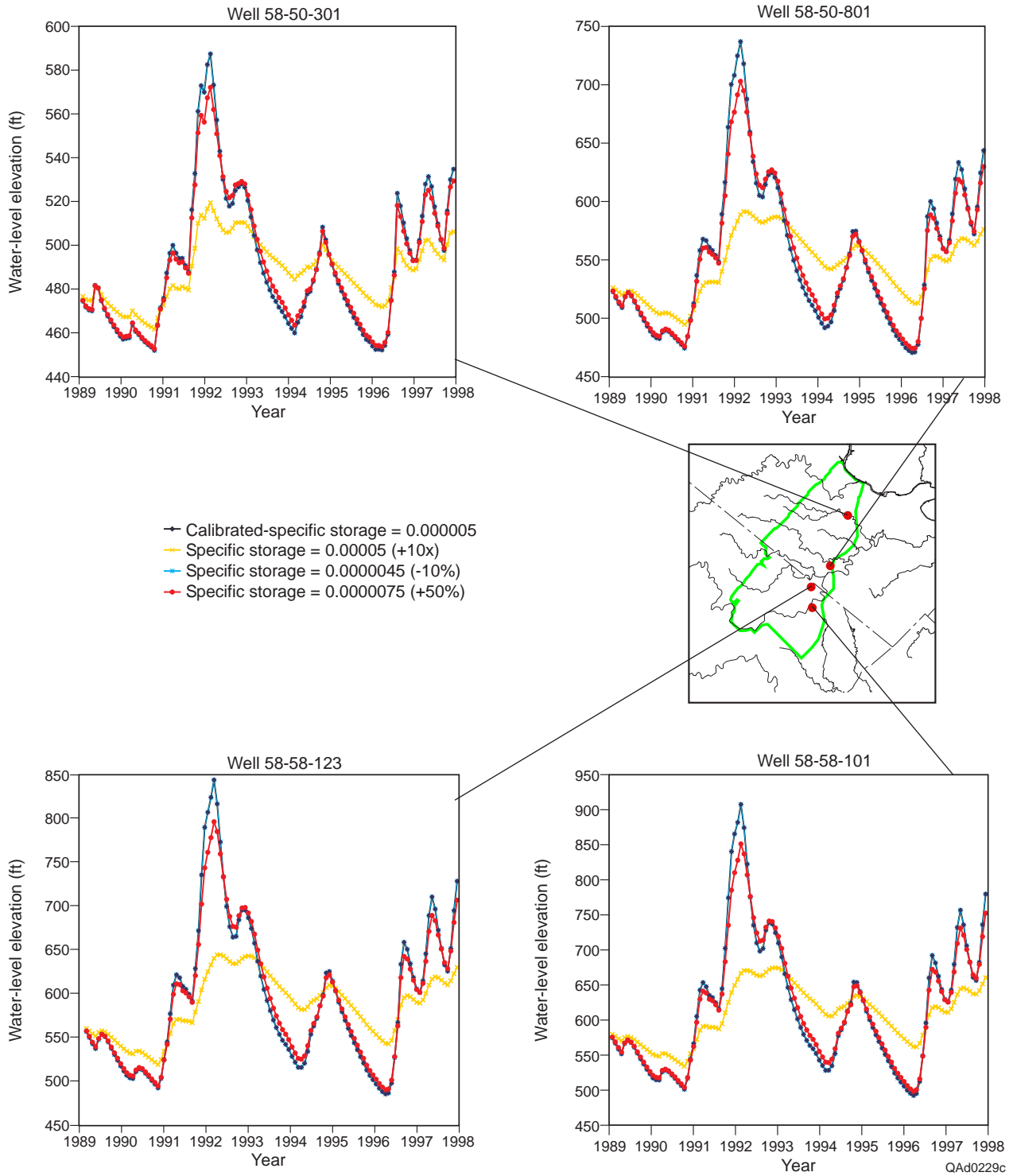
Figure 45. Sensitivity of the transient calibration water levels to specific storage.
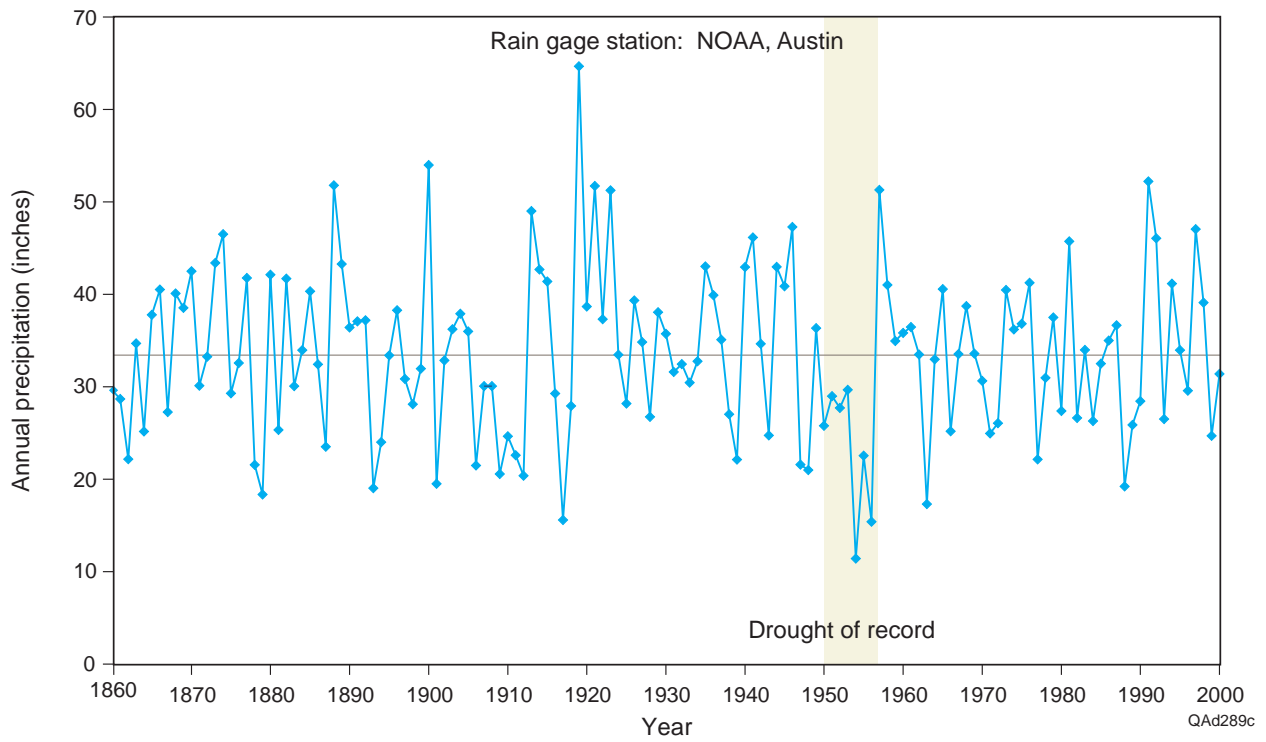
Figure 46. Precipitation from 1860 through 2000 measured at the rainfall gaging station in Camp Mabry and Mueller Airport in Austin (NOAA), showing the drought of record during the 1950's.
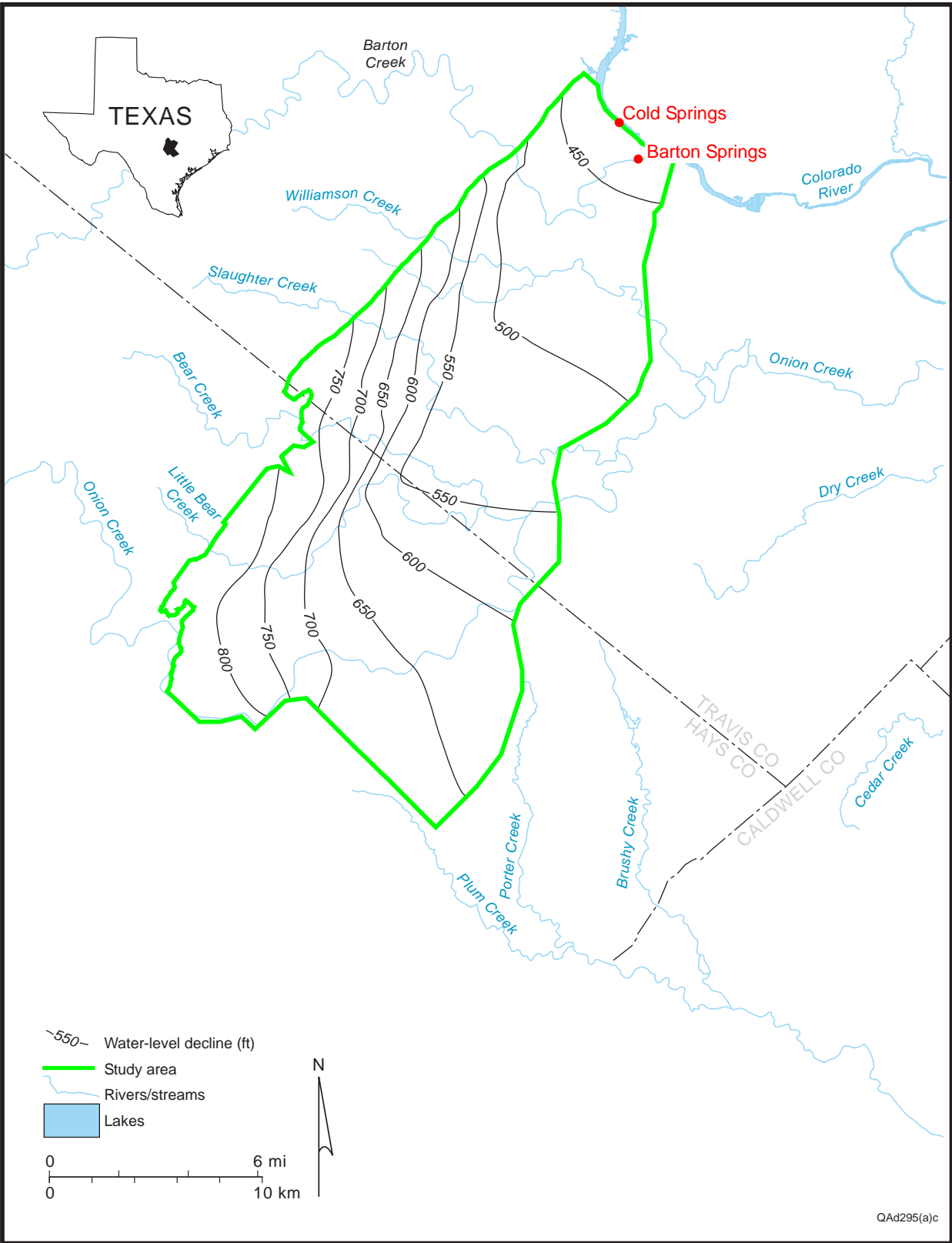
Figure 47.  Baseline water levels based on average recharge (55 cfs) and current pumpage (2000) at the end of a 10-yr simulation for comparison with future simulations.
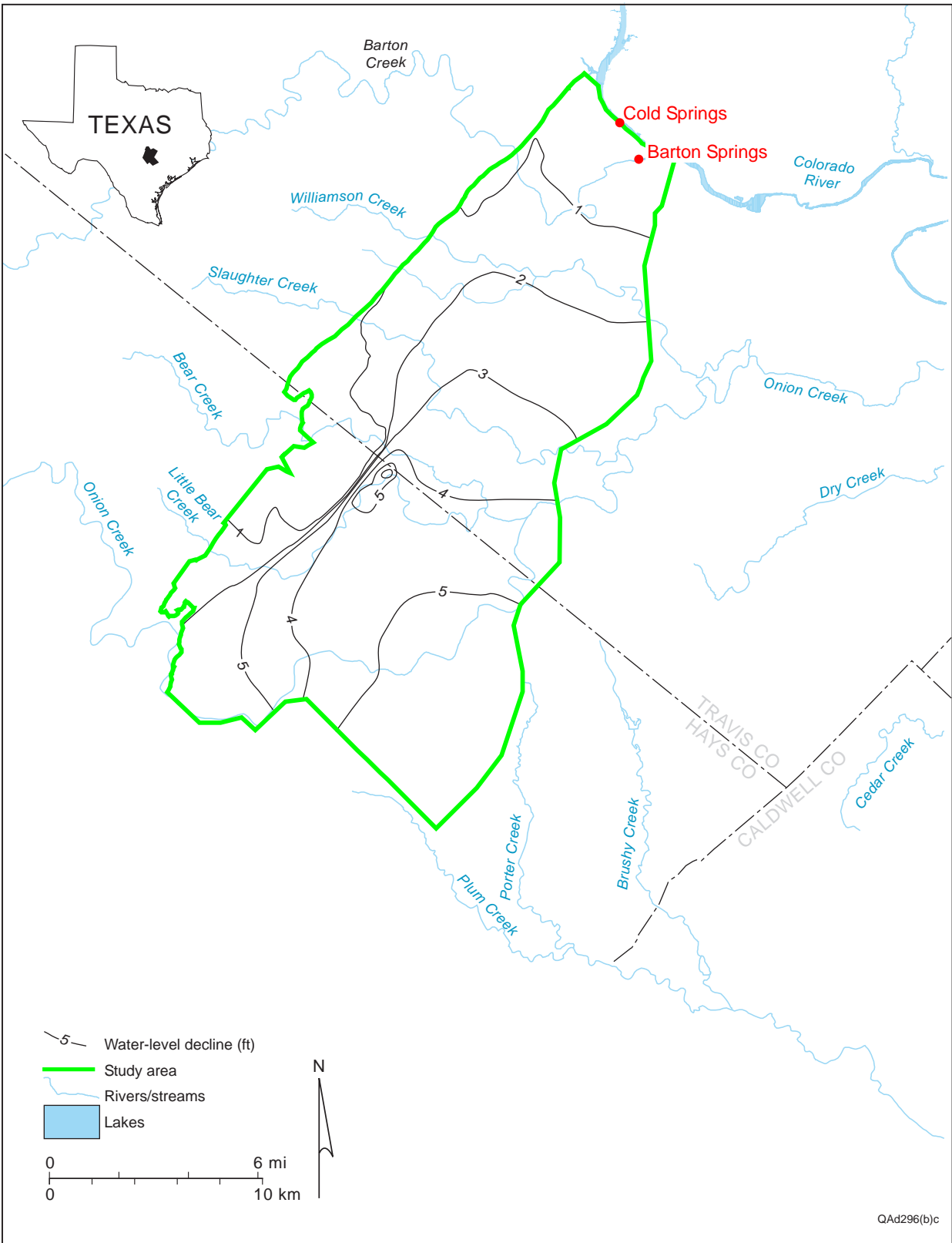
Figure 48(a).  Simulated water-level declines in 2010 (relative to baseline water levels (Fig. 47)) using average recharge conditions through 2010.
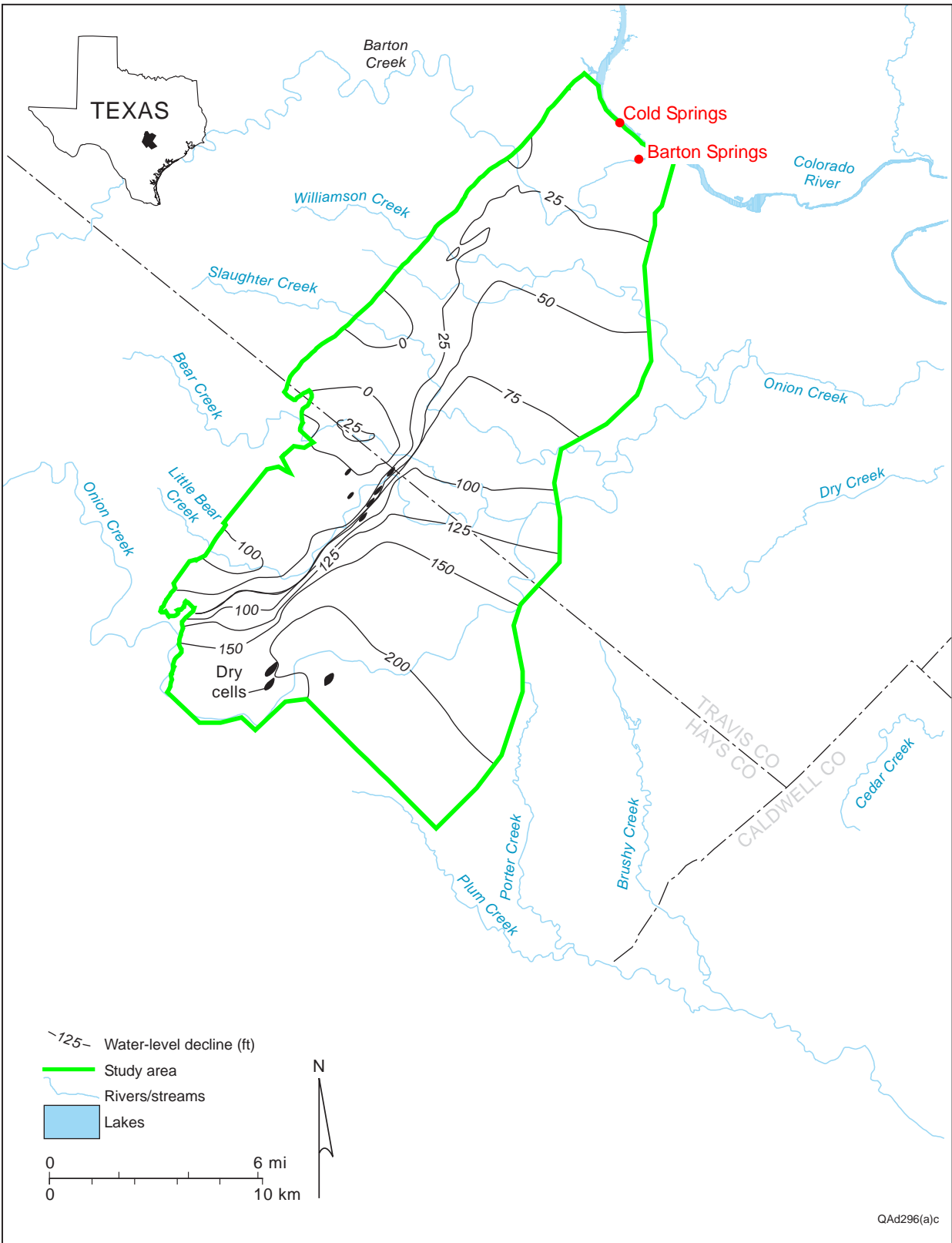
Figure 48(b).  Simulated water-level declines in 2010 (relative to baseline water levels (Fig. 47)) using average recharge conditions through 2003 and drought-of-record recharge conditions from 2004 to 2010.
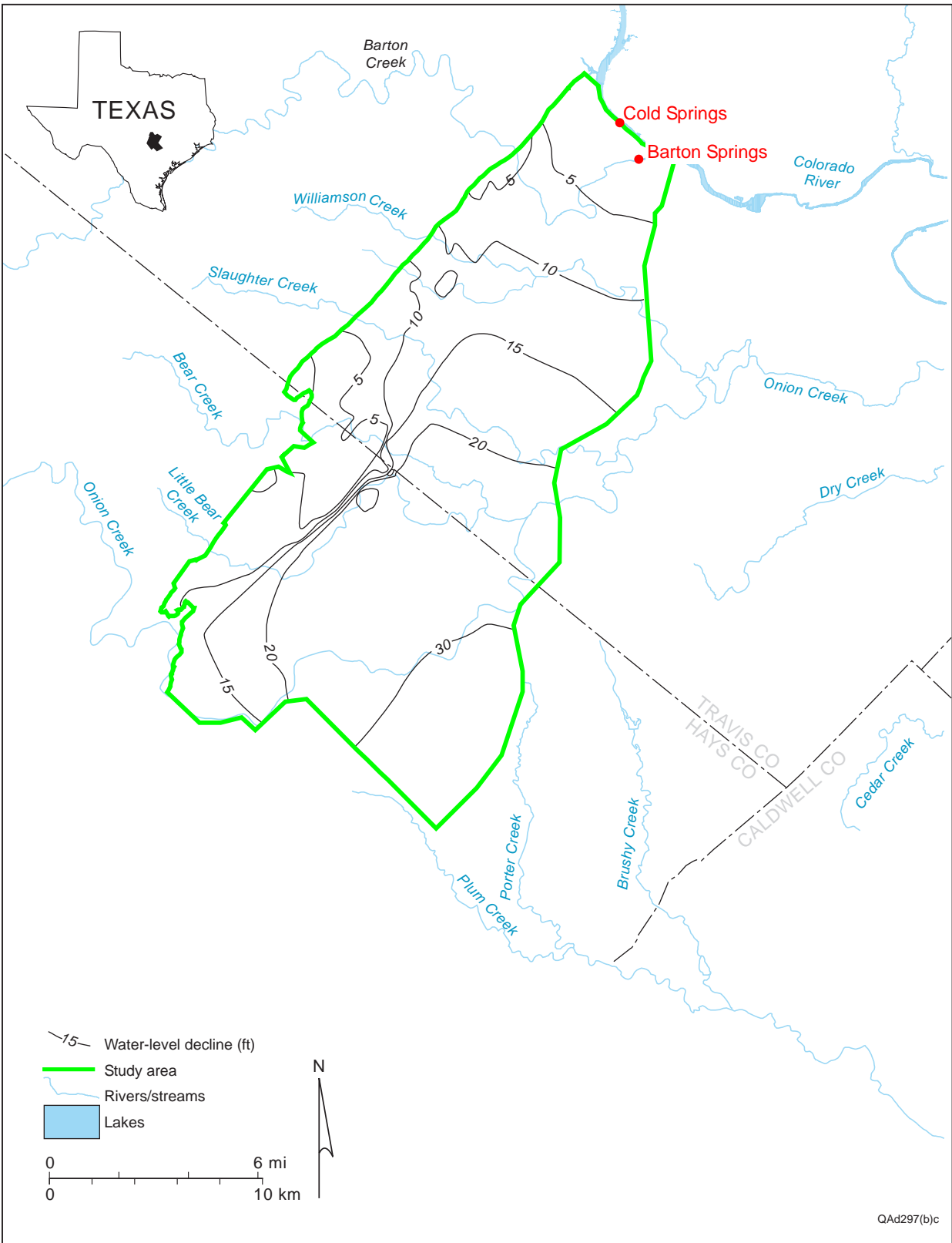
Figure 49(a). Simulated water-level declines in 2050 (relative to baseline water levels (Fig. 47)) using average recharge conditions through 2050.
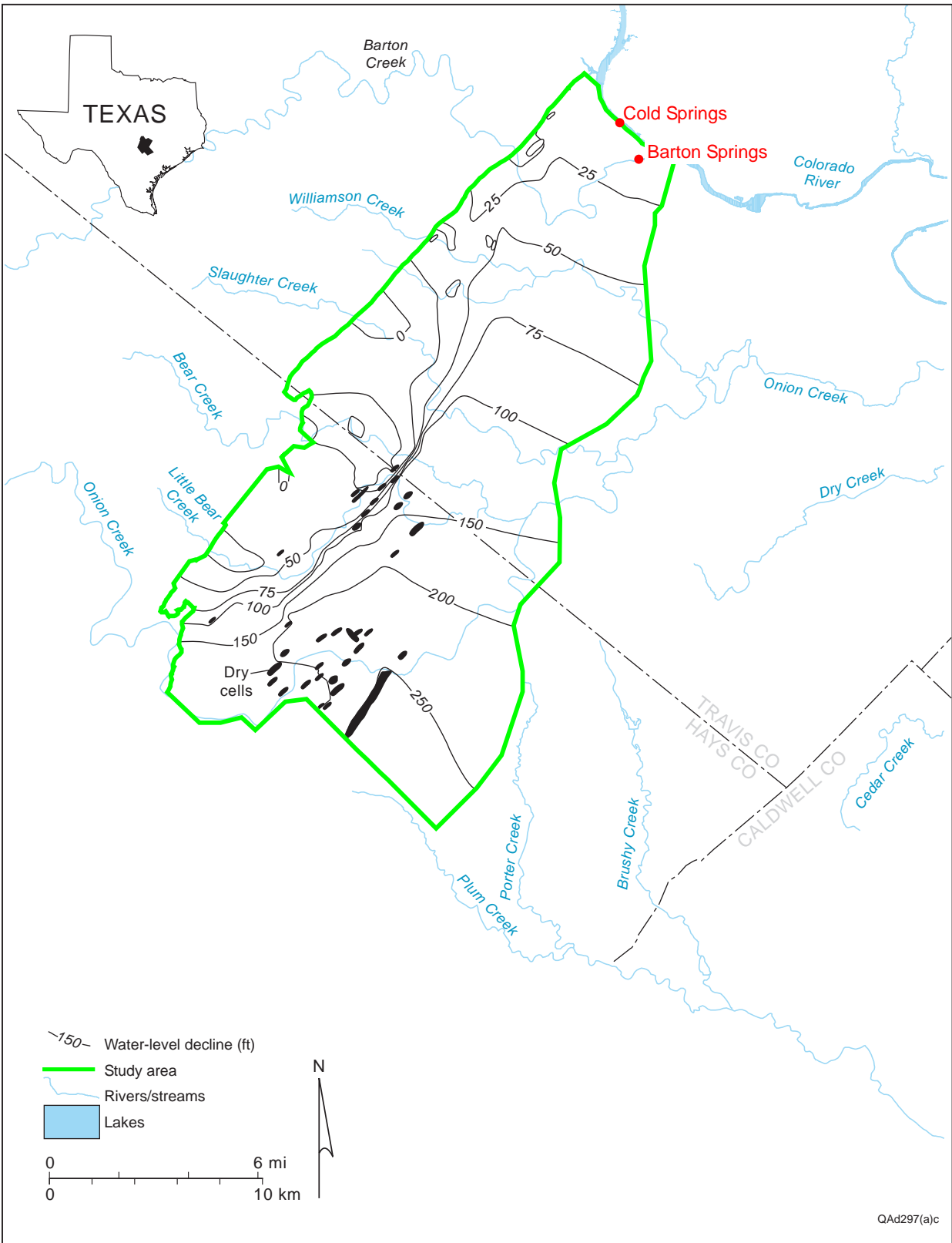
Figure 49(b). Simulated water-level declines in 2050 (relative to baseline water levels (Fig. 47)) using average recharge conditions through 2043 and drought-of-record recharge conditions from 2043 to 2050.
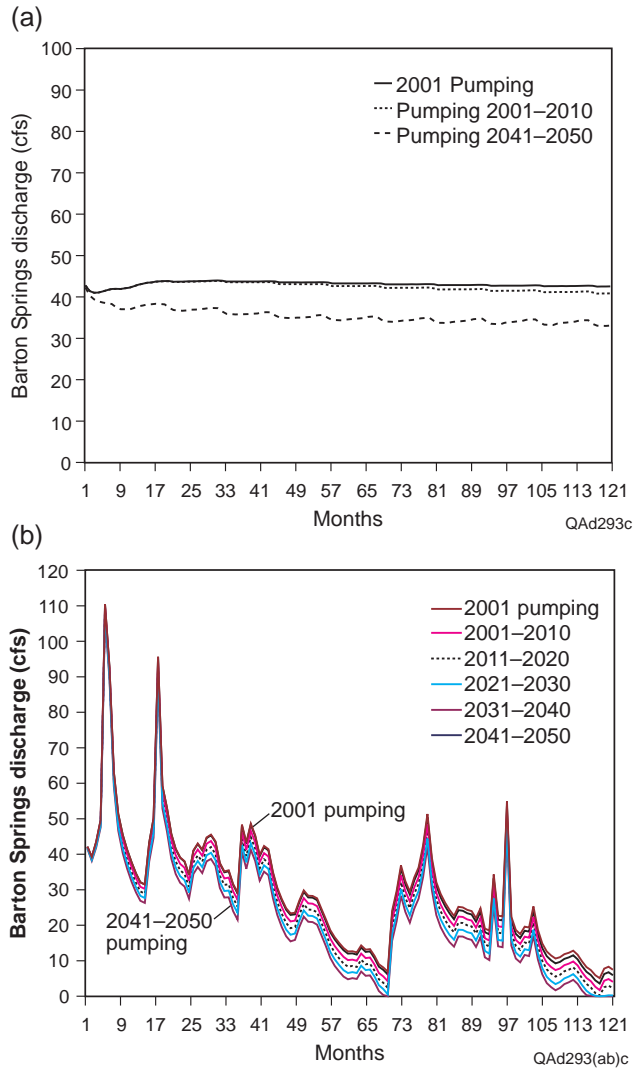
Figure 50. Simulated spring discharge for 10-yr periods using (a) average recharge conditions through 2050 and (b) average recharge conditions for the first three years and drought of record for the last seven years of each 10-yr period. The order in the legend reflects the vertical order in the line graphs.

Table 1. Stream-gauge data, including location, length of record, and maximum recharge.

| Creek name | Station no. | Latitude/longitude | Upstream/ downstream | Length of gauging record | Maximum recharge ($ft^3$/s) |
|---|---|---|---|---|---|
| Barton (Lost Creek) | 8155240 | 301626,0975040 | Upstream | 12/28/88–9/30/98 | 250 |
| Barton (Loop 360) | 8155300 | 301440, 0974807 | Downstream | 2/1/77–12/29/98 | |
| Williamson Creek | 8158920 | 301406, 975136 | Upstream | 12/29/93 | 13 |
| Williamson Creek | 8158922 | 301334,0975228 | Upstream | 3/1/93–12/29/98 | |
| Slaughter Creek | 8158840 | 301232,0975411 | | 1/1/78–12/29/98 | 52 |
| Bear Creek | 8158810 | 300919,09752623 | | 7/1/79–12/29/98 | 66 |
| Onion Creek (Drift) | 8158700 | 300458,0980027 | Upstream | 7/1/79–12/29/98 | 120 |
| Onion Creek (Buda) | 8158800 | 300509,975052 | Downstream | 7/1/79–9/30/83 | |

Table 2. Distribution of recharge among creeks calculated from daily data from 1/1/1980 through 12/31/1998.

| | Recharge ($ft^3$/yr) | Total creek recharge (%) |
|---|---|---|
| Barton Creek | 6.35E+08 | 29 |
| Williamson Creek | 4.95E+07 | 2 |
| Slaughter Creek | 1.22E+08 | 5 |
| Bear and Little Bear Creeks | 4.19E+08 | 19 |
| Onion Creek | 1.00E+09 | 45 |
| Total | 2.23E+09 | 100 |

Table 3. Statistical summary of hydraulic conductivity values for the Barton Springs segment of the Edwards aquifer.

| n | $p_{25}$ | $p_{50}$ | $p_{75}$ | $x_g$ | $x_{g+s}$ | $x_{g--s}$ | $s^2$ |
|---|---|---|---|---|---|---|---|
| 24 | 1.3 | 4.9 | 13.8 | 0.6 | 1.4 | -0.2 | 0.6 |

n—number of points
$p_{25}$— 25th percentile (medial) (ft/d)
$p_{50}$—50th percentile (median) (ft/d)
$p_{75}$—75th percentile (median) (ft/d)
$x_g$—geometric mean
$x_{g-s}$—geometric mean minus a standard deviation (ft/d)
$x_{g+s}$—geometric mean plus a standard deviation
$s^2$—variance $(log[ft/d])^2$
Standard deviations are calculated from the log-normal distribution.

Table 4. Annual precipitation, recharge, pumpage, and number of reported users for the transient simulation (1989 through 1998) and predicted recharge for average conditions (2041 through 2043) and potential future drought (2044 through 2050) estimated from the 1950's drought for the future simulations.

| Time (yr) | Precipitation (inches) | Recharge (cfs) | Pumpage (reported + domestic) (cfs) | Pumpage as % of recharge | Number of users |
|---|---|---|---|---|---|
| 1989 | 25.87 | 28.84 | 5.11 | 18 | 100 |
| 1990 | 28.44 | 20.91 | 3.88 | 19 | 103 |
| 1991 | 52.21 | 140.98 | 3.92 | 3 | 116 |
| 1992 | 46.05 | 168.56 | 4.57 | 3 | 126 |
| 1993 | 26.5 | 66.07 | 5.41 | 8 | 129 |
| 1994 | 41.16 | 33.38 | 5.23 | 16 | 131 |
| 1995 | 33.97 | 82.86 | 5.29 | 6 | 136 |
| 1996 | 29.58 | 4.15 | 5.73 | 138 | 139 |
| 1997 | 47.06 | 127.39 | 5.56 | 4 | 140 |
| 1998 | 39.11 | 153.45 | 6.29 | 4 | 142 |

Table 5. Sensitivity of transient spring discharge to variations in recharge, pumpage, specific yield, and specific storage.

| | Mean (cfs) | Minimum (cfs) | Maximum (cfs) | Range (cfs) | Coefficient of variation |
|---|---|---|---|---|---|
| Calibrated value | 67.6 | 19 | 196 | 177 | 0.61 |
| Recharge (-10%) | 60.8 | 18 | 172 | 154 | 0.59 |
| Recharge (50%) | 102.7 | 26 | 319 | 293 | 0.68 |
| | | | | | |
| Pumpage (-10%) | 68.1 | 20 | 197 | 178 | 0.61 |
| Pumpage (+50%) | 65.4 | 17 | 194 | 177 | 0.63 |
| | | | | | |
| Specific yield (-10%) | 67.9 | 18 | 200 | 182 | 0.63 |
| Specific yield (+50%) | 66.5 | 23 | 177 | 154 | 0.52 |
| | | | | | |
| Specific storage (-10%) | 67.8 | 19 | 207 | 188 | 0.63 |
| Specific storage (+50%) | 67.1 | 20 | 178 | 158 | 0.56 |
| Specific storage (10x) | 64.2 | 28 | 133 | 105 | 0.35 |

Table 6. Water budget for the calibrated steady-state, transient, and predictive runs. All values are in cubic feet per second (cfs).

| Model Run | Recharge | Wells | Springs | Storage |
|---|---|---|---|---|
| | cfs | cfs | cfs | cfs |
| Steady State | 60.0 | -5.1 | -54.8 | NA |
| Transient 89-98 | 82.7 | -5.1 | -71.9 | 5.7 |
| 2010 | 13.5 | -11.2 | -7.6 | -5.3 |
| 2020 | 13.5 | -13.2 | -5.8 | -5.5 |
| 2030 | 13.5 | -15.3 | -4.1 | -5.9 |
| 2040 | 13.5 | -17.3 | -2.3 | -6.1 |
| 2050 | 13.5 | -19.4 | -1.5 | -7.4 |
| 2010 (no drought) | 55.0 | -11.2 | -41.1 | 2.7 |
| 2050 (no drought) | 55.0 | -19.4 | -33.7 | 1.9 |

To convert cfs to acre-ft/yr, multiply by 723.97
A positive sign indicates additions to the water budget and negative signs indicate removals.
Numbers represent fluxes for the year listed. The transient calibration model represents the average flux for 1989 – 1998.

ATTACHMENT 1
TEXAS WATER DEVELOPMENT BOARD
Review of the draft Final Report: Contract No. 2001-483-399
"Groundwater Availability of the Barton Springs Segment of the Edwards Aquifer,
Texas: Numerical Simulations through 2050:

Board staff offers the following comments:

1.    Report is well written and easy to read and understand

2.    Cover page, need to note that Brian Smith is with BSEACD.

Brian Smith's affiliation has been noted on the cover page.

3.    Page 2, 1st and 3rd sentence: It would be clearer if Barton Springs pool was defined
and then described.

Sentences reordered to clarify meaning.

4.    Page 2, paragraph 2: "in a computer" does not seem like correct terminology,
perhaps "using" or some other word would be more appropriate.

Changed in a computer to using a computer.

5.    Page 2, paragraph 2, 2nd sentence: Calibrated is introduced here but it is unclear
what it means.

Model calibration is a standard process in modeling and is explained in detail in the
Methods section

6.    Page 3, paragraph 1, 1st sentence: The statement "(1,000 x 500 versus a minimum
of 1,500 ft)" does not seem to be parallel and is hard to understand. Whether it means
500,000 vs 1500 or 1000 versus 1500 or something else entirely is not clear.

Changed sentence to indicate that minimum cell spacing of 500 ft versus 1,500 ft.

7.    Page 4, geology section (and many places afterward): Comment on aquifer
nomenclature. TWDB calls the aquifer the Edwards (Balcones Fault Zone) aquifer. This
aquifer consists of three segments: the San Antonio segment, the Barton Springs
segment, and the northern segment. In the report, you refer to the San Antonio segment
as the Balcones Fault Zone segment.

Balcones Fault Zone segment renamed the San Antonio segment throughout.

8.    Page 10, paragrapa 4: This statement seems to compare a description "stratigraphic thickness" to a process "thinning as a result fo normal faulting" to each other and is hard to understand.

Changed thinning to reduction in thickness.

9.    Page 21, paragraph 1, equation 1: The m in hm needs to be a subscript. The i in hi should be a subscript s according to the equation.

Changes made.

10.    Page 21, RMS equation: Explanation of terms in the text is inconsistent with the equation 1.

Explanation corrected to correspond to equation.

11.    Page 26, paragraph 1: The use of the word recession here is confusing. Perhaps a definition should be included.

The term recession is replaced with low-flow period.

12.    Pate 29, Drought of Record: "1960 through 2000' should be 1860 through 2000'.

Change made.

13.    Figures difficult to impossible to read without being in color. Impossible to address now, but will need to be looked at in Final Report.

Color figures included in report where it was difficult to decipher material in black and white.

14.    Please include a budget table in the Final Report

Table included.